IRDR

Intractable & Rare Diseases Research

IRCA
BSSA

IACMHR

www.irdrjournal.com

IRDR
Intractable & Rare Diseases Research

Intractable & Rare Diseases Research is one of a series of peer-reviewed journals of the International Research and Cooperation Association for Bio & Socio-Sciences Advancement (IRCA-BSSA) Group and is published quarterly by the International Advancement Center for Medicine & Health Research Co., Ltd. (IACMHR Co., Ltd.) and supported by the IRCA-BSSA.

Intractable & Rare Diseases Research devotes to publishing the latest and most significant research in intractable and rare diseases. Articles cover all aspects of intractable and rare diseases research such as molecular biology, genetics, clinical diagnosis, prevention and treatment, epidemiology, health economics, health management, medical care system, and social science in order to encourage cooperation and exchange among scientists and clinical researchers.

Intractable & Rare Diseases Research publishes Original Articles, Brief Reports, Reviews, Policy Forum articles, Case Reports, Communications, Editorials, News, and Letters on all aspects of the field of intractable and rare diseases research. All contributions should seek to promote international collaboration.

IRCA-BSSA Group Journals

ISSN: 1881-7815
Online ISSN: 1881-7823
CODEN: BTIRCZ
Issues/Year: 6
Language: English
Publisher: IACMHR Co., Ltd.
www.biosciencetrends.com
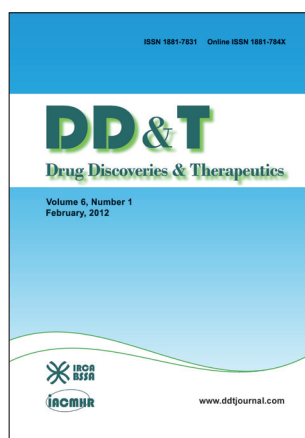
ISSN: 1881-7831
Online ISSN: 1881-784X
CODEN: DDTRBX
Issues/Year: 6
Language: English
Publisher: IACMHR Co., Ltd.
www.ddtjournal.com
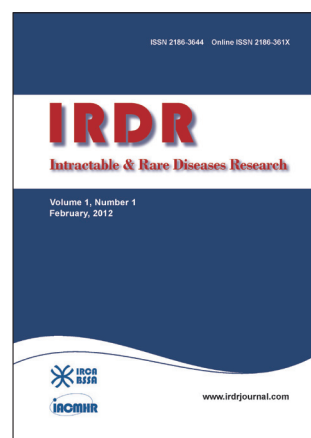
ISSN: 2186-3644
Online ISSN: 2186-361X
CODEN: IRDRA3
Issues/Year: 4
Language: English
Publisher: IACMHR Co., Ltd.
www.irdrjournal.com

Intractable & Rare Diseases Research

Editorial and Head Office

Pearl City Koishikawa 603, 2-4-5 Kasuga, Bunkyo-ku,
Tokyo 112-0003, Japan

E-mail: office@irdrjournal.com
URL: www.irdrjournal.com

Editorial Board

Editor-in-Chief:

Takashi KARAKO
National Center for Global Health and Medicine, Tokyo, Japan

Co-Editors-in-Chief:

Jinxiang HAN
Shandong Academy of Medical Sciences, Ji'nan, China

Jose-Alain SAHEL
Pierre and Marie Curie University, Paris, France

Editorial Board Members

CONTENTS   *Volume 10, Number 3, 2021*

CONTENTS   (*Continued*)

An update on China's national policies regarding rare diseases

Zhiye Ying[1], Li Gong[2], Chunyang Li[1,*]

[1] Biomedical Big Data Center, West China Hospital, Sichuan University, Chengdu, Sichuan, China;
[2] Rare Diseases Center, West China Hospital, Sichuan University, Chengdu, Sichuan, China.

SUMMARY   Over the past few years, China has paid greater attention to the topic of rare diseases. The Chinese Government has made considerable efforts to gradually improve the situation of patients with rare diseases in terms of diagnosis and treatment, access to medication, and affordability of care. The National Health Commission implemented a raft of measures, including the first Catalog of Rare Diseases, establishment of a rare diseases alliance, establishment of the Network for Collaboration in Rare Disease Diagnosis and Treatment, formulation of the Guidelines for the Diagnosis and Treatment of Rare Diseases, sharing of diagnostic and treatment information, and creation of expert committees, to ensure the standardization of rare disease diagnosis and treatment and to promote the improvement of rare disease diagnosis and treatment capabilities nationwide. In order to encourage the research, development, and production of drugs to treat rare diseases, the National Medical Products Administration has drafted a series of policies to accelerate the review and approval of drug registration and to support the research and development of drugs to treat rare diseases. The Ministry of Finance has also helped to implement tax incentives for drugs to treat rare diseases, to encourage the marketing and importation of drugs to treat rare diseases, and to reduce the cost of drugs for patients with rare diseases. Through adjustment of the List of Drugs Covered by National Medical Insurance, the National Healthcare Security Administration has covered an increasing number of drugs to treat rare diseases under basic medical insurance. It has also negotiated to reduce the price of some drugs to treat rare diseases, further reducing the economic burden on patients with rare diseases.

Keywords   rare diseases, drugs, policies, China

1. Introduction

Rare diseases refer to diseases with a very low prevalence. The definition of rare diseases varies in different countries around the world. An article in the internationally renowned academic journal Nature Reviews Drug Discovery in 2020 stated that by integrating multiple rare disease-related knowledge bases and databases, more than 10,000 rare diseases have been evaluated (*1*). Currently, China has more than 20 million people with rare diseases who have very few treatment options (*2*). Misdiagnosis and difficulties related to drug options are among the main challenges in diagnosing and treating rare diseases. China has emphasized the diagnosis, treatment, and relief of rare diseases. Since China implemented the New Drug Registration Regulation in May 1999, it has made considerable efforts to support the development of rare diseases. The current study describes three key aspects of recent national policies regarding rare diseases in order to examine the current state of management of rare diseases in China.

2. Three key aspects of national policies on rare diseases

2.1. Promoting the improvement of rare disease diagnosis and treatment capabilities nationwide

We listed current national policies on diagnosis and treatment of rare diseases in Table 1. In May 2018, five authorities announced the "First Catalog of Rare Diseases," which included 121 rare diseases (*3*). This was the first time that the Chinese Government drafted a list of rare diseases, providing an opportunity to discuss rare diseases in public.

In October 2018, a Chinese medical research alliance was set up to accelerate the study of rare diseases (*4*). The China Alliance for Rare Diseases consists of more than 50 entities including medical

Table 1. Current national policies on diagnosis and treatment of rare diseases

Effective time (*Ref.*)	Issuing agency	Policy & Regulation	Content about rare diseases
May, 2018 (*3*)	Five authorities	China's First National List of Rare Diseases	121 rare diseases
October, 2018 (*4*)	China Alliance for Rare Diseases	An explanation of China's first Catalog of Rare Diseases	It includes the basic concepts, clinical manifestations, diagnosis, differential diagnoses, and treatment principles for 60 rare diseases.
February, 2019 (*5*)	National Health Commission	Notice on establishing the National Network for Collaboration in Rare Disease Diagnosis and Treatment	To establish a mechanism to facilitate collaboration, to relatively centralize diagnosis and treatment, and to provide two-way referrals for patients with rare diseases.
February, 2019 (*6*)	National Health Commission	Guidelines for the Diagnosis and Treatment of Rare Diseases (2019 ed.)	The definitions, causes, and procedures for diagnosis and treatment of 121 rare diseases.
October, 2019 (*7*)	National Health Commission	Notice on entry of information on the diagnosis and treatment of rare diseases	To establish a registry for patients with rare diseases.
January, 2020 (*8*)	National Health Commission	Office of the National Network for Collaboration in Rare Disease Diagnosis and Treatment	The Office is mainly responsible for daily contact with and management of hospitals in the collaborative network.
September, 2020 (*9*)	National Health Commission	Notice on publication and dissemination of the roster of the National Health Commission's second Expert Committee on the diagnosis and treatment of rare diseases and welfare for patients	The special committee will make recommendations to relevant departments.

facilities, universities, academic institutions, and companies. The Alliance is instrumental in concentrating resources and will encourage the treatment of rare diseases in China. During its launch on October 24, the Alliance published an explanation of China's first Catalog of Rare Diseases.

In February 2019, the National Health Commission issued the "Notice on Establishing the National Network for Collaboration in Rare Disease Diagnosis and Treatment," and 324 hospitals were included in the collaborative network. Member hospitals are required to include drugs to treat rare diseases in the hospital formulary and essential drug catalog in a timely manner, to conduct clinical monitoring of drugs to treat rare diseases, to warn of shortages and to report information as required, and to strive to meet the clinical demand for drugs (*5*). Enhanced coordination with the catalog of drugs to treat rare diseases at member hospitals, inter-hospital adjustment of drugs, and enhanced distribution and logistics allow patients with rare diseases to more easily obtain medicines nearby. The establishment of the National Network for Collaboration in Rare Disease Diagnosis and Treatment marks the beginning of the establishment of a mechanism for collaboration in the diagnosis and treatment of rare diseases and also provides a reference for treatment paths for patients with rare diseases in various regions.

In February 2019, China's first Guidelines for the Diagnosis and Treatment of Rare Diseases were published (*6*). Experts referred to relevant international guidelines while drafting the Chinese guidelines. The guidelines include definitions of 121 rare diseases included in the catalog released by the National Health

Commission, their causes, and procedures for diagnosis and treatment in order to improve the diagnosis and treatment of rare diseases and to benefit patients in China. In general, medical facilities in China lack personnel with sufficient skills to effectively diagnose and treat rare diseases, and the guidelines can help to train medical staff and improve their diagnostic and treatment skills.

There is no official figure on the number of people with rare diseases in China. In October 2019, the National Health Commission announced a notice on entry of information on the diagnosis and treatment of rare diseases in a bid to establish a system to collect relevant data to understand the epidemiology, clinical diagnosis and treatment of, and welfare for rare diseases in China. Now that data are being collected, the diagnosis and treatment of rare diseases and access to medicines should improve (*7*).

In January 2020, the National Health Commission established an Office for the National Network for Collaboration in Rare Disease Diagnosis and Treatment in order to enhance the organization and management of the National Network for Rare Disease Diagnosis and Treatment, to facilitate collaboration, and to effectively fulfil the overall role of a collaborative network (*8*).

Building on the original expert committee, the roster of the second expert committee on the diagnosis and treatment of rare diseases and welfare for patients was updated in September 2020 (*9*). Under the leadership of the National Health Commission, the special committee will research and define rare diseases and offer recommendations for changes to the rare disease catalog in conjunction with conditions in China,

Table 2. Current national policies on drugs to treat rare diseases

Effective time (*Ref.*)	Issuing agency	Policy/Regulation	Content related to rare diseases
October, 2017 (*10*)	The General Office of the State Council	The Opinions of the State Council on further reform of the review and approval system to encourage innovations in pharmaceuticals and medical devices.	To support the development of drugs and medical devices to treat rare diseases.
April, 2018 (*11*)	The State Council	Opinions on reforming and improving policies to ensure the supply and govern the use of generic drugs	To encourage the creation of generic drugs to treat rare diseases.
October, 2018 (*12*)	National Medical Products Administration	Guidelines for the Registration and Review of Medical Devices to Prevent and Treatment Rare Diseases	To resolve difficulties with the clinical evaluation of medical devices used to prevent and treat rare diseases.
March, 2019 (*13*)	Ministry of Finance of the People&s Republic of China	Notice on the value-added tax policy for drugs to treat rare diseases	The VAT rate for imported drugs to treat rare diseases has been reduced to 3%.
August, 2019 (*14*)	Standing Committee of the National People's Congress	The Pharmaceutical Administration Law	Greenlights the development and manufacture of drugs to treat rare diseases.
October, 2019 (*15*)	The Central Committee of the Communist Party of China and the State Council	The Opinions on promoting the passing down of, innovation in, and the development of traditional Chinese medicine	Encourages the use of traditional Chinese medicine to treat rare diseases.

draft and update technical specifications and devise clinical pathways for the prevention and treatment of rare diseases, screen for rare diseases, and make recommendations to relevant departments regarding diagnosis and treatment, medications, rehabilitation, and welfare for patients.

2.2. Encouraging the research, development, and production of drugs to treat diseases

Current national policies on drugs to treat rare diseases were summarized in Table 2. In October 2017, the General Office of the Central Committee of the Communist Party of China and the General Office of the State Council issued its "Opinions of the State Council on further reform of the review and approval system to encourage innovations in pharmaceuticals and medical devices" to encourage and accelerate the development of drugs and medical devices for rare diseases (*10*).

China is promoting research on and increased availability of generic drugs with improved quality and efficacy in order to lower healthcare costs and to better meet public demand, according to a document issued by the State Council on April 3, 2018 (*11*). Drug companies are encouraged to make generic versions of drugs that are essential for clinical treatment and that are in short supply, and especially drugs to treat major infectious diseases, rare diseases, pediatric diseases, and public healthcare crises.

In October 2018, the State Drug Administration drafted the Guidelines for the Registration and Review of Medical Devices to Prevent and Treatment Rare Diseases in order to implement the "Opinions on further reform of the review and approval system to encourage innovations in pharmaceuticals and medical devices" from the General Office of the Central Committee of the Communist Party of China and the General Office of the State Council (Notice No. 42 [2017]) (*12*). These guidelines focus on benefiting patients with rare diseases by scientifically resolving difficulties with the clinical evaluation of medical devices to prevent and treat rare diseases, reasonably reducing the clinical use of those devices, and promoting the clinical introduction of those devices as soon as possible through conditional approval.

A total of 21 drugs to treat rare diseases and 4 active pharmaceutical ingredients were the subject of China's first attempt at a policy to reduce the value-added tax (VAT) on certain drugs, which took effect in March 2019. The policy aimed to lower the cost for patients with rare diseases and to encourage drug development by the pharmaceutical industry. According to the policy, the VAT rate for imported drugs to treat rare diseases was reduced to 3%. The VAT for the production and sale of drugs to treat rare diseases was also reduced to 3% as of March 1 (*13*).

In August 2019, the Pharmaceutical Administration Law of the People's Republic of China encouraged innovation in the development of drugs that have confirmed or special curative effects or a new mechanism of action and drugs that can cure life-threatening or rare diseases. The Law greenlights urgently needed drugs, new drugs, drugs to treat pediatric diseases, and drugs that could prevent or cure serious infectious or rare diseases (*14*).

Table 3. Current national policies on medications for patients with rare diseases

Effective time (*Ref.*)	Issuing agency	Policy/Regulation	Content related to rare diseases
August 2019 (*16*)	National Healthcare Security Administration and Ministry of Human Resources and Social Security	List of drugs for national basic medical insurance, workmen's compensation, and maternity insurance.	New drugs to treat rare diseases are added.
January 2020 (*17*)	National Healthcare Security Administration	China implements a new list of drugs covered by national medical insurance.	7 drugs to treat rare diseases are included in the List of Drugs Covered by National Medical Insurance.
March 2020 (*18*)	National Health Commission	Opinions on further reform of the medical insurance system.	Cites the need to explore forms of welfare to cover drugs to treat rare diseases.
January 2021 (*19*)	Ministry of Finance	Import tariffs on some commodities are adjusted.	No tariffs are imposed on constituents of drugs to treat rare diseases.
December 2020 (*20*)	National Healthcare Security Administration and Ministry of Human Resources and Social Security	Notice on the drug list for national basic medical insurance, workmen's compensation, and maternity insurance (2020 ed.).	Some drugs to treat rare diseases have been added to the latest national essential drug list.
January 2020 (*21*)	The State Council of the People's Republic of China	Further reform of centralized bulk drug purchasing to ease the financial burden on patients.	Special arrangements will be made to procure drugs to treat rare diseases.

In October 2019, the Opinions of the Central Committee of the Communist Party of China and the State Council on promoting the passing down of, innovation in, and the development of traditional Chinese medicine stated that under the framework of the central financial science and technology plan (special projects, funds, *etc*.), China will conduct clinical research on the prevention and treatment of major, refractory, and rare diseases and emerging infectious diseases and accelerate the research and development of new traditional Chinese medicines (*15*).

2.3. Improving access to medications for patients with rare diseases

As shown in Table 3, some policies on medications for patients with rare diseases were implemented since 2019. In August 2019, a total of 148 new drugs were added to the regularly referenced portion of the drug list for national basic medical insurance, workmen's compensation, and maternity insurance. The added drugs include national essential drugs, drugs to treat major diseases such as cancer and rare diseases, drugs to treat chronic diseases, and drugs to treat pediatric diseases. In addition, some of the aforementioned types of drugs, and especially those to treat cancer and rare diseases, are mainly included in the list to be negotiated. If reasonable prices are negotiated in the next step, then those drugs will be included in the list as required (*16*).

China's new list of drugs covered by national medical insurance came into effect on January 1, 2020. It includes 70 new drugs with prices reduced by 60.7%, on average. Some 22 anti-cancer drugs, 7 drugs to treat diseases, 14 drugs to treat chronic diseases, and 4 drugs to treat

pediatric diseases will be included in the list. After the price reduction and medical insurance reimbursements, the financial burden on patients should be eased by more than 80% (*17*).

In March 2020, the "Opinions of the Central Committee of the Communist Party of China and the State Council on further reform of the medical insurance system" clearly stated that "forms of welfare to cover drugs to treat rare diseases need to be explored" (*18*). This shows that the Chinese Government is seeking to improve welfare for patients with rare diseases.

In order to reduce the economic burden on patients and improve the quality of life of the people in 2021, a notice issued by the Ministry of Finance in December 2020 stipulated that no tariffs would be imposed on the second set of anti-cancer drugs, constituents of drugs to treat rare diseases, and foods needed by particular patients (*19*).

After considerable reductions in their prices, a total of 119 drugs have been added to the latest national essential drug list for reimbursement, according to the National Healthcare Security Administration on December 28, 2020. This long-expected move will greatly relieve the financial burden on patients with serious conditions ranging from cancer and rare diseases to COVID-19 (*20*).

China will proceed with its centralized bulk drug purchasing program and regularly seek to lower medical costs for the general public, as decided at the executive meeting of the State Council chaired by Premier Li Keqiang on January 15, 2021. Special arrangements will be made to procure drugs to treat rare diseases (*21*).

China Hospital (ZYJC18010) and a project funded by the Science & Technology Department of Sichuan Province (no. 2016FZ0108).

Conflict of Interest: The authors have no conflicts of interest to disclose.

References

1. Haendel M, Vasilevsky N, Unni D, et al. How many rare diseases are there? Nat Rev Drug Discov. 2020; 19:77-78.
2. Guangming Daily. A series of policies benefit 20 million patients with rare diseases. *https://news.gmw.cn/2019-03/02/content_32590501.htm* (accessed November 30, 2020) (in Chinese).
3. He JJ, Kang Q, Hu JH, Song PP, Jin CL. China has officially released its first national list of rare diseases. Intractable Rare Dis Res. 2018; 7:145-147.
4. Xinhua News Agency. China Rare Disease Alliance established. *http://www.xinhuanet.com/politics/2018-10/26/c_1123619519.htm* (accessed December 2, 2020) (in Chinese).
5. National Health Commission of the People's Republic of China. Notice of the General Office of the National Health Commission on the establishment of a National Network for Collaboration in Rare Disease Diagnosis and Treatment. *http://www.nhc.gov.cn/yzygj/s7659/201902/3a8228589bf94e6d9356008763387cc4.shtml* (accessed December 2, 2020) (in Chinese).
6. National Health Commission of the People's Republic of China. Notice of the General Office of the National Health Commission on issuance of the Guidelines for the Diagnosis and Treatment of Rare Diseases (2019 edition). *http://www.nhc.gov.cn/yzygj/s7659/201902/61d06b4916c348e0810ce1fceb844333.shtml* (accessed December 2, 2020) (in Chinese).
7. National Health Commission of the People's Republic of China. Notice of the General Office of the National Health Commission on entry of information on the diagnosis and treatment of rare diseases. *http://www.nhc.gov.cn/yzygj/s7659/201910/be9343380e414adb8c8d641ae8967492.shtml* (accessed December 3, 2020) (in Chinese).
8. National Health Commission of the People's Republic of China. Notice of the General Office of the National Health Commission on the establishment of the Office of the National Network for Collaboration in Rare Disease Diagnosis and Treatment. *http://www.nhc.gov.cn/yzygj/s7659/202001/c07900d864b64c79aa3e5c2457e46f90.shtml* (accessed December 3, 2020) (in Chinese).
9. National Health Commission of the People's Republic of China. Notice of the General Office of the National Health Commission on publication and dissemination of the roster of the National Health Commission's second committee of experts on the diagnosis and treatment of rare diseases and welfare for patients. *http://www.nhc.gov.cn/cms-search/xxgk/getManuscriptXxgk.htm?id=c4cf28e6b54a4d248f0611b50dc023e7* (accessed December 3, 2020) (in Chinese).
10. The General Office of the State Council. The Opinions of the State Council on further reform of the review and approval system to encourage innovations in pharmaceuticals and medical devices. *http://www.gov.cn/xinwen/2017-10/08/content_5230105.htm* (accessed March 19, 2021) (in Chinese).
11. National Health Commission of the People's Republic of China. Opinions of the General Office of the State Council on reforming and improving policies to ensure the supply and govern the use of generic drugs. *http://www.nhc.gov.cn/wjw/gwywj/201804/ac9eb7a6c3594ec4b419fd7fcb76a9a6.shtml* (accessed December 8, 2020) (in Chinese).
12. National Medical Products Administration. Notice of the State Drug Administration on Issuance of the Guidelines for the Registration and Review of Medical Devices to Prevent and Treatment Rare Diseases (No. 101 of 2018). *https://www.nmpa.gov.cn/xxgk/ggtg/qtggtg/20181018162101924.html* (accessed January 10, 2021) (in Chinese).
13. Ministry of Finance of the People's Republic of China. Notice on the value-added tax policy regarding drugs to treat rare diseases. *http://szs.mof.gov.cn/zhengcefabu/201902/t20190222_3176415.htm* (accessed December 10, 2020) (in Chinese).
14. Xinhua News Agency. The Pharmaceutical Administration Law of the People's Republic of China. *http://m.xinhuanet.com/2019-08/26/c_1124924302.htm* (accessed December 11, 2020) (in Chinese).
15. Xinhua News Agency. Opinions of the Central Committee of the Communist Party of China and the State Council on promoting the passing down of, innovation in, and the development of Traditional Chinese Medicine. *http://www.gov.cn/zhengce/2019-10/26/content_5445336.htm* (accessed December 14, 2020) (in Chinese).
16. National Healthcare Security Administration. Interpretation of the drug list for national basic medical insurance, workmen's compensation, and maternity insurance. *http://www.nhsa.gov.cn/art/2019/8/22/art_38_1677.html* (accessed December 18, 2020) (in Chinese).
17. Xinhua News Agency. Seventy new drugs are included in the list of drugs covered by medical insurance, Many groundbreaking and innovative drugs that are domestically produced are listed. *http://www.gov.cn/xinwen/2019-11/28/content_5456718.htm* (accessed December 20, 2020). (in Chinese)
18. National Healthcare Security Administration. Opinions of the Central Committee of the Communist Party of China and the State Council on further reform of the medical insurance system. *http://www.nhsa.gov.cn/art/2020/3/5/art_14_2812.html* (accessed December 21, 2020) (in Chinese).
19. Guangming Daily. Starting January 1st next year, China will adjust import tariffs on some commodities and impose no tariffs on the second set of anticancer drugs and drugs to treat rare diseases. *https://news.gmw.cn/2020-12/25/content_34491886.htm* (accessed January 10, 2021) (in Chinese).
20. National Healthcare Security Administration. Policy Interpretation of the "Notice of the National Medical Insurance Administration and the Ministry of Human Resources and Social Security on publication and dissemination of the drug list for national basic medical insurance, workmen's compensation, and maternity insurance (2020 ed.)". *http://www.nhsa.gov.cn/art/2020/12/28/art_38_4219.html* (accessed January 10,

2021) (in Chinese).

21. The State Council of the People's Republic of China. Li Keqiang presided over an executive meeting of the State Council to implement a "Chinese New Year" period to enhance welfare and subsistence assistance for people impacted by the [COVID-19] pandemic. *http://www.gov. cn/premier/2021-01/15/content_5580263.htm* (accessed January 18, 2021) (in Chinese).

**Address correspondence to:*
Chunyang Li, Biomedical Big Data Center, West China Hospital, Sichuan University, No.37 Guo Xue Xiang, Chengdu 610041, Sichuan, China.
E-mail: lichunyang@wchscu.cn

Review

Immunopathogenic mechanisms of rheumatoid arthritis and the use of anti-inflammatory drugs

Ling Zhang[1,2,3]**, Yihang Zhang**[1,2,3]**, Jihong Pan**[1,2,3,*]

[1] Biomedical Sciences College, Shandong Medicinal Biotechnology Centre, Shandong First Medical University, Ji'nan, China;
[2] Key Lab for Biotech-Drugs of National Health Commission, Shandong First Medical University, Ji'nan, China;
[3] Key Lab for Rare & Uncommon Diseases of Shandong Province, Shandong First Medical University, Ji'nan, China.

SUMMARY   Rheumatoid arthritis (RA) is a chronic, progressive autoimmune disease characterized by synovitis and symmetrical joint destruction. RA has become one of the key diseases endangering human health, but its etiology is not clear. Therefore, identifying the immunopathogenic mechanisms of RA and developing therapeutic drugs to treat autoimmune diseases have always been difficult. This article mainly reviews the immunopathogenic mechanism of RA and advances in the study of anti-inflammatory drugs in order to provide a reference for the treatment of RA and drug development in the future.

Keywords   rheumatoid arthritis, immunopathogenesis, cytokines, inflammatory drugs

1. Introduction

Rheumatoid arthritis (RA) is a chronic, inflammatory, systemic autoimmune disease with an incidence of 5-10 cases per 1,000 people (*1,2*). Nonsuppurative joint and joint tissue inflammation is a main feature of RA, which mainly manifests as joint synovitis, resulting in damage to the cartilage, ligaments, tendons, and other joint tissues as well as multiple organ damage. The basic pathological changes in RA are synovitis, acute synovial swelling and exudation, chronic granulocyte infiltration, synovial hyperplasia and hypertrophy, and vasculitis. The latter is the pathological basis of joint injury, deformity, and obstruction and causes the disease to progress to the irreversible stage. The initial symptoms of RA are swelling and pain in the joints of the hands and feet, and especially the palms, toes, and proximal interphalangeal joints. Large joints, including the elbows, shoulders, ankles, and knees, can also be involved (*1*). In addition to joint symptoms, patients with RA often experience other symptoms such as fever, anemia, scleritis, pericarditis, vasculitis, and enlarged lymph nodes, and a variety of autoantibodies can be found in their serum. Without proper treatment, RA mainly affects the small joints of the limbs, such as the hands, feet, and wrists; symptoms are usually symmetrical and can be temporarily relieved. Without systematic treatment, however, RA can occur repeatedly for many years, eventually leading to joint deformities and loss of function.

Treatment of RA has two objectives: symptom relief and maintenance of function, and slowing the process of tissue injury. Currently, drugs used to treat RA are mainly divided into non-steroidal anti-inflammatory drugs (NSAIDs), disease-modifying anti-rheumatic drugs (DMARDs) and glucocorticoids (GCs). NSAIDs play an anti-inflammatory, antipyretic and analgesic role by inhibiting the activity of cyclooxygenase (COX), reducing the generation of prostaglandin (PG), and inhibiting the secretion of various cytokines. DMARDs can interfere with RA symptoms and signs, improve body function, and inhibit the progression of joint injury (*3*). Currently, IL-6R antibodies and JAK inhibitors are the most effective biological DMARDs (*4*). Although these drugs have a certain therapeutic effect, there are still some patients who fail to respond to the therapeutic drugs or who do not continue to respond (*5*). Therefore, there is an urgent need to develop drugs with new targets or new mechanisms to meet the clinical needs of these patients.

This review focuses on the current understanding of the immunopathogenic mechanisms of bone and cartilage damage caused by inflammatory disorders and progress in the use of anti-inflammatory drugs to treat patients with RA.

2. Immune mechanisms of RA

Cascade responses of innate and adaptive immunity are important mechanisms of the RA inflammatory process

(6). Many inflammatory cytokines and autoantibodies drive RA-associated inflammation and are maintained by epigenetic changes in fibroblast-like synovial cells, facilitating further inflammation *(7,8)*. During this process, many immune cells (neutrophils, granulocytes, macrophages, and B and T cells) invade the synovium and the synovial fluid. This invasion results in the release of many cytokines, chemokines, autoantibodies, and reactive oxidative species (ROS) in the synovial and joint spaces, leading to joint injury. The serological markers of the disease are the presence of high titers of rheumatoid factor (RF) and anti-citrullinated peptide antigens and antibodies (ACPAs) *(9,10)*. This complex pathogenic mechanism will be discussed in more detail below.

2.1. Immune cells

Synovial inflammation reflects subsequent immune activation, which is characterized by leukocyte invasion by innate immune cells (*e.g.*, monocytes, macrophages, dendritic cells, and neutrophils) and adaptive immune cells (*e.g.*, Th1, Th2, Th17 cells, B cells, and plasma cells) *(11,12)*.

2.1.1. T cells

T cells play an important role in the RA immune-mediated inflammatory response. In experimental models of collagen-induced RA, activated T cells aggregate in the inflamed joints as the disease progresses *(13,14)*. Naive CD4+T helper cells (Th) can differentiate into different cell lines (Th1, Th2, and Th17), characterized by the specific expression of transcription factors and proinflammatory cytokines in the system under antigen stimulation *(15,16)*.

In the past, the pathogenesis of RA was generally believed to involve the abnormal differentiation of CD4+T lymphocytes, which mainly manifested as a Th1/Th2 imbalance. As the pathogenesis of RA has been better understood and key transcription factors in the differentiation and development of different T cell subsets have been examined, Th17 and regulatory T cells (Tregs) have been found to play an important role in mediating the inflammatory response, articular cartilage and bone destruction, and bone erosion in RA *(17,18)*.

Th17 cells can secrete interleukin-17 (IL-17) as well as cytokines such as IL-21 and IL-22. IL-17 can aggravate the inflammatory response and it participates in many autoimmune diseases. IL-17 expression increased significantly in the serum and joint fluid of patients with RA, which promoted synovial cells to secrete a variety of inflammatory cells to make chondrocytes to synthesize matrix, enhance osteoclast activity, and cause bone erosion *(19)*. Tregs are a subgroup of CD4+ T cells with immunosuppressive

activity. Treg cells can inhibit T cells and antigen-presenting cells by releasing the cytokines IL-10 and TGF-β and by reducing the production of inflammatory cytokines and antibody secretion, thereby exhibiting an immunosuppressive effect. Th17 and Treg cells can transform each other under specific cytokine microenvironment conditions. CD4+T cells can differentiate into Treg cells when induced with TGF-β alone. When IL-6 is also present, it can induce RORγt expression, inhibit Treg cell production, and promote the differentiation of initial CD4+T cells into Th17 cells *(20)*. Therefore, the body's immune status can be regulated and the pathogenesis and progression of RA can be managed by controlling differing factors in the Th17 cell environment, inhibiting Th17 cell differentiation and proinflammatory cytokine expression, enhancing Treg activity, and regulating the balance of Th17 cells/Tregs in the body. This may provide a new therapeutic direction for prevention and control of RA.

2.1.2. B cells

In patients with RA, citrulline antigen-oriented B cells and B cells that react with citrulline antigens have significant effects *in vitro* *(21)*. This citrullinated antigen-directed B cell response contributes to the initiation and persistence of inflammatory processes. Thus, the ACPA response is the major humoral immune response associated with RA *(22)*. An abnormal dynamic between immune cells leads to abnormal aggregation of activated T cells, B cells, mast cells, neutrophils, macrophages, and cells entering APCs, which contribute to the cellular immune response in the course of RA *(23)*.

2.1.3. Macrophages

Macrophages are full-time antigen-presenting cells that activate T cells through their costimulatory molecules such as CD80/86 and CD40. Macrophages play an important role in many inflammatory responses, and their number is strongly associated with symptoms of RA and joint damage *(24)*. Macrophages abound in the synovium and cartilage pannus of inflamed joints. The increased number of macrophages in RA may be due to the lack of apoptosis. Macrophages in synovial fluid of patients with RA overexpress the FADD-like IL-1 invertase inhibitor protein (FLIP), which prevents tumor necrosis factor receptor FAS-mediated macrophage apoptosis. Moreover, macrophage activation, such as through overexpression of MHCII molecules, produces proinflammatory cytokines, chemokines, macrophage inflammatory protein-1 (MIP-1), monocyte chemoattractant protein-1 (MCP-1), matrix metalloproteinases (MMPs), and neopterin, which can exacerbate inflammatory responses *(25)*.

2.2. Factors related to RA

A variety of cytokines play important roles in the development and progression of RA. Cytokines such as interleukin-1 (IL-1), IL-6, IL-17, and tumor necrosis factor α (TNF-α) promote osteoclast production, whereas cytokines such as interferon-α (IFN-α), IFN-β, and IFN-γ antagonize this cell production, thereby regulating the bone balance and participating in bone and cartilage destruction and repair. In addition, cytokines can directly or indirectly regulate immune active cells or regulatory T cells and participate in regulation of the inflammatory response. A variety of cytokine-targeting biological agents has been developed to achieve disease relief in patients with RA.

2.2.1. Interleukins (IL)

IL-6 is produced by a variety of cells such as endothelial cells, fibroblasts, keratinocytes, chondrocytes, some tumor cells, and immune cells including monocytes, macrophages, T cells, and B cells. High levels of IL-6 are detected in the blood and synovial fluid of most patients with RA. IL-6 promotes the secretion of ROS and protease by neutrophils, increases inflammation, and causes joint injury (*26*). In addition, IL-6 stimulates osteoclast differentiation by activating RANKL-dependent or independent mechanisms (*27*). Hence, IL-6 may be related to osteochondral destruction and osteoporosis in patients with RA. A current RA therapy blocks IL-6 and IL-6R (*28,29*). Humanized anti-IL-6R antibodies can block the binding of IL-6 and IL-6R and affect the role of IL-6. Therefore, interfering with IL-6 activity is a treatment approach for RA (*30*).

IL-37 levels in plasma or peripheral blood mononuclear cells (PBMCs) in patients with RA are significantly higher than those in healthy controls and increase with increased disease activity (*31,32*). IL-37 levels in plasma of patients with RA are positively correlated with levels of TNF-α, IL-6, IL-17A, and C-reactive protein as well as the Disease Activity Score in 28 joints (DAS28) but are significantly reduced after DMARD treatment. Wang *et al.* (*33*) found higher levels of IL-37+CD4+ T cells, total IL-37+ lymphocytes, IL-18Rα+CD4+ cells, IL-18Rα+ CD4– cells, and total IL-18Rα + lymphocytes in the PBMCs of patients with RA than in those in the healthy control group. Patients with RA have higher IL-37 levels than healthy individuals, but *in vitro* and *in vivo* experiments indicated that IL-37 has anti-inflammatory action. When patients receive DMARD, their IL-37 level decreases, indicating that the increase in IL-37 expression in RA is a feedback increase, that is, a response that limits disease severity.

The cytokine IL-34 has recently been found to have multiple effects on the immune system. Although research is still in the preliminary stage, the IL-34 produced by epithelial cells is indispensable for the development of tissue macrophage-like cells (*34*). Interestingly, recent studies indicated that IL-34 is also expressed in synovial fibroblasts and the sublining and intimal lining of the synovium in patients with RA. IL-34 expression is also significantly correlated with synovitis severity (*35*). IL-34 levels in fibroblast-like synoviocytes (FLS), serum, and synovial fluid are significantly increased in patients with RA compared to healthy individuals and patients with osteoarthritis (OA) (*36-39*), and IL-34 levels are associated with total leukocytes in synovial fluid (*35*). In addition, serum IL-34 levels in patients with RA are positively correlated with rheumatoid factor and anti-cyclic citrullinated peptide antibody titers (*40*). Therefore, an abnormal level of IL-34 may be an effective marker of RA activity, and real-time fluorescence quantitative PCR may reveal a high level of IL-34 expression in osteoblasts. These studies have clearly indicated that IL-34 plays a role in the pathogenesis of RA.

2.2.2. TNF-α

Animal experiments (*41*) have demonstrated that TNF-α overexpression can cause severe arthritis in mice and that TNF-α suppression can prevent its development. Drugs that block TNF-α activity can alleviate the clinical symptoms of RA. In the affected joints of patients with RA, TNF-α promotes IL-6 production in synovial cells and co-induces vascular endothelial growth factor. TNF-α is encoded in the major histocompatibility complex (MHC). The presentation of peptides by the MHC is dictated by the TNF-α gene, which may be related to the therapeutic effect of blocking TNF-α.

2.2.3. Chemokines

Chemokines are inducible pro-inflammatory cytokines and are divided into four subgroups: CXC, CC, C, and CX3C (*42*). Chemokines and chemokine receptors play a key role in leukocyte migration into inflammatory tissues. Chemokines CCL5 and CCL15 belong to the CC subgroup. The increased specificity of CCL5 and CCL15 in RA may be related to the infiltration and aggregation of Th1 cells in inflamed joints. CXCL16 of the chemokine CXC subfamily increases in the synovial membrane and plays an important role in T cell aggregation and synovial inflammation. Therefore, CXCL16 may become a new target for RA therapy. IL-8 normal T cells in in the serum of patients with rheumatoid synovitis have significantly higher levels of regulatory activation chemokines (RANTES) and McP-1 than those in patients with other types of synovitis, and serum levels of IL-8 and RANTES are associated with rheumatic synovitis in different tissue types (*43*).

2.2.4. Interferon (IFN)

IFN-γ has a wide range of immunomodulatory actions that can activate NK cells, improve their killing ability, and induce the expression of macrophages, T cells, B cells and other cells, thus improving their ability to present antigens. The level of serum IFN-γ in patients with RA is reported to be significantly higher than that in healthy controls (*44*).

2.3. JAK/STAT signaling pathway

Four members (JAK1, JAK2, JAK3, and TYK2) of the JAK family and seven members (STAT 1-4, STAT 5A/B, and STAT 6) of the STAT family are found in mammals. They share a structurally and functionally common region, called the JAK homologous (JH) region (Figure 1). JAK/STAT proteins are ubiquitous, and different combinations of them respond to specific cytokine or growth factor signals, guaranteeing a high level of specificity with different roles *in vivo* (*45-47*). IL-6/JAK/STAT mechanisms of signaling cascades allow direct communication between transmembrane receptors and nuclei, which can be summarized in the following steps (Figure 2): IL-6 ligands bind IL-6r-Gp130

Figure 1. JH domains and JAK3 phosphorylation sites found in JAK/STAT proteins. FERM, four-point.1-ezrin-radaxin-moesin domain; JAK, Janus kinase; JH, JAK homology; kinase-like, pseudokinase domain; SH2, Src homology domain; Tyr kinase, tyrosine kinase domain.

receptor complexes and activate JAK tyrosine kinases recruited to their receptor intracellular regions. Once a JAK protein is activated, it undergoes dimerization, it phosphorylates tyrosines, and it activates its main substrate, the STAT protein. Tyrosine-phosphorylated STAT proteins homo- or hetero- dimerize and shift to the nucleus, where they interact with coactivators and bind to specific regulatory elements in the promoter regions of thousands of different target protein-coding genes, as well as micro-RNAs and long noncoding RNAs. STAT activity is regulated by phosphorylation, acetylation, and methylation, promoting STAT dimer stabilization, DNA binding, interaction with transcription costimulatory factors, and target cell expression (*48-50*). Negative regulators of JAK/STAT signaling provide further levels of control, guaranteeing cell feedback inhibition that can induce specific cytokine receptor signaling (*45,51,52*). Indeed, a soluble IL-6 receptor (SIL-6R), including its extracellular portion, can bind IL-6 and IL-6-SIL-6R complexes and activate gp130 homodimers in cells lacking membrane-bound IL-6R (*53,54*). Hence, JAK/STAT signaling cascades provide a significant direct and tuned translation of extracellular signals into transcriptional responses in many cells.

Levels of cytokines IL-6, IL-15, IFN, and granulocyte-macrophage colony stimulating factor (GM-CSF), which are involved in pathogenesis of synovial inflammation and joint destruction, increase significantly in patients with RA (*55*). These factors can activate JAK/STAT1 signaling pathways, IL-6, IL-15, IL-10, and IFN binding to JAK1, as well as platelet-derived factor (PDGF), EGF, GM-CSF, and IL-6 binding to JAK3. Using immunohistochemistry, Kasperkovitz *et al.* (*56*) verified that the total STAT1 protein level in the synovial tissue of patients with RA was significantly higher than that in patients with OA and was mainly expressed in T
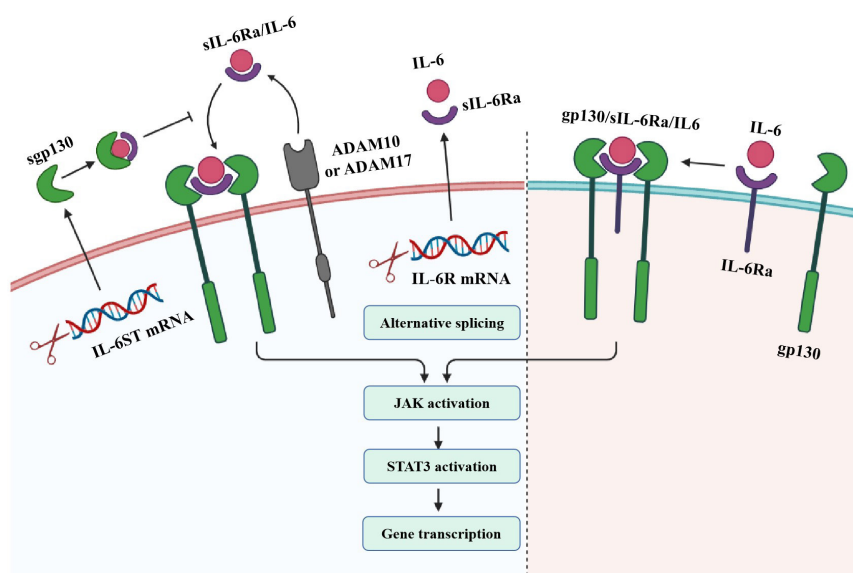

Figure 2. IL-6 signaling pathways (*58*).

cells and B cells at the site of inflammatory infiltration as well as in FLS in the intimal lining of the synovium. Activation of the STAT signaling pathway in the synovial membrane may be achieved by inducing STAT1 expression to promote synovial inflammation. However, Krause *et al.* (*57*) found that a STAT3 deficiency induces accelerated apoptosis of RA-FLS, suggesting an important role of STAT3 in RA-FLS. Thus, STAT may have dual regulatory effects on exacerbating symptoms and protecting joints in synovial inflammation associated with RA.

IL-6 binds to membrane-bound IL-6 receptors (IL-6R), inducing the formation of a heterodimer complex consisting of two molecules each of IL-6, IL-6R, and IL-6 receptor subunits (gp130). Formation of this complex leads to activation of the JAK/STAT3 signaling pathway, resulting in target gene transcription. Soluble IL-6R (SIL-6R) binds to IL-6 in the signaling pathway. SIL-6R can be produced by alternative splicing of IL6R mRNA or cleavage of disintegrin and metalloprotein-containing domain protein 170 (ADAM10) or cleavage of IL-6R by ADAM17. When IL-6 binds to SIL-6R, the complex is able to bind to gp130 and induce its dimerization, thereby activating downstream signaling pathways. While IL-6R is expressed in limited cell types, gp130 is widely expressed. IL-6 acts on cells with limited or missing IL-6R expression through SIL-6R transfer. IL-6 transduction signals can be negatively regulated by soluble gp130 (sgp130), which is produced by alternative splicing. Gp130 competes with the membrane binding of IL-6-SIL-6R complexes, thereby inhibiting IL-6 signal transduction but not classical IL-6 signaling pathways.

3. Immunotherapy and therapeutic drugs for RA

3.1. NSAIDs

NSAIDs are commonly used in autoimmune diseases such as RA and ankylosing spondylitis (AS) and can effectively reduce the clinical symptoms and signs of disease and eliminate local joint inflammation. However, such drugs can only treat the symptoms rather than the causes of disease and cannot control the activity or progression of the disease. Common adverse reactions to NSAIDs include central nervous system symptoms (pain, dizziness, tinnitus, *etc.*), cardiovascular damage (high blood pressure, edema, myocardial infarction, heart failure, *etc.*), gastrointestinal symptoms (abdominal pain, poor appetite, vomiting, ulcers, bleeding, *etc.*), changes in the hematopoietic system (thrombocytopenia), liver and kidney dysfunction, asthma, and skin eruptions. Following aspirin, many NSAIDs have been developed for clinical use (*59*).

3.2. Conventional DMARDs

Conventional DMARDs commonly used in clinical

practice include methotrexate (MTX), leflunomide (LEF), cyclophosphamide (CTX), azathioprine (AZA), cyclosporin A (CsA), mycophenolate mofetil (MMF), tacrolimus (FK506), and salazosulfapyridine (*60*). These drugs are widely used in autoimmune diseases, chronic kidney disease, transplant rejection, and tumors. Although the chemical structures and pharmacological mechanisms of the various conventional DMARDs differ, they work in a similar slow-acting manner, inhibiting the progression of RA after a few weeks or months and allowing the symptoms and signs of the disease to remain relatively stable for a long time. LEF mainly inhibits the activity of dihydroorotate dehydrogenase, it affects the synthesis of lymphocytic pyrimidine, and it alleviates the clinical symptoms and improves the laboratory markers of RA.

3.3. Glucocorticoids (GCs)

GCs are widely used in RA and can have potent anti-inflammatory and immunomodulatory actions, reduce the number of mononuclear macrophages in the circulatory system, reduce inflammatory factor and prostaglandin synthesis, and reduce Fc receptor expression (*61*). At the same time, GCs can prevent inflammatory cell exudation, reduce osteoclast formation, and reduce articular cartilage destruction. GCs have potent therapeutic action on immune cells, humoral factors, osteoblasts, and chondrocytes. GCs are divided into endogenous GCs and exogenous GCs. Endogenous GCs are a class of steroid hormones secreted by the adrenal cortex in the physiological state and include cortisone and hydrocortisone. Exogenous GCs such as dexamethasone and methylprednisolone are often used to treat RA.

3.4. Biological agents

Biological agents act as therapeutic agents by blocking key inflammatory cytokines or cell surface molecules, such as monoclonal antibodies targeting IL-1, IL-6, TNF-α, and IL-17, anti-CD20 monoclonal antibodies, B lymphocyte-stimulating factor (BAFF) inhibitors, T cell inhibitors, integrin monoclonal antibodies, and selective adhesion molecule inhibitors (*4*).

3.4.1. T cell inhibitors

Abatacept, a fusion protein consisting of the Fc region of IgG1 and the extracellular domain of CTLA4, is a selective T-cell co-stimulation inhibitor. Abatacept inhibits T cell activation by binding to CD80 and CD86 on antigen-presenting cells, thereby inhibiting the production of inflammatory factors such as TNF-α, IFN-γ, and IL-2. It can be used clinically to treat patients with moderate to severe active RA who have not sufficiently responded to one or more conventional DMARDs, as well as patients with juvenile idiopathic

arthritis (JIA). Abatacept can reduce serum LL-6, RF, C-reactive protein, MMP-3, and TNF- levels, delay the process of structural destruction of tissue, and reduce the symptoms and signs of RA.

3.4.2. Targeted B-cell therapy

In 2004, the first randomized, double-blind, placebo-controlled trial of rituximab in patients with long-term active RA noted significant results when rituximab was combined with MTX or CTX (*62*). In addition, a clinical study by the current authors examined the efficacy and safety of different doses of rituximab combined with MTX (with or without glucocorticoids) in patients with active RA who did not respond to conventional DMARDs; both low and high doses of rituximab were effective and well-tolerated (*63,64*).

Rituximab combined with MTX in one course of treatment can significantly slow the clinical progression of disease activity and alleviate radiation injury in patients with RA not sufficiently responding to anti-TNF-α therapy (*65*). An open-label prospective study further confirmed that rituximab is a therapeutic option for patients, and especially for seropositive patients (CCP- or RF-positive patients), with no response to single-dose TNF-α inhibitors (*66*).

3.4.3. IL-6 inhibitors

Tozumab is an anti-IL-6 receptor monoclonal antibody that can inhibit IL-6-mediated signaling by binding to IL-6 transmembrane receptors and inhibiting the production of autoantibodies such as rheumatoid factor (RF) and ACPA. It is mainly used to treat moderate and severe RA as well as JIA. With the success of TOCili-Zumab, multiple biological agents targeting the IL-6 signaling pathway are being developed for treatment of RA. The main adverse reactions to IL-6 inhibitors include an infusion reaction, infection, tumor risk, gastrointestinal ulcer, dyslipidemia, elevated liver transaminase, and neutropenia (*67*).

Tofacitinib is a novel oral Janus kinase (JAK) inhibitor mediated by JAK1, JAK3, STAT1, and STAT3 *via* the IL-6/GP130/STAT3 signaling pathway. Tofacitinib is effective in relieving arthritis symptoms in patients with RA, and both the Food and Drug Administration (FDA) and European Medicines Agency (EMA) have approved oral administration of tofacitinib for the treatment of RA (*27,68*). In addition, tofacitinib can down-regulate the production of pro-inflammatory cytokines IL-17 and IFN-r and the proliferation of CD4+T cells in patients with RA (*69,70*).

Global data have indicated that patients with RA with an inadequate or poorly tolerated response to anti-TNF-α inhibitors can usually be effectively managed by switching to drugs with new mechanisms of action, such as IL-6R inhibitors (*71*). IL-6 blockade of signaling pathways (*via* tocilizumab, which is a monoclonal antibody that binds to IL-6 receptors) can enhance Tregs and inhibit monocyte IL-6 mRNA expression, thereby inducing monocyte apoptosis (*72-74*). Samalizumab, a monoclonal antibody against IL-6R in humans, was effective and safe in patients with RA with a limited response to MTX in randomized clinical trials (*75,76*). Other IL-6 inhibitors are shown in Table 1.

3.4.4. Anti-IL-12/23 monoclonal antibody

TGF-β, IL-23, and pro-inflammatory cytokines play a role in driving and regulating the human Th17 response in RA (*77,78*). In addition, an increased Th17 cell count and poor clinical outcomes in patients with RA are associated with IL4R gene variation (*79*). Therefore, IL-12 and IL-23 participate in the pathogenesis of RA and may be considered potential molecules for immune targeting of RA. Currently, the most widely used anti-IL-12/23 antibody is ustekinumab, which was approved by the US FDA for the treatment of psoriasis in 2009 and which has clinical efficacy significantly superior to that of other biological agents (*80*). Other anti-IL-12/23

Table 1. Biological agents targeting cytokines

Cytokine	Drug	Mechanism of action	Phase
IL-6	Tocilizumab Sarilumab Clazakizumab ALX-0061	Inhibit IL-6-mediated signaling involving ubiquitous signal-transducing gp130 and STAT3	Appeared on the market in 2010 Phase III Phase II B Phase II
IL-1	Anakinra	Blocks IL-1 binding to IL-1RI, resulting in intracellular signaling	Appeared on the market in 2001
IL-12/23	Ustekinumab Canakinumab	Bind to the cytokines IL-12 and IL-23 and down-modulate lymphocyte function	Appeared on the market in 2005 Appeared on the market in 2009
TNF-α	Infliximab Adalimumab Etanercept Golimumab Certolizumab	Induce antibody-dependent cytotoxicity (ADCC); the complement pathway triggers cell-dependent cytotoxicity (CDC) and targets immune cell apoptosis	Appeared on the market in 1998 Appeared on the market in 2002 Appeared on the market in 1998 Appeared on the market in 2009 Appeared on the market in 2008

monoclonal antibodies are shown in Table 1.

3.4.5. TNF-α inhibitors

The strategy of blocking TNF-α was introduced into clinical practice at the end of the last century and revolutionized the treatment of RA and many other inflammatory conditions. Steeland *et al.* recently conducted an impressive review of the successful use of tumor necrosis factor inhibitors including etanercept, infliximab, adamab, cetuximab, and golimumab in RA therapy (*81*). Infliximab, adalimumab, and golimumab are full-length monoclonal antibodies. In addition to blocking the growth of tumor cells, they act as Fc effectors. They induce antibody-dependent cellular cytotoxicity (ADCC), trigger complement pathways that lead to cell-dependent cytotoxicity (CDC), and target immune cell apoptosis. Etanercept is a soluble TNF receptor that contains truncated Fc domains and that does not contain IgG1 CH1 domains; therefore, etanercept induces less potent ADCC and CDC than monoclonal antibodies such as infliximab (*82*).

The total number of B cells in the blood of patients with RA is lower than that in healthy controls but it is significantly higher (normal) in patients receiving antitumor necrosis factor therapy. Cardiovascular disease, including heart failure and infection, is the leading cause of disability and death in patients with RA (*83*). Patients treated with anti-TNF or MTX alone appear to have a further risk of severe infection, such as tuberculosis (*84,85*). Therefore, anti-TNF-α inhibitory therapy is contraindicated in all patients with heart failure, which represents a considerable proportion of patients with RA (*86*). Despite the risks associated with anti-TNF-α therapy, it is the treatment of choice for patients with RA when MTX does not provide relief. Other TNF-α inhibitors are shown in Table 1.

3.5. Small molecule inhibitors targeting JAK

3.5.1. Decernotinib

Decernotinib is a next-generation jakinib, and kinase assays revealed its 5-fold selectivity for JAK3 compared to JAK1, JAK2, and TYK2 (*87*). Decernotinib yielded satisfactory results in animal models of autoimmune diseases (*88*) and thus entered clinical trials for treatment of RA.

Decernotinib appears to offer promise in the treatment of RA. Phase II trials indicated that a 50-150 mg dose of decernotinib BID improved the American College of Rheumatology (ACR) response criteria and DAS28 joint count for RA with CRP (DAS28-CRP) compared to a placebo. Adverse events reported were similar to those caused by first-generation jakinibs, such as infection, rhinitis, and hyperlipidemia (*89-91*). Anemia was not observed, which is consistent with decernotinib's selectivity for JAK3 over JAK2. Surprisingly, many patients developed neutropenia, which indicates that the drug may have some off-target effects (*87*). Recent phase IIb studies have indicated that decernotinib with conventional DMARDs can alleviate synovitis and osteitis in patients with RA (*92*).

3.5.2. Filgotinib (GLPG0634)

Filgotinib inhibits JAK1 and JAK2 in CBC and kinase assays, but is 30-fold more selective for JAK1 (*89*). *In vitro* studies also demonstrated its dose-dependent inhibition of Th1, Th2 and, to a lesser extent, Th17 cell differentiation.

Filgotinib is currently being studied as a potential treatment for RA (*93*). A phase IIa study indicated that filgotinib was more effective than the placebo at a daily dose of 30 mg or higher (*89,94*). This was followed by two phase IIb trials: Darwin 1 and Darwin 2. Darwin 1 was a study of 595 patients with RA receiving MTX who were also given filgotinib in a dose ranging from 50 to 100 mg per day. The Darwin 2 study evaluated filgotinib monotherapy in 280 patients with RA at doses ranging from 50 to 200 mg per day (*89*). In both studies, filgotinib outperformed the placebo in controlling disease activity according to the ACR 20/50

Table 2. Small molecule inhibitors targeting JAK

JAK inhibitor	Molecular target	Mechanism of action	Phase
Tofacitinib	JAK1, JAK3	Interferes with the binding of IL-6 to the IL-6Rα/gp130 complex, STAT proteins	Appeared on the market in 2017
Baricitinib	JAK1, JAK2	Blocks intracellular signaling, facilitates the turnover of active (phosphorylated) STAT1 and STAT3	Appeared on the market in 2018
Filgotinib	JAK1	Blocks intracellular signaling, facilitates the turnover of active (phosphorylated) STAT1	Phase III
Peficitinib	JAK1, JAK3	Interferes with the binding of IL-6 to the IL-6Rα/gp130 complex, STAT proteins	Phase III
SHR0302	JAK1	Blocks intracellular signal transduction, facilitates the turnover of active (phosphorylated) STAT1	Phase II

criteria, DAS28-CRP, the Simplified Disease Activity Index (SDAI), and the Clinical Disease Activity Index (*95,96*). Other small molecule inhibitors targeting JAK are shown in Table 2.

4. Summary and prospects for the future

NSAIDs, GCs, conventional DMARDs, biological agents, and other drugs for treatment of RA have definite efficacy but are associated with adverse reactions such as immunosuppression, infection, and the development of new tumors. Therefore, development of anti-inflammatory immunomodulatory drugs for soft regulation of inflammatory immune responses (SRIIR) is important. SRIIR drugs selectively control physiological tissue and cell function and promote recovery from pathological gene and protein changes. Their mechanism may involve one or more key signaling molecules regulating abnormal signaling pathway activity, thus appropriately restoring the static balance of the human body. When SRIIR drugs are used clinically, they can reduce adverse reactions without diminishing physiological function. Paeoniflorin - 6-oxybenzenesulfonic acid ester (code name CP-25) comes from the structural modification of paeoniflorin, an active ingredient of an herbal medicine (*97*). Cp-25 can suppress inflammation associated with adjuvant arthritis in rats and collagen-induced arthritis in mice by down-regulating inflammatory mediator production and the immune response, reducing bone damage (*98,99*). *In vitro*, CP-25 can inhibit TNF-α or PGE2 stimulation of mature dendritic cells by regulating the expression of CD40, CD80, CD83, CD86, and MHC- II. Cp-25 can down-regulate BAFF-stimulated proliferation of B cells, including CD19+ B cells, CD19+ CD20+ B cells, CD19+ CD27+ B cells, and CD19+CD20+CD27+ B cells, and inhibit the expression of BAFFR, TRAF2, and P52. Compared to etanercept and rituximab, CP-25 moderately down-regulates the abnormal rise in B-cell proliferation.

In conclusion, further understanding of the pathological mechanism of autoimmune diseases and the discovery of new drug targets has led to the rapid development of new biological agents targeting cytokines and cell surface molecules in addition to NSAIDs, SAIDs and conventional DMARDs. Biological agents such as monoclonal antibodies targeting IL-1, IL-6, TNF-α, IL-17, and CD20, BAFF inhibitors, T cell inhibitors, integrin monoclonal antibodies, and selective adhesion molecular inhibitors exhibit therapeutic action by blocking inflammatory cytokines or cell surface molecules.

Several small molecule drugs targeting the JAK/ STAT signaling pathway such as tofacitinib, baricitinib, upadacitinib, and filgotinib (see Table 2) have also been developed and used in clinical practice in recent years. Although these drugs are effective, they also cause adverse reactions such as gastrointestinal symptoms, immunosuppression, myelosuppression, and infection. The focus now is on developing an SRIIR with anti-inflammatory immunomodulatory action. Cp-25 may be a new SRIIR with the potential to treat autoimmune diseases. SRIIRs, which control excessive activation of inflammatory immune response-related cells without harming their physiological function, are a new therapeutic strategy and a major direction for development of drugs to treat autoimmune diseases.

Conflict of Interest: The authors have no conflicts of interest to disclose.

References

1. Wasserman AM. Diagnosis and management of rheumatoid arthritis. Am Fam Physician. 2011; 84:1245-1252.
2. Silman AJ, Pearson JE. Epidemiology and genetics of rheumatoid arthritis. Arthritis Res. 2002; 4 Suppl 3:S265-272.
3. Smolen JS, van der Heijde D, Machold KP, Aletaha D, Landewe R. Proposal for a new nomenclature of disease-modifying antirheumatic drugs. Ann Rheum Dis. 2014; 73:3-5.
4. Smolen JS, Landewe R, Bijlsma J, *et al.* EULAR recommendations for the management of rheumatoid arthritis with synthetic and biological disease-modifying antirheumatic drugs: 2016 update. Ann Rheum Dis. 2017; 76:960-977.
5. Chandrupatla D, Molthoff CFM, Lammertsma AA, van der Laken CJ, Jansen G. The folate receptor beta as a macrophage-mediated imaging and therapeutic target in rheumatoid arthritis. Drug Deliv Transl Res. 2019; 9:366-378.
6. Holmdahl R, Malmstrom V, Burkhardt H. Autoimmune priming, tissue attack and chronic inflammation - The three stages of rheumatoid arthritis. Eur J Immunol. 2014; 44:1593-1599.
7. Harre U, Schett G. Cellular and molecular pathways of structural damage in rheumatoid arthritis. Semin Immunopathol. 2017; 39:355-363.
8. Mateen S, Zafar A, Moin S, Khan A Q, Zubair S. Understanding the role of cytokines in the pathogenesis of rheumatoid arthritis. Clin Chim Acta. 2016; 455:161-171.
9. Cohen E, Nisonoff A, Hermes P, Norcross BM, Lockie LM. Agglutination of sensitized alligator erythrocytes by rheumatoid factor(s). Nature. 1961; 190:552-553.
10. Scherer HU, Huizinga TWJ, Kronke G, Schett G, Toes REM. The B cell response to citrullinated antigens in the development of rheumatoid arthritis. Nat Rev Rheumatol. 2018; 14:157-169.
11. Cuda CM, Pope RM, Perlman H. The inflammatory role of phagocyte apoptotic pathways in rheumatic diseases. Nat Rev Rheumatol. 2016; 12:543-558.
12. Bazzazi H, Aghaei M, Memarian A, Asgarian-Omran H, Behnampour N, Yazdani Y. Th1-Th17 ratio as a new insight in rheumatoid arthritis disease. Iran J Allergy Asthma Immunol. 2018; 17:68-77.

13. Jung SM, Lee J, Baek SY, Lee J, Jang SG, Hong SM, Park JS, Cho ML, Park SH, Kwok SK. Fraxinellone attenuates rheumatoid inflammation in mice. Int J Mol Sci. 2018; 19.

14. Myers LK, Stuart JM, Kang AH. A CD4 cell is capable of transferring suppression of collagen-induced arthritis. J Immunol. 1989; 143:3976-3980.

15. Chiocchia G, Boissier M C, Ronziere M C, Herbage D, Fournier C. T cell regulation of collagen-induced arthritis in mice. I. Isolation of Type II collagen-reactive T cell hybridomas with specific cytotoxic function. J Immunol. 1990; 145:519-525.

16. Sakaguchi S, Benham H, Cope A P, Thomas R. T-cell receptor signaling and the pathogenesis of autoimmune arthritis: Insights from mouse and man. Immunol Cell Biol. 2012; 90:277-287.

17. Mai J, Wang H, Yang X F. Th 17 cells interplay with Foxp3+ Tregs in regulation of inflammation and autoimmunity. Front Biosci (Landmark Ed). 2010; 15:986-1006.

18. Kelchtermans H, Geboes L, Mitera T, Huskens D, Leclercq G, Matthys P. Activated CD4+CD25+ regulatory T cells inhibit osteoclastogenesis and collagen-induced arthritis. Ann Rheum Dis. 2009; 68:744-750.

19. Zizzo G, De Santis M, Bosello S L, Fedele A L, Peluso G, Gremese E, Tolusso B, Ferraccioli G. Synovial fluid-derived T helper 17 cells correlate with inflammatory activity in arthritis, irrespectively of diagnosis. Clin Immunol. 2011; 138:107-116.

20. Lina C, Conghua W, Nan L, Ping Z. Combined treatment of etanercept and MTX reverses Th1/Th2, Th17/Treg imbalance in patients with rheumatoid arthritis. J Clin Immunol. 2011; 31:596-605.

21. Kerkman P F, Rombouts Y, van der Voort E I, Trouw L A, Huizinga T W, Toes R E, Scherer H U. Circulating plasmablasts/plasmacells as a source of anticitrullinated protein antibodies in patients with rheumatoid arthritis. Ann Rheum Dis. 2013; 72:1259-1263.

22. Pelzek AJ, Gronwall C, Rosenthal P, Greenberg JD, McGeachy M, Moreland L, Rigby WFC, Silverman GJ. Persistence of disease-associated anti-citrullinated protein antibody-expressing memory B cells in rheumatoid arthritis in clinical remission. Arthritis Rheumatol. 2017; 69:1176-1186.

23. Malemud C J. The role of the JAK/STAT signal pathway in rheumatoid arthritis. Ther Adv Musculoskelet Dis. 2018; 10:117-127.

24. Araki Y, Mimura T. The mechanisms underlying chronic inflammation in rheumatoid arthritis from the perspective of the epigenetic landscape. J Immunol Res. 2016; 2016:6290682.

25. Weyand CM, Zeisbrich M, Goronzy JJ. Metabolic signatures of T-cells and macrophages in rheumatoid arthritis. Curr Opin Immunol. 2017; 46:112-120.

26. Narazaki M, Tanaka T, Kishimoto T. The role and therapeutic targeting of IL-6 in rheumatoid arthritis. Expert Rev Clin Immunol. 2017; 13:535-551.

27. Tournadre A, Pereira B, Dutheil F, Giraud C, Courteix D, Sapin V, Frayssac T, Mathieu S, Malochet-Guinamand S, Soubrier M. Changes in body composition and metabolic profile during interleukin 6 inhibition in rheumatoid arthritis. J Cachexia Sarcopenia Muscle. 2017; 8:639-646.

28. Kishimoto T, Kang S, Tanaka T. IL-6: A new era for the treatment of autoimmune inflammatory diseases. In: Innovative Medicine: Basic Research and Development. Edited by Nakao K, Minato N, Uemoto S. Tokyo; 2015:

131-147.

29. Venuturupalli S. Immune mechanisms and novel targets in rheumatoid arthritis. Immunol Allergy Clin North Am. 2017; 37:301-313.

30. Rose-John S. Interleukin-6 family cytokines. Cold Spring Harb Perspect Biol. 2018; 10.

31. Xu W D, Zhao Y, Liu Y. Insights into IL-37, the role in autoimmune diseases. Autoimmun Rev. 2015; 14:1170-1175.

32. Zhao P W, Jiang W G, Wang L, Jiang Z Y, Shan Y X, Jiang Y F. Plasma levels of IL-37 and correlation with TNF-alpha, IL-17A, and disease activity during DMARD treatment of rheumatoid arthritis. PLoS One. 2014; 9:e95346.

33. Wang L, Wang Y, Xia L, Shen H, Lu J. Elevated frequency of IL-37- and IL-18Ralpha-positive T cells in the peripheral blood of rheumatoid arthritis patients. Cytokine. 2018; 110:291-297.

34. Jin S, Sonobe Y, Kawanokuchi J, Horiuchi H, Cheng Y, Wang Y, Mizuno T, Takeuchi H, Suzumura A. Interleukin-34 restores blood-brain barrier integrity by upregulating tight junction proteins in endothelial cells. PLoS One. 2014; 9:e115981.

35. Chemel M, Le Goff B, Brion R, Cozic C, Berreur M, Amiaud J, Bougras G, Touchais S, Blanchard F, Heymann M F, Berthelot J M, Verrecchia F, Heymann D. Interleukin 34 expression is associated with synovitis severity in rheumatoid arthritis patients. Ann Rheum Dis. 2012; 71:150-154.

36. Garcia S, Hartkamp L M, Malvar-Fernandez B, van Es I E, Lin H, Wong J, Long L, Zanghi J A, Rankin A L, Masteller E L, Wong B R, Radstake T R, Tak P P, Reedquist K A. Colony-stimulating factor (CSF) 1 receptor blockade reduces inflammation in human and murine models of rheumatoid arthritis. Arthritis Res Ther. 2016; 18:75.

37. Tian Y, Shen H, Xia L, Lu J. Elevated serum and synovial fluid levels of interleukin-34 in rheumatoid arthritis: possible association with disease progression *via* interleukin-17 production. J Interferon Cytokine Res. 2013; 33:398-401.

38. Hwang SJ, Choi B, Kang SS, Chang JH, Kim YG, Chung YH, Sohn DH, So MW, Lee CK, Robinson WH, Chang EJ. Interleukin-34 produced by human fibroblast-like synovial cells in rheumatoid arthritis supports osteoclastogenesis. Arthritis Res Ther. 2012; 14:R14.

39. Chang SH, Choi BY, Choi J, Yoo JJ, Ha YJ, Cho HJ, Kang EH, Song YW, Lee YJ. Baseline serum interleukin-34 levels independently predict radiographic progression in patients with rheumatoid arthritis. Rheumatol Int. 2015; 35:71-79.

40. Moon SJ, Hong YS, Ju JH, Kwok SK, Park SH, Min JK. Increased levels of interleukin 34 in serum and synovial fluid are associated with rheumatoid factor and anticyclic citrullinated peptide antibody titers in patients with rheumatoid arthritis. J Rheumatol. 2013; 40:1842-1849.

41. Llanos C, Soto L, Sabugo F, Bastias MJ, Salazar L, Aguillon JC, Cuchacovich M. The influence of -238 and -308 TNF alpha polymorphisms on the pathogenesis and response to treatment in rheumatoid arthritis. Rev Med Chil. 2005; 133:1089-1095.

42. Haringman JJ, Smeets TJ, Reinders-Blankert P, Tak PP. Chemokine and chemokine receptor expression in paired peripheral blood mononuclear cells and synovial tissue of patients with rheumatoid arthritis, osteoarthritis, and reactive arthritis. Ann Rheum Dis. 2006; 65:294-300.

43. Klimiuk PA, Sierakowski S, Latosiewicz R, Skowronski J, Cylwik JP, Cylwik B, Chwiecko J. Histological patterns of synovitis and serum chemokines in patients with rheumatoid arthritis. J Rheumatol. 2005; 32:1666-1672.

44. Canete JD, Martinez SE, Farres J, Sanmarti R, Blay M, Gomez A, Salvador G, Munoz-Gomez J. Differential Th1/Th2 cytokine patterns in chronic arthritis: Interferon gamma is highly expressed in synovium of rheumatoid arthritis compared with seronegative spondyloarthropathies. Ann Rheum Dis. 2000; 59:263-268.

45. Aaronson DS, Horvath CM. A road map for those who don't know JAK-STAT. Science. 2002; 296:1653-1655.

46. Kisseleva T, Bhattacharya S, Braunstein J, Schindler CW. Signaling through the JAK/STAT pathway, recent advances and future challenges. Gene. 2002; 285:1-24.

47. Yan Z, Gibson SA, Buckley JA, Qin H, Benveniste EN. Role of the JAK/STAT signaling pathway in regulation of innate immunity in neuroinflammatory diseases. Clin Immunol. 2018; 189:4-13.

48. Zhuang S. Regulation of STAT signaling by acetylation. Cell Signal. 2013; 25:1924-1931.

49. Yu H, Lee H, Herrmann A, Buettner R, Jove R. Revisiting STAT3 signalling in cancer: New and unexpected biological functions. Nat Rev Cancer. 2014; 14:736-746.

50. Zimmers TA, Fishel ML, Bonetto A. STAT3 in the systemic inflammation of cancer cachexia. Semin Cell Dev Biol. 2016; 54:28-41.

51. Yoshimura A, Ito M, Chikuma S, Akanuma T, Nakatsukasa H. Negative regulation of cytokine signaling in immunity. Cold Spring Harb Perspect Biol. 2018; 10.

52. Linossi EM, Babon JJ, Hilton DJ, Nicholson SE. Suppression of cytokine signaling: The SOCS perspective. Cytokine Growth Factor Rev. 2013; 24:241-248.

53. Kallen KJ. The role of transsignalling *via* the agonistic soluble IL-6 receptor in human diseases. Biochim Biophys Acta. 2002; 1592:323-343.

54. Scheller J, Ohnesorge N, Rose-John S. Interleukin-6 trans-signalling in chronic inflammation and cancer. Scand J Immunol. 2006; 63:321-329.

55. Walker JG, Smith MD. The Jak-STAT pathway in rheumatoid arthritis. J Rheumatol. 2005; 32:1650-1653.

56. Kasperkovitz PV, Verbeet NL, Smeets TJ, van Rietschoten JG, Kraan MC, van der Pouw Kraan TC, Tak PP, Verweij CL. Activation of the STAT1 pathway in rheumatoid arthritis. Ann Rheum Dis. 2004; 63:233-239.

57. Krause A, Scaletta N, Ji JD, Ivashkiv LB. Rheumatoid arthritis synoviocyte survival is dependent on Stat3. J Immunol. 2002; 169:6610-6616.

58. Johnson DE, O'Keefe RA, Grandis JR. Targeting the IL-6/JAK/STAT3 signalling axis in cancer. Nat Rev Clin Oncol. 2018; 15:234-248.

59. Bermas B L. Non-steroidal anti inflammatory drugs, glucocorticoids and disease modifying anti-rheumatic drugs for the management of rheumatoid arthritis before and during pregnancy. Curr Opin Rheumatol. 2014; 26:334-340.

60. Combe B, Landewe R, Daien C I, *et al.* 2016 update of the EULAR recommendations for the management of early arthritis. Ann Rheum Dis. 2017; 76:948-959.

61. Strehl C, Buttgereit F. Optimized glucocorticoid therapy: Teaching old drugs new tricks. Mol Cell Endocrinol. 2013; 380:32-40.

62. Edwards JC, Szczepanski L, Szechinski J, Filipowicz-Sosnowska A, Emery P, Close DR, Stevens RM, Shaw T. Efficacy of B-cell-targeted therapy with rituximab in patients with rheumatoid arthritis. N Engl J Med. 2004; 350:2572-2581.

63. Schioppo T, Ingegnoli F. Current perspective on rituximab in rheumatic diseases. Drug Des Devel Ther. 2017; 11:2891-2904.

64. Emery P, Fleischmann R, Filipowicz-Sosnowska A, Schechtman J, Szczepanski L, Kavanaugh A, Racewicz AJ, van Vollenhoven RF, Li NF, Agarwal S, Hessey EW, Shaw TM, Group DS. The efficacy and safety of rituximab in patients with active rheumatoid arthritis despite methotrexate treatment: Results of a phase IIB randomized, double-blind, placebo-controlled, dose-ranging trial. Arthritis Rheum. 2006; 54:1390-1400.

65. Mease PJ, Cohen S, Gaylis NB, Chubick A, Kaell AT, Greenwald M, Agarwal S, Yin M, Kelman A. Efficacy and safety of retreatment in patients with rheumatoid arthritis with previous inadequate response to tumor necrosis factor inhibitors: Results from the SUNRISE trial. J Rheumatol. 2010; 37:917-927.

66. Emery P, Gottenberg J E, Rubbert-Roth A, *et al.* Rituximab versus an alternative TNF inhibitor in patients with rheumatoid arthritis who failed to respond to a single previous TNF inhibitor: SWITCH-RA, a global, observational, comparative effectiveness study. Ann Rheum Dis. 2015; 74:979-984.

67. Rubbert-Roth A, Furst DE, Nebesky JM, Jin A, Berber E. A review of recent advances using tocilizumab in the treatment of rheumatic diseases. Rheumatol Ther. 2018; 5:21-42.

68. Traynor K. FDA approves tofacitinib for rheumatoid arthritis. Am J Health Syst Pharm. 2012; 69:2120.

69. Gertel S, Mahagna H, Karmon G, Watad A, Amital H. Tofacitinib attenuates arthritis manifestations and reduces the pathogenic CD4 T cells in adjuvant arthritis rats. Clin Immunol. 2017; 184:77-81.

70. Cheung TT, McInnes IB. Future therapeutic targets in rheumatoid arthritis? Semin Immunopathol. 2017; 39:487-500.

71. Chastek B, Becker LK, Chen CI, Mahajan P, Curtis JR. Outcomes of tumor necrosis factor inhibitor cycling versus switching to a disease-modifying anti-rheumatic drug with a new mechanism of action among patients with rheumatoid arthritis. J Med Econ. 2017; 20:464-473.

72. Samson M, Audia S, Janikashvili N, Ciudad M, Trad M, Fraszczak J, Ornetti P, Maillefert JF, Miossec P, Bonnotte B. Brief report: Inhibition of interleukin-6 function corrects Th17/Treg cell imbalance in patients with rheumatoid arthritis. Arthritis Rheum. 2012; 64:2499-2503.

73. Pesce B, Soto L, Sabugo F, Wurmann P, Cuchacovich M, Lopez MN, Sotelo PH, Molina MC, Aguillon JC, Catalan D. Effect of interleukin-6 receptor blockade on the balance between regulatory T cells and T helper type 17 cells in rheumatoid arthritis patients. Clin Exp Immunol. 2013; 171:237-242.

74. Sarantopoulos A, Tselios K, Gkougkourelas I, Pantoura M, Georgiadou AM, Boura P. Tocilizumab treatment leads to a rapid and sustained increase in Treg cell levels in rheumatoid arthritis patients: Comment on the article by Thiolat *et al.* Arthritis Rheumatol. 2014; 66:2638.

75. Tono T, Aihara S, Hoshiyama T, Arinuma Y, Nagai T, Hirohata S. Effects of anti-IL-6 receptor antibody on human monocytes. Mod Rheumatol. 2015; 25:79-84.

76. Huizinga T W, Fleischmann R M, Jasson M, Radin A R, van Adelsberg J, Fiore S, Huang X, Yancopoulos G

D, Stahl N, Genovese M C. Sarilumab, a fully human monoclonal antibody against IL-6Ralpha in patients with rheumatoid arthritis and an inadequate response to methotrexate: Efficacy and safety results from the randomised SARIL-RA-MOBILITY Part A trial. Ann Rheum Dis. 2014; 73:1626-1634.

77. Genovese MC, Fleischmann R, Kivitz AJ, *et al.* Sarilumab plus methotrexate in patients with active rheumatoid arthritis and inadequate response to methotrexate: Results of a phase III study. Arthritis Rheumatol. 2015; 67:1424-1437.

78. Volpe E, Servant N, Zollinger R, Bogiatzi SI, Hupe P, Barillot E, Soumelis V. A critical function for transforming growth factor-beta, interleukin 23 and proinflammatory cytokines in driving and modulating human T(H)-17 responses. Nat Immunol. 2008; 9:650-657.

79. Kirkham BW, Kavanaugh A, Reich K. Interleukin-17A: A unique pathway in immune-mediated diseases: Psoriasis, psoriatic arthritis and rheumatoid arthritis. Immunology. 2014; 141:133-142.

80. Leipe J, Schramm MA, Prots I, Schulze-Koops H, Skapenko A. Increased Th17 cell frequency and poor clinical outcome in rheumatoid arthritis are associated with a genetic variant in the IL4R gene, rs1805010. Arthritis Rheumatol. 2014; 66:1165-1175.

81. Molinelli E, Campanati A, Brisigotti V, Offidani A. Biologic therapy in psoriasis (part II): Efficacy and safety of new treatment targeting IL23/IL-17 pathways. Curr Pharm Biotechnol. 2017; 18:964-978.

82. Steeland S, Libert C, Vandenbroucke RE. A new venue of TNF targeting. Int J Mol Sci. 2018; 19.

83. Billmeier U, Dieterich W, Neurath MF, Atreya R. Molecular mechanism of action of anti-tumor necrosis factor antibodies in inflammatory bowel diseases. World J Gastroenterol. 2016; 22:9300-9313.

84. Levy L, Fautrel B, Barnetche T, Schaeverbeke T. Incidence and risk of fatal myocardial infarction and stroke events in rheumatoid arthritis patients. A systematic review of the literature. Clin Exp Rheumatol. 2008; 26:673-679.

85. Pala O, Diaz A, Blomberg BB, Frasca D. B lymphocytes in rheumatoid arthritis and the effects of anti-TNF-alpha agents on B lymphocytes: A review of the literature. Clin Ther. 2018; 40:1034-1045.

86. Kroesen S, Widmer A F, Tyndall A, Hasler P. Serious bacterial infections in patients with rheumatoid arthritis under anti-TNF-alpha therapy. Rheumatology (Oxford). 2003; 42:617-621.

87. Kotyla P J. Bimodal function of anti-TNF treatment: Shall we be concerned about anti-TNF treatment in patients with rheumatoid arthritis and heart failure? Int J Mol Sci. 2018; 19.

88. Mahajan S, Hogan JK, Shlyakhter D, Oh L, Salituro FG, Farmer L, Hoock TC. VX-509 (decernotinib) is a potent and selective janus kinase 3 inhibitor that attenuates inflammation in animal models of autoimmune disease. J Pharmacol Exp Ther. 2015; 353:405-414.

89. Norman P. Selective JAK inhibitors in development for rheumatoid arthritis. Expert Opin Investig Drugs. 2014; 23:1067-1077.

90. Genovese MC, van Vollenhoven RF, Pacheco-Tena C, Zhang Y, Kinnman N. VX-509 (Decernotinib), an oral selective JAK-3 inhibitor, in combination with methotrexate in patients with rheumatoid arthritis. Arthritis

Rheumatol. 2016; 68:46-55.

91. Fleischmann RM, Damjanov NS, Kivitz AJ, Legedza A, Hoock T, Kinnman N. A randomized, double-blind, placebo-controlled, twelve-week, dose-ranging study of decernotinib, an oral selective JAK-3 inhibitor, as monotherapy in patients with active rheumatoid arthritis. Arthritis Rheumatol. 2015; 67:334-343.

92. Genovese MC, Yang F, Ostergaard M, Kinnman N. Efficacy of VX-509 (decernotinib) in combination with a disease-modifying antirheumatic drug in patients with rheumatoid arthritis: Clinical and MRI findings. Ann Rheum Dis. 2016; 75:1979-1983.

93. Namour F, Diderichsen PM, Cox E, Vayssiere B, Van der Aa A, Tasset C, Van't Klooster G. Pharmacokinetics and pharmacokinetic/pharmacodynamic modeling of filgotinib (GLPG0634), a selective JAK1 inhibitor, in support of phase IIB dose selection. Clin Pharmacokinet. 2015; 54:859-874.

94. Namour F, Diderichsen P M, Cox E, Vayssiere B, Van der Aa A, Tasset C, Van't Klooster G. Pharmacokinetics and Pharmacokinetic/Pharmacodynamic Modeling of Filgotinib (GLPG0634), a Selective JAK1 Inhibitor, in Support of Phase IIB Dose Selection. Clin Pharmacokinet. 2015; 54:859-874.

95. Kavanaugh A, Kremer J, Ponce L, Cseuz R, Reshetko O V, Stanislavchuk M, Greenwald M, Van der Aa A, Vanhoutte F, Tasset C, Harrison P. Filgotinib (GLPG0634/GS-6034), an oral selective JAK1 inhibitor, is effective as monotherapy in patients with active rheumatoid arthritis: results from a randomised, dose-finding study (DARWIN 2). Ann Rheum Dis. 2017; 76:1009-1019.

96. Yang XD, Wang C, Zhou P, Yu J, Asenso J, Ma Y, Wei W. Absorption characteristic of paeoniflorin-6'-O-benzene sulfonate (CP-25) in in situ single-pass intestinal perfusion in rats. Xenobiotica. 2016; 46:775-783.

97. Chang Y, Jia X, Wei F, Wang C, Sun X, Xu S, Yang X, Zhao Y, Chen J, Wu H, Zhang L, Wei W. CP-25, a novel compound, protects against autoimmune arthritis by modulating immune mediators of inflammation and bone damage. Sci Rep. 2016; 6:26239.

98. Chen J, Wang Y, Wu H, Yan S, Chang Y, Wei W. A Modified Compound From Paeoniflorin, CP-25, Suppressed immune responses and synovium inflammation in collagen-induced arthritis mice. Front Pharmacol. 2018; 9:563.

99. Zhang F, Shu JL, Li Y, Wu YJ, Zhang XZ, Han L, Tang XY, Wang C, Wang QT, Chen JY, Chang Y, Wu HX, Zhang LL, Wei W. CP-25, a novel anti-inflammatory and immunomodulatory drug, inhibits the functions of activated human B cells through regulating BAFF and TNF-alpha signaling and comparative efficacy with biological agents. Front Pharmacol. 2017; 8:933.

*Address correspondence to:
Pan Jihong, Biomedical Sciences College, Shandong Medicinal Biotechnology Centre, Shandong First Medical University, # 6699 Qingdao Road, Ji'nan 250117, China.
E-mail: panjihong@sdfmu.edu.cn

Integrative overview of IFITMs family based on Bioinformatics analysis

Pengchao Liu[1,2]**, Yongtao Zhang**[1,2]**, Shanshan Zhang**[1,2]**, Chuanming Peng**[1,2]**, Wei Yang**[1,2]**, Xianxian Li**[1,2]**, Chao Zhang**[1,2]**, Mian Li**[1,2]**, Jinxiang Han**[1,2]**, Yanqin Lu**[1,2,]*****

[1] Department of Endocrinology, The First Affiliated Hospital of Shandong First Medical University, Ji'nan, Shandong, China;

[2] Key Laboratory for Biotech-Drugs of National Health Commission, Key Laboratory for Rare & Uncommon Diseases of Shandong Province, Biomedical Sciences College & Shandong Medicinal Biotechnology Centre, Shandong First Medical University & Shandong Academy of Medical Sciences, Ji'nan, Shandong, China.

SUMMARY   Human interferon-induced transmembrane proteins (IFITMs) family is a multi-functional biomacromolecule family playing a critical role in various physiological processes, such as, antiviral immunity, tumor suppression, and bone formation. Although there are many studies proving that a subset of tumors strongly links to the changes of IFITMs, the link between different IFITMs mutant types and diverse tumors has not been studied thoroughly. To investigate the law of expression among IFITMs internal members and the linking of IFITMs mutant types and cancers, online databases were used to pool together relevant data for bioinformatics analysis. Here, we summarize mutations, expression, and functions of human *IFITMs*, analyze diverse expression levels of *IFITMs* in physiological and pathological tissues, predict protein-protein interaction (PPI) networks, and target miRNAs and relevant signaling pathways of *IFITMs*. The results show that *IFITM1*, *IFITM2*, and *IFITM3* have similar motif pattern constructions and physiological functions, while *IFITM5* and *IFITM10* show far diversity from them. Particularly, *IFITM1-3*, in conjunction with interacting proteins, is strongly related to development and overall survival rates of a portion of cancers, including renal cancer and uveal melanoma (UVM). This trait may make *IFITM1-3* become a prognostic marker of cancers. Meanwhile, hsa_circ_0116375 has been found as the common circRNA for *IFITM2*, *IFITM3*, *IFITM5*, and *IFITM10*.

Keywords   IFITM, IFITM mutations, IFITM expression, Tumor, In silico prediction

1. Introduction

Human interferon-induced transmembrane proteins (IFITMs), first reported in 1984, are proteins that can be induced by interferon (IFN) (*1*). There are five members of human IFITMs namely IFITM1, IFITM2, IFITM3, IFITM5 and IFITM10, respectively (*2*). IFITMs, clustering in a 26.5 kb region on human chromosome 11, play a critical role in physiological functions (*3*). IFITMs process the CD225 domain, which is also shared by more than 300 members of the CD225 and pfam04505 family (*4*). Significantly, the CD225 domain of IFITMs is highly conserved among family members, while the family's respective N-terminal domains (NTDs) display heterogeneity in both sequence and length, which is being considered as the functional structure of antiviral specificities (*5*).

There are studies showing that *IFITM* expression or genetic variation may result in diseases. Specifically,

the extent of variation in *IFITMs* are considered strongly associated with illness severity, and there is proof that specific mutations can reverse the function of IFITMs, from inhibiting to promoting the infection of coronaviruses (*6,7*). Functionally, IFITMs mainly play a role in immune signal transduction, cell adhesion, tumorigenesis, and antiviral activity (*8*). Specifically, IFITM1, IFITM2 and IFITM3 have important roles in antiviral invasion and act as tumor markers, while mutations of *IFITM5* cause type V osteogenesis imperfecta. Additionally, *IFITM10* with Cathepsin D (*CTSD*) has been regarded as a molecular marker for breast cancer (*9-11*). Studies indicated that the homotypic interactions between IFITM proteins, are essential for their antiviral activity and signaling pathways associated with IFITMs (*5,12*). Our study summarizes the expression, mutation, interacting molecular function and signaling pathways related to human *IFITMs* based on comprehensive bioinformatics analysis. The study

provides a basis for further understanding of IFITMs and explores its potential functions and applications.

2. Materials and Methods

2.1. Phylogenetic analysis of IFITMs

The protein sequences of the IFITMs with Fasta format were downloaded from the NCBI database (*https://www.ncbi.nlm.nih.gov/*). Multiple sequences alignments were performed with CLUSTAL 2.0 software. A phylogenetic tree was constructed using molecular evolutionary genetic analysis (MEGA) software. Motif detection of IFITMs protein sequences was performed in MEME tools (*https://meme-suite.org/meme/index.html*), and visualized by TBtools software (*13*).

2.2. Analysis of human diseases related to IFITMs

IFITMs-related human diseases were pooled with the published data of the GCBI website (*https://www.gcbi.com.cn*). The mutation profiles and copy number changes of the *IFITMs* in different cancers were summarized by cBioPortal (*http://www.cbioportal.org*) (*14,15*). The mutation types and nucleotide changes of *IFITMs* were analyzed by the Catalogue of Somatic Mutations in Cancer (COSMIC) tools (https://cancer.sanger.ac.uk/cosmic).

2.3. IFITMs expression in tumors and survival analysis of IFITMs-related cancers

Standardized analysis of *IFITMs* expression data in different normal tissues, obtained from Human Protein Atlas database (*https://www.proteinatlas.org*), was based on transcriptome provided by GTEx database. We analyzed the co-expression of both human *IFITMs* genes with the GEPIA2 (*http://gepia2.cancer-pku.cn/#index*) website, and a heatmap was mapped by TBStools through the co-expression results. The GCBI database was used to distinguish the difference of *IFITMs* expression between normal tissues and tumor tissues. The cancers related to *IFITMs* were screened from the PrognoScan database (*http://dna00.bio.kyutech.ac.jp/PrognoScan/*), and the survival curves of the corresponding cancers were drawn by TCGA and GTEx databases on the GEPIA2 website (*http://gepia2.cancer-pku.cn/#index*).

2.4. Prediction of coexisting proteins, PPI networks, targeted miRNA and signaling pathway of IFITMs

The IFITMs-related protein-protein interactions networks were predicted with GeneMANIA database (*http://genemania.org*) and STRING (*https://string-db.org/cgi/input.pl*) online tools (*16,17*). The targeted miRNAs of IFITMs were predicted based on the data extracted from MiRWalk database (*http://mirwalk.umm.uni-heidelberg.de/search_genes*), and then the concurrent targeted miRNAs of different *IFITM* members were found from the predicted miRNAs. The corresponding circRNAs of the concurrent targeted miRNAs were predicted with circBank database (http://www.circbank.cn), and then the concurrent target circRNAs were selected from the predictions. The relationship among *IFITMs*, targeted miRNA and targeted circRNA were mapped by Cytoscape software. KEGG database (http://www.kegg.jp) was used to predict the pathways relevant to *IFITMs* (*18,19*).

3. Results

3.1. Phylogenetic analysis of IFITMs protein

Human *IFITMs* family, located on human chromosome 11, can be divided into five subtypes: *IFITM1*, *IFITM2*, *IFITM3*, *IFITM5*, and *IFITM10*. Phylogenetic analysis was performed with the amino acid sequences of IFITMs proteins based on the results of multiple sequence alignments. IFITM2 and IFITM3 are very close in the phylogenetic tree (Figure 1A) and share the same motif structure of motif1, motif2, and motif3. Compared to IFITM2 and IFITM3, motif 2 is absent in IFITM1 (Figure 1B). The results are consistent with the findings of existing studies that IFITM1, IFITM2, and IFITM3 have similar physiological functions.

3.2 Human diseases related to IFITMs mutations

As listed in GCBI database, all *IFITMs* family members are all related to human immunodeficiency virus (HIV) infections (Figure 2A). IFITM1, IFITM2, and IFITM3 are, particularly, related to influenza, neoplasms, amino acid metabolism, infection, and hepatitis C. Interestingly, there are studies that show *IFITM1* is one of the hub-genes of schizophrenia (*20*), and *IFITM3* is responsible for leukemia and acute liver injury (*21,22*), *IFITM1* and *IFITM3* are related to tumors, and *IFITM5* is the pathogenic gene for type V osteogenesis imperfecta (*2,23-25*).

Five mutation types of *IFITMs*, including mutations, fusions, amplifications, deep deletions, and multiple
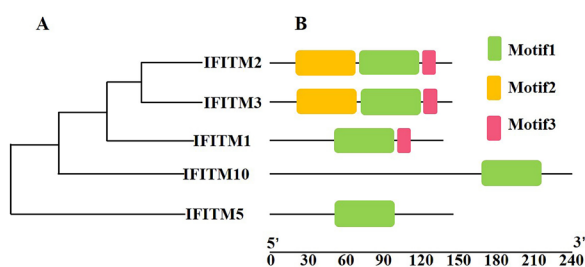

Figure 1. Phylogenetic analysis of IFITMs and motif prediction. (A) Phylogenetic Tree, **(B)** Motif prediction.
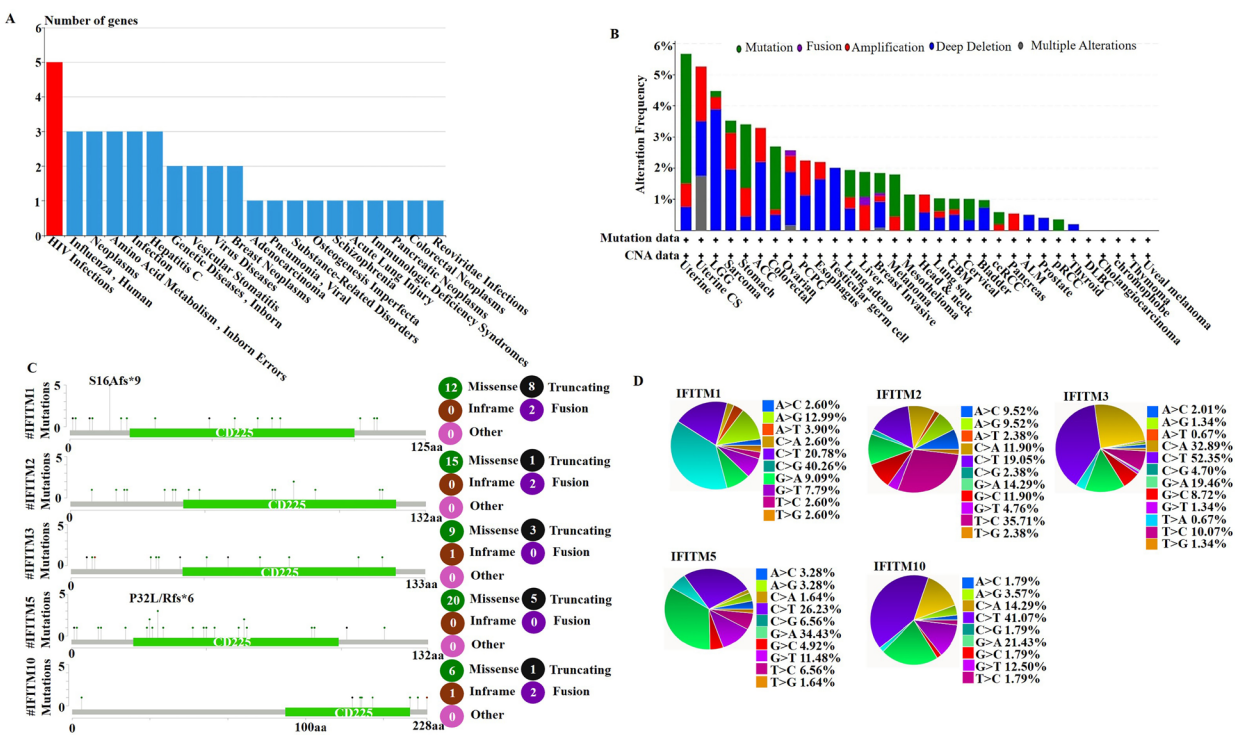
Figure 2. Human diseases related to *IFITMs* mutations. (A) Diseases related to *IFITMs*, **(B)** Mutation frequency of *IFITMs* in different tumors, **(C)** Mutation types of *IFITMs* in cBioPortal database, **(D)** The distribution of different mutation types recorded in COSMIC database.

alterations, were analyzed with 10,967 samples which we obtained from 10,953 patients in 32 types of cancer using cBioPortal tools (Figure 2B). Uterine corpus endometrial carcinoma and uterine carcinosarcoma have the highest mutation frequency, accounting for more than 5%. Most of the mutation types are missense mutations among all *IFITMs* mutations, and the C>T substitution mutations are the most common according to all the base mutation types (Figure 2C and 2D).

Different mutation types of *IFITMs* have been found in the amino acid sequences of these samples (Table S1 (*http://www.irdrjournal.com/action/getSupplementalData.php?ID=76*), Figure 2C). The S16Afs*9 change of IFITM1 is included in numerous tumors, including astrocytoma, colon adenocarcinoma, diffuse type stomach adenocarcinoma, intestinal type stomach adenocarcinoma and tubular stomach adenocarcinoma. Moreover, the other mutation types of *IFITM1* exist in tumors such as colon adenocarcinoma, stomach adenocarcinoma, uterine endometrioid carcinoma, *etc*. As for *IFITM5*, P32L change was related to tumors of rectal adenocarcinoma and breast invasive lobular carcinoma. *PTDSS2*, and *IGF2BP2* were identified fused with *IFITM1* and *IFITM2* to cause hepatocellular carcinoma, and uterine carcinoma, respectively. *DENND5A* and *CFLL1* were fused with *IFITM10* (Table S1 (*http://www.irdrjournal.com/action/getSupplementalData.php?ID=76*), Figure 2C). According to the mutation samples, we can see that *IFITMs* may cause different tumors, and the missense mutation was the most common mutation type among

all tumor-related *IFITMs* mutations.

3.3. IFITMs expression in tumors and survival analysis of IFITMs-related cancers

The expressions of *IFITMs* in different tissues were obtained from the Human Protein Atlas database. There are 34 normal tissues that express *IFITM1*, *IFITM2*, *IFITM3*, and *IFITM10*, while only 13 normal tissues express *IFITM5*, according to the transcriptome data on the GTEx database (Figure 3A). Based on this database, the expression of *IFITM1*, *IFITM2*, *IFITM3*, compared with *IFITM5* and *IFITM10*, is higher in the uterus, ovary, fallopian tube, and adipose tissue. However, the tissues with highest level of *IFITM5* expression are the pancreas, lung, and thyroid gland. The highest level of *IFITM10* expression is in the adrenal gland and urinary bladder. The expression levels of *IFITM5* and *IFITM10* were significantly lower than those of other *IFITM* family members in normal tissues. Then, we analyzed the co-expression profiles of *IFITMs* family members in partial normal physiological tissues (Figure 3B). It can be found that the relevance among *IFITM1*, *IFITM2*, and *IFITM3* were closer than other *IFITMs* members in expression.

The differential levels of *IFITM1*, *IFITM2*, *IFITM3* and *IFITM5* expression in normal and tumor tissues have been searched in the GCBI database (Figure 3C). In totality, the expression levels of *IFITMs* in most tumor tissues were higher than that in normal tissues. The expression of *IFITM1*, *IFITM2* and *IFITM3* were
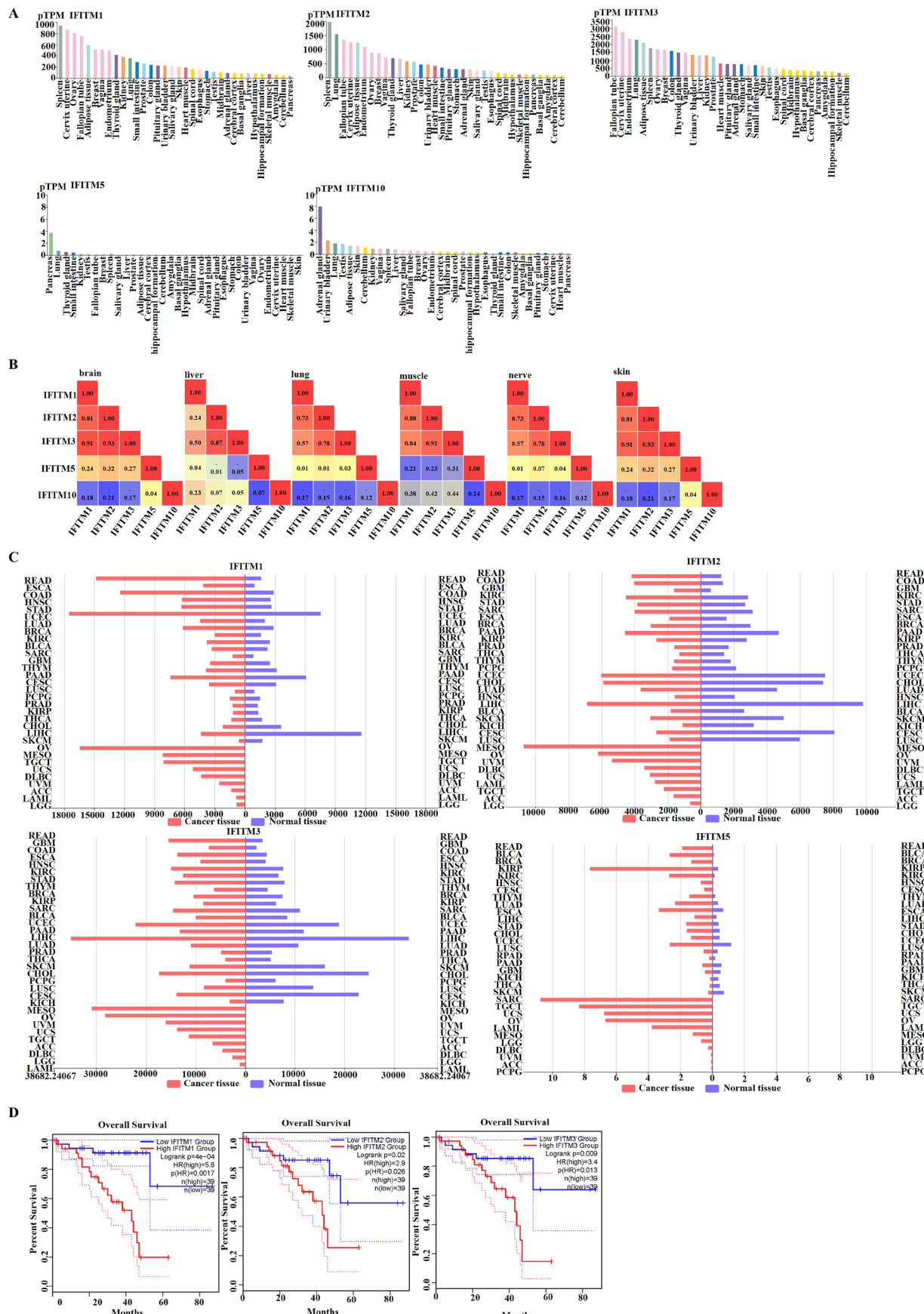
Figure 3. *IFITMs* **expression and survival analysis of UVM cancer.** **(A)** Expression of *IFITMs* in different normal tissues, **(B)** Co-expression HeatMap of *IFITMs* in normal tissues, **(C)** Expression of *IFITMs* in tumor tissues, **(D)** Overall survival curve for the *IFITM1-3* signature in UVM.

Table 1. Tumors related to *IFITMs* in PrognoScan database

Tumors	IFITM1	IFITM2	IFITM3	IFITM5	IFITM10
acute myeloid leukemia (LALM)	√	×	√	×	√
breast invasive carcinoma (BRCA)	√	√	√	×	√
bladder urothelial carci-noma (BLCA)	√	√	√	×	×
Colon adenocarcinoma (COAD)	√	×	×	×	√
glioma (GBMLGG)	√	√	√	×	√
lung adenocarcinoma (LUAD)	√	√	√	√	√
lung squamous cell carci-noma (LUSC)	√	×	×	×	×
ovarian serous cystadeno-carcinoma (OV)	√	×	×	×	×
uveal melanoma (UVM)	√	√	√	×	√

tissues, including adrenocortical carcinoma (ACC), lymphoid neoplasm diffuse large b-cell lymphoma (DLBC), mesothelioma (MESO), acute myeloid leukemia (LAML), brain lower grade glioma (LGG), ovarian serous cystadenocarcinoma (OV), testicular germ cell tumors (TGCT), uterine carcinosarcoma (UCS) and uveal melanoma (UVM), were not studied, so that there are no data showing the corresponding information.

Different types of tumors associated with *IFITMs* are summarized through the PrognoScan database. By setting the selection condition COX P-VALUE < 0.05, the cancers related to *IFITMs* are listed (Table 1). Accordingly IFITMs show significant expression differences in different tumors, and cancer survival curves were drawn with GEPIA2 tools based on TCGA and GTEx databases. The log rank $P < 0.05$ is the screening condition to show significantly different curves of the overall survival analysis (Figure 3D). The log rank values of *IFITM1*, *IFITM2*, *IFITM3* were < 0.05 in UVM, and the survival percentage of *IFITM1*, *IFITM2*, *IFITM3* low-expression group was significantly higher than that of the high-expression group. The log rank $p > 0.05$ of *IFITM5* and *IFITM10* showed no significant difference in overall survival (OS). Based on the above data, the high expression of *IFITM1*, *IFITM2*, *IFITM3* is an unfavorable factor in UVM.

The expressions of *IFITM1*, *IFITM2*, and *IFITM3* are very significant in renal cancer and can be used as a prognostic marker (unfavorable), while *IFITM5* and *IFITM10* products are not prognostic according to Human Protein Atlas database.

3.4. Prediction of PPI networks, targeted miRNA and signaling pathway of IFITMs

Twenty proteins related to the function of IFITMs were predicted with the GeneMANIA database (Figure 4A and 4B). GeneMANIA and String databases predict that IFITM1, 2, 3 are related to CD81, IFIT1, IFIT3, IFI35, IFI6, and IFITM5, and IFITM10 are not significantly related to IFITM1, IFITM2, IFITM3 (Figure 4A-4C). IFITM1-3 interacts with CD81 to inhibit the entry of hepatitis C; IFITMs interact with MX1, ISG15, ISG20, IRF9, IFIT1, IFIT2, IFIT3, IFI, BST2, GBP2 and RSAD2 to play an antiviral immunity role (*26-29*). There is evidence confirmed that IFITM1 combines with CD81 and makes a complex with CD19 and CD21 (*30*). Moreover, there are reports that showed the constitutive up-regulation of CD81 associated with tumor progression in mouse skin tumor models (*31,32*).

The target miRNAs and circRNAs of *IFITMs*, gathered from MiRWalk and circBank, are listed in Table S2 and Table S3 (*http://www.irdrjournal. com/action/getSupplementalData.php?ID=76*). The interactions among IFITMs, the concurrent target miRNA and the concurrent target circRNA has been drawn in the Cytoscape software (Figure 4D). Interestingly, there are 13 miRNAs jointly targeted by *IFITM5* and *IFITM10*, with *IFITM1* sharing no common miRNAs among the family members. Among all the 22 coexisting targeted miRNAs, there are 7 miRNAs, including miR-29b-2-5p, miR-4418, miR-4463, miR-4519, miR-5093, miR-6860, and miR-6895-5p, related to *IFITM2*, *IFITM3*, *IFITM5*, and *IFITM10*, targeting to the hsa_circ_0116375.

According to the prediction results based on KEGG database, the disease related to the IFITM family is osteogenesis imperfecta, and the signaling pathway related to IFITM1 is B cell receptor signaling pathway.

4. Discussion

IFITMs family is associated with various human diseases including anti-virus, immunity, osteogenesis imperfecta, and tumors. The induced type interferons activate many interferon-stimulating genes (ISG) that have direct antiviral effects and block viruses from entering the human body (*33*). The immune defense against a variety of viruses is mainly participated by IFITM1, 2, and 3 (*34*). However, the IFITMs family has also been involved in other processes, such as tumorigenesis, and bone mineralization (IFITM5) (*35*). Also, *IFITMs* mutations may cause different effects on diseases, for example, a single recurrent mutation in the 5'-UTR of *BRIL* (bone-restricted *IFITM*-like, or *IFITM5*) causes osteogenesis imperfecta type V in humans (*36*). Interestingly, most of the mutations in *IFITMs* family are mistranslation mutations, and the location of the mutations is not limited to NTDs.
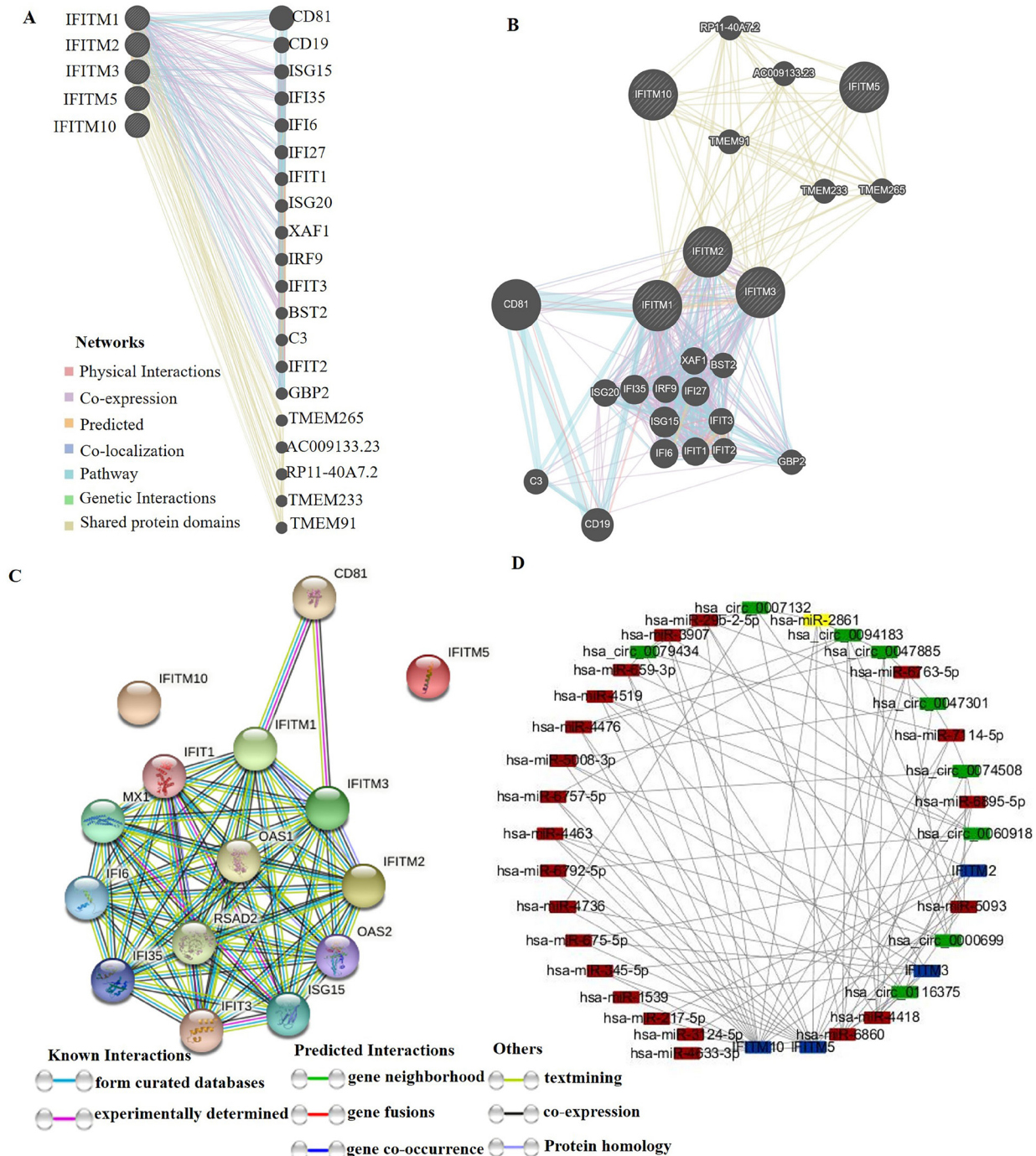
Figure 4. Predicted IFITMs- interacting proteins and targeting non-coding RNAs. (A-C) IFITMs -related proteins predicted by GeneMania and String, respectively, **(D)** MiRNAs and circRNAs targeting IFITMs predicted by MiRWalk and circBank, respectively.

The corresponding mutations in CD225 structure have been found in our study. Tissues of colorectal cancer in humans were confirmed with over-expressed *IFITM3*, while *IFITM3* knock-offs caused significant suppression of the proliferation, colony formation, and migration (*37,38*). Also, *IFITM1* knock-offs significantly suppressed the invasiveness of head and neck tumor cells (*31*). There is evidence, which showed that deletion of adenomatous polyposis coli (APC) alleles, which leads to the formation of colon

adenomas, results in *IFITM3* expression dropping sharply in conditional APC mutant mice (*39*). Based on the mutation samples, different *IFITMs* are related to different tumors, and diverse mutants may appear in one type of tumor. Among all the mutation types of IFITMs in tumors, missense mutations were the most frequent mutation type, and the C > T substitution mutation was the most common mutation according to all the tumor-related *IFITMs* mutations.

IFITM1, IFITM2, IFITM3 have higher similarity

in motif structure, while IFITM5 and IFITM10 have lower similarity compared to them. Based on the online database, the similarity of *IFITM1*, *IFITM2* and *IFITM3* expression in normal tissues and tumor tissues has been found through our study. In normal tissues, the expression levels of *IFITM1-3* were significantly higher than those of *IFITM5*, *IFITM10*, and *IFITM1-3* was highly expressed in female reproductive organs, but lower in brain tissues. These findings support *IFITM1*, *IFITM2* and *IFITM3* are similar not only in structure but also in function.

More and more studies have shown that *IFITMs* can be used as markers for tumor prognosis. *IFITMs* are reported to be frequently overexpressed in colorectal tumors (*38*), and the IFITMs family can be used as marker molecules for human colorectal cancer (*39*), and *IFITM1* can be used as a rare type of squamous cell/ adenosquamous carcinoma (SC/ASC) and common adenocarcinoma (AC) marker molecule (*40*).

The comprehensive bioinformatics analysis of our study indicated that *IFITM1*, *IFITM2*, and *IFITM3* can be used as prognostic markers of kidney cancer (unfavorable), while the products of *IFITM5* and *IFITM10* cannot be used as markers of tumor prognosis. It is consistent with this result that the expression levels of *IFITMs* in tumor tissues, including rectum adenocarcinoma (READ), COAD, kidney renal clear cell carcinoma (KIRC) and esophageal carcinoma (ESCA), were higher than that in normal tissues. In addition, for several kinds of tumors without normal tissue as control, we found that high expression of *IFITM1-3* is closely related to the decline in overall survival, which indicates that the expression level of *IFITM1-3* can be used as a diagnostic indicator for UVM.

Our study summarized the mutation, expression, and function of the human IFITMs family based on comprehensive bioinformatics analysis. The expression of IFITM and proteins interacting with it was involved in various cancers and is significantly related to survival in some cancers. The altered expression of *IFITMs* and proteins interacting with it may be a prognostic marker in some cancers.

Conflict of Interest: The authors have no conflicts of interest to disclose.

References

1. Alber D, Staeheli P. Partial inhibition of vesicular stomatitis virus by the interferon-induced human 9-27 protein. J Interferon Cytokine Res. 1996; 16:375-380.

2. Yánez DC, Ross S, Crompton T. The IFITM protein family in adaptive immunity. Immunology. 2020; 159:365-372.

3. Jia R, Ding S, Pan Q, Liu SL, Qiao W, Liang C. The C-terminal sequence of IFITM1 regulates its anti-HIV-1 activity. PloS One. 2015; 10:e0118794.

4. Punta M, Coggill PC, Eberhardt RY, *et al.* The Pfam protein families database. Nucleic Acids Res. 2012; 40:D290-D301.

5. John SP, Chin CR, Perreira JM, Feeley EM, Aker AM, Savidis G, Smith SE, Elia AE, Everitt AR, Vora M, Pertel T, Elledge SJ, Kellam P, Brass AL. The CD225 domain of IFITM3 is required for both IFITM protein association and inhibition of influenza A virus and dengue virus replication. J Virol. 2013; 87:7837-7852.

6. Zhao X, Li J, Winkler CA, An P, Guo JT. IFITM genes, variants, and their roles in the control and pathogenesis of viral infections. Front Microbiol. 2018; 9:3228.

7. Zhao X, Sehgal M, Hou Z, Cheng J, Shu S, Wu S, Guo F, Le Marchand SJ, Lin H, Chang J, Guo JT. Identification of residues controlling restriction versus enhancing activities of IFITM proteins on entry of human coronaviruses. J Virol. 2018; 92.

8. Siegrist F, Ebeling M, Certa U. The small interferon-induced transmembrane genes and proteins. J Interferon Cytokine Res. 2011; 31:183-197.

9. Zhang Z, Liu J, Li M, Yang H, Zhang C. Evolutionary dynamics of the interferon-induced transmembrane gene family in vertebrates. PloS one. 2012; 7:e49265.

10. Lu Y, Zuo Q, Zhang Y, Wang Y, Li T, Han J. The expression profile of IFITM family gene in rats. Intractable Rare Dis Res. 2017; 6:274-280.

11. Tirosh B, Daniel-Carmi V, Carmon L, Paz A, Lugassy G, Vadai E, Machlenkin A, Bar-Haim E, Do MS, Ahn IS, Fridkin M, Tzehoval E, Eisenbach L. '1-8 interferon inducible gene family': putative colon carcinoma-associated antigens. Br J Cancer. 2007; 97:1655-1663.

12. Winkler M, Wrensch F, Bosch P, Knoth M, Schindler M, Gärtner S, Pöhlmann S. Analysis of IFITM-IFITM Interactions by a flow cytometry-based FRET assay. Int J Mol Sci. 2019; 20.

13. Bailey TL, Elkan C. Fitting a mixture model by expectation maximization to discover motifs in biopolymers. Proc Int Conf Intell Syst Mol Biol. 1994; 2:28-36.

14. Gao J, Aksoy BA, Dogrusoz U, Dresdner G, Gross B, Sumer SO, Sun Y, Jacobsen A, Sinha R, Larsson E, Cerami E, Sander C, Schultz N. Integrative analysis of complex cancer genomics and clinical profiles using the cBioPortal. Sci Signal. 2013; 6: pl1.

15. Cerami E, Gao J, Dogrusoz U, *et al.* The cBio cancer genomics portal: an open platform for exploring multidimensional cancer genomics data. Cancer Discov. 2012; 2:401-404.

16. Warde-Farley D, Donaldson SL, Comes O, *et al.* The GeneMANIA prediction server: biological network integration for gene prioritization and predicting gene function. Nucleic Acids Res. 2010; 38:W214-220.

17. Szklarczyk D, Franceschini A, Wyder S, Forslund K, Heller D, Huerta-Cepas J, Simonovic M, Roth A, Santos A, Tsafou KP, Kuhn M, Bork P, Jensen LJ, von Mering C. STRING v10: protein-protein interaction networks, integrated over the tree of life. Nucleic Acids Res. 2015; 43:D447-452.

18. Kanehisa M, Furumichi M, Tanabe M, Sato Y,

Morishima K. KEGG: new perspectives on genomes, pathways, diseases and drugs. Nucleic Acids Res. 2017; 45:D353-d361.

19. Carbon S, Ireland A, Mungall CJ, Shu S, Marshall B, Lewis S. AmiGO: online access to ontology and annotation data. Bioinformatics. 2009; 25:288-289.

20. Siegel BI, Sengupta EJ, Edelson JR, Lewis DA, Volk DW. Elevated viral restriction factor levels in cortical blood vessels in schizophrenia. Biol Psychiatry. 2014; 76:160-167.

21. Chan YK, Huang IC, Farzan M. IFITM proteins restrict antibody-dependent enhancement of dengue virus infection. PloS one. 2012; 7:e34508.

22. Zhang LQ, Adyshev DM, Singleton P, Li H, Cepeda J, Huang SY, Zou X, Verin AD, Tu J, Garcia JG, Ye SQ. Interactions between PBEF and oxidative stress proteins--a potential new mechanism underlying PBEF in the pathogenesis of acute lung injury. FEBS Lett. 2008; 582:1802-1808.

23. Hanagata N. IFITM5 mutations and osteogenesis imperfecta. J Bone Miner Metab. 2016; 34:123-131.

24. Yang M, Gao H, Chen P, Jia J, Wu S. Knockdown of interferon-induced transmembrane protein 3 expression suppresses breast cancer cell growth and colony formation and affects the cell cycle. Oncol Rep. 2013; 30:171-178.

25. Ogony J, Choi HJ, Lui A, Cristofanilli M, Lewis-Wambi J. Interferon-induced transmembrane protein 1 (IFITM1) overexpression enhances the aggressive phenotype of SUM149 inflammatory breast cancer cells in a signal transducer and activator of transcription 2 (STAT2)-dependent manner. Breast Cancer Res. 2016; 18:25.

26. El-Asmi F, McManus FP, Brantis-de-Carvalho CE, Valle-Casuso JC, Thibault P, Chelbi-Alix MK. Cross-talk between SUMOylation and ISGylation in response to interferon. Cytokine. 2020; 129:155025.

27. Narayana SK, Helbig KJ, McCartney EM, Eyre NS, Bull RA, Eltahla A, Lloyd AR, Beard MR. The interferon-induced transmembrane proteins, IFITM1, IFITM2, and IFITM3 inhibit hepatitis C virus Entry. J Biol Chem. 2015; 290:25946-25959.

28. Ashley CL, Abendroth A, McSharry BP, Slobedman B. Interferon-independent innate responses to cytomegalovirus. Front Immunol. 2019; 10:2751.

29. Tsuji R, Yamamoto N, Yamada S, Fujii T, Yamamoto N, Kanauchi O. Induction of anti-viral genes mediated by humoral factors upon stimulation with Lactococcus lactis strain plasma results in repression of dengue virus replication in vitro. Antiviral Res. 2018; 160:101-108.

30. Levy S, Todd SC, Maecker HT. CD81 (TAPA-1): a molecule involved in signal transduction and cell adhesion in the immune system. Annu Rev Immunol. 1998; 16:89-109.

31. Hatano H, Kudo Y, Ogawa I, Tsunematsu T, Kikuchi A, Abiko Y, Takata T. IFN-induced transmembrane protein 1 promotes invasion at early stage of head and neck cancer progression. Clin Cancer Res. 2008; 14:6097-6105.

32. Owens DM, Watt FM. Influence of beta1 integrins on epidermal squamous cell carcinoma formation in a transgenic mouse model: alpha3beta1, but not alpha2beta1, suppresses malignant conversion. Cancer Res. 2001; 61:5248-5254.

33. Liu SY, Sanchez DJ, Cheng G. New developments in the induction and antiviral effectors of type I interferon. Curr Opin Immunol. 2011; 23:57-64.

34. Huang IC, Bailey CC, Weyer JL, *et al.* Distinct patterns of IFITM-mediated restriction of filoviruses, SARS coronavirus, and influenza A virus. PLoS Pathog. 2011; 7:e1001258.

35. Sällman Almén M, Bringeland N, Fredriksson R, Schiöth HB. The dispanins: a novel gene family of ancient origin that contains 14 human members. PloS one. 2012; 7:e31961.

36. Kasaai B, Gaumond MH, Moffatt P. Regulation of the bone-restricted IFITM-like (Bril) gene transcription by Sp and Gli family members and CpG methylation. J Biol Chem. 2013; 288:13278-13294.

37. Li D, Peng Z, Tang H, Wei P, Kong X, Yan D, Huang F, Li Q, Le X, Li Q, Xie K. KLF4-mediated negative regulation of IFITM3 expression plays a critical role in colon cancer pathogenesis. Clin Cancer Res. 2011; 17:3558-3568.

38. Miyamoto C, Miyamoto N, Yamamoto H, Imai K, Shinomura Y. Detection of fecal interferon-induced transmembrane protein messenger RNA for colorectal cancer screening. Oncol Lett. 2011; 2:95-100.

39. Andreu P, Colnot S, Godard C, Laurent-Puig P, Lamarque D, Kahn A, Perret C, Romagnolo B. Identification of the IFITM family as a new molecular marker in human colorectal tumors. Cancer Res. 2006; 66:1949-1955.

40. Li D, Yang Z, Liu Z, Zou Q, Yuan Y. DDR2 and IFITM1 are prognostic markers in gallbladder squamous cell/adenosquamous carcinomas and adenocarcinomas. Pathol Oncol Res. 2019; 25:157-167.

Original Article

Myoblast differentiation of C2C12 cell may related with oxidative stress

Xianxian Li[1,2], Shanshan Zhang[1,2], Yongtao Zhang[1,2], Pengchao Liu[1,2], Mian Li[1,2], Yanqin Lu[1,2,*], Jinxiang Han[1,2,*]

[1] Department of Endocrinology and Metabolism, The First Affiliated Hospital of Shandong First Medical University & Shandong Provincial Qianfoshan Hospital, Ji'nan, Shandong, China;

[2] Key Laboratory for Biotech-Drugs of National Health Commission, Key Laboratory for Rare & Uncommon Diseases of Shandong Province, Biomedical Sciences College & Shandong Medicinal Biotechnology Centre, Shandong First Medical University & Shandong Academy of Medical Sciences, Ji'nan, Shandong, China.

SUMMARY   Muscle is a contractile tissue responsible for maintaining posture and the movement of all parts of the body. Prolonged oxidizative stress can lead to the damage of cells, tissues, and organs. In this study, we investigated the possibility of oxidative stress in the process of myoblast differentiation of C2C12 cells. First, the myoblast differentiation model of C2C12 cells was constructed and verified by Giemsa staining. The expression of hypoxia inducible factor1-alpha (HIF1-α), hypoxia inducible factor1-beta (HIF1-β), Von Hippel-Lindau (VHL), lysyl oxidase (Lox), EGL-9 family hypoxia-inducible factor 1 (EGLN1), proline 4-hydroxylase alpha 1 (P4HA1) and heme oxygenase-1 (HOMX1) in the process of myoblast differentiation was verified by *in vitro* experiments and Gene Expression Omnibus (GEO) bioinformatic analysis. We found that with the increased expression of myogenic factor 5 (MYF5), myogenic differentiation 1 (MYOD1), and Desmin, myotube fusion became more obvious during the process of C2C12 cell differentiation. Both experimental and GEO analysis indicated that the expression of HIF1-α, HIF1-β, VHL, LOX, EGLN1 and P4HA1 increased, and the expression of HOMX1 decreased during myogenic differentiation. Therefore, we suggest that the myoblast differentiation of C2C12 cells may be related to oxidative stress. Their possible relationship was proposed, though further studies are needed.

Keywords   C2C12 cells, myoblast differentiation, oxidative stress

1. Introduction

Skeletal muscle differentiates through clonal proliferation of myoblasts, directed differentiation, and mutual fusion into multinucleated myotubules to finally become mature muscle fibers (*1*). Myogenic differentiation is a process regulated by myogenic regulation-transcription factors (MRFs) including MYOD1, myogenin and MYF5 (*2-4*). The early stages of development are dominated by induction of MYF5 and MYOD1 (*5*). MYF5 leads to rapid proliferation of myoblasts (*6*), while the up-regulation of MYOD1 results in stagnation of the cell cycle and transition from proliferation to differentiation.

Oxidative stress (OS) is an imbalance between production and accumulation of oxygen reactive species (ROS) in cells and tissues and the ability of the body to detoxify these reactive products (*7*), and is highly related to the process of homeostasis and the function of skeletal muscle. Active oxygen can not only damage the

structure of cells and thus their function, but also affect cell's growth, proliferation, and differentiation (*8*). Redox signal is an important regulator of skeletal muscle protein synthesis and proteolytic cell signaling pathways (*9*). Previous studies have shown that oxidative stress also plays a vital role in the pathogenesis of sarcopenia (*10*). High ROS levels can modify the structure and function of cell proteins and lipids, leading to cell dysfunction, including impaired energy metabolism, altered cell signaling and cell cycle control (*7*). The production of ROS in the sarcoplasmic reticulum physiologically enhances muscle contractility (*11*) and regeneration of skeletal muscle (*12*). Recent studies have shown that ROS is produced by mitochondrial electron transport chain complex I and is an indispensable mediator of muscle differentiation (*13*).

The oxygen concentration in mature skeletal muscle cells is about 1-10%, and physiological hypoxia is the optimal condition for myoblast differentiation. Therefore,

oxidative stress promotes myoblast differentiation, which is very important for the repair of muscle injury. However, how oxidative stress relates to myogenic differentiation and the potential mechanism has never been investigated extensively. It has been reported that HIF1-α, HIF1-β, VHL, Lox, EGLN1, P4HA1 and HOMX1 are associated with tissue myoblast differentiation and oxidative stress. The following experiments were conducted to explore the molecular mechanisms involved.

2. Materials and Methods

2.1. Cell culture and differentiation

C2C12 cells were cultured in high dulbecco's modified eagle medium (Gibco) containing 10% fetal bovine serum (Gibco), 100 IU/mL penicillin and 100 IU/mL streptomycin (Beyotime). Subsequently, the cells were switched to differentiation medium (DM) containing 2% horse serum (Gibco), 100 UI/mL penicillin and 100 μg/mL streptomycin in DMEM for 0, 3, 5 and 7 days of differentiation.

2.2. Giemsa dyeing

The cells were gently washed 3 times with phosphate buffered saline (PBS) before addition of anhydrous methanol solution to fix them (cover the cells) for 15 min. The methanol solution was aspirated and the monolayer of cells were rinsed twice with fresh anhydrous methanol. Before staining, anhydrous ethanol was added to absorb water, and then diluted 10% Giemsa working dye was added. The cells were incubated at 37℃ for 15 min, and washed with PBS.

2.3. Real-time Quantitative PCR

The cells were cultured in a six-well plate. Total RNA was extracted from three replicates per group using Trizol. RNA purity and integrity were evaluated using a NanoDrop-2000 spectrophotometer.

Complementary DNA (cDNA) was generated using a TAKARA kit. The first step is to remove genomic DNA: Random Primer (6 mer) 1μL, dNTP Mix (10 nm) 1μL, template RNA 2000 ng, RNase-free ddH$_2$O supplemented 10 μL, 65℃ for 5 min, 4℃ for 2 min; Step 2 Reverse transcriptional reaction: 4 μL 5X Primer Script Buffer, 0.5 μL RNase Inhibitor, 1 μL Primer Script Reverse Transcriptase and 4.5 μL RNase-free ddH$_2$O were added into the reaction products of the first step. The cDNA was synthesized using the following reaction conditions: 30℃ for 10 min; 42 ℃ 60 min; 70 ℃ for 15 min. The product was stored at -80℃.

QPCR was performed using 2X SYBR Green qPCR Mix (SparkJade, Bio, China) on a Lightcycler 480 to confirm the relative levels of expression of genes in the C2C12 cells. The total volume of the PCR reaction was 10 μL, containing 0.5 μL of each primer (10 μM), 1 μL cDNA, 5 μL 2X SYBR Green qPCR Mix, 3 μL RNase-free ddH$_2$O. PCR cycling conditions were as follows: initial 5 min denaturation at 95℃, followed by 45 cycles of amplification at 95℃ for 10 sec, 60℃ for 10 sec and 72℃ for 15 sec. To quantify the expression of each candidate gene, the mRNA expression levels were normalized to the level of glyceraldehyde 3-phosphate dehydrogenase (GAPDH) mRNA. Relative gene expression was analyzed using a comparative cycle threshold (Ct) method ($2^{-\Delta\Delta Ct}$). RT-qPCR was performed in triplicate for each sample and was repeated three times for each assay. Sequences of the forward and reverse primers used are shown in Table 1.

2.4. Western blotting

Protein concentration was determined using the BCA protein concentration assay kit (Biosharp, China) after lysing cells in RIPA Buffer (CWBIO, China) supplemented with 1% PMSF (CWBIO, China). The cells were washed with ice-cold PBS and exposed to RIPA Buffer supplemented with 1% PMSF cocktail solution for 1 h on ice. Insoluble material was removed by centrifugation at 16600g for 25 min at 4℃. Proteins (50-100 μg) were separated by 12% sodium dodecyl sulfate-polyacrylamide gel electrophoresis and transferred to a polyvinylidene fluoride membrane (0.45 μm, Biosharp, China). The membranes were blocked with 5% skim milk in Tris-buffered saline containing 0.1% Tween 20 (TBST) for 2 h at room temperature. The blots were then incubated with primary antibody overnight at 4℃. Antibodies used for western blot analysis were rabbit

Table 1. Q-PCR primer sequences

Primer Name	Primer sequence (5′-3′)
Mus-HIF1-α	F: CATGATGGCTCCCTTTTTCA
	R: GTCACCTGGTTGCTGCAATA
Mus-HIF1-β	F: TGCCTCATCTGGTACTGCTG
	R: TGTCCTGTGGTCTGTCCAGT
Mus-VHL	F: CTGCGTCTGCCCTTTGTAG
	R: TCACCAGGAAGCAAAACTGA
Mus-Lox	F: CAGGCTGCACAATTTCACC
	R: CAAACACCAGGTACGGCTTT
Mus-P4HA1	F: CGTGGGGAGGGTATCAAAAT
	R: ATGGTAGCGGCAGAACAGTC
Mus-EGLN1	F: CGTCTCTCAGTGATTCCAACC
	R: ACTGTTAGGTCGGTCGAAGC
Mus-Desmin	F: GTGAAGATGGCCTTGGATGT
	R: AAGGTCTGGATCGGAAGGTT
Mus-MYOD1	F: AGCACTACAGTGGCGACTCA
	R: GGCCGCTGTAATCCATCAT
Mus-MYF5	F: CTGCTCTGAGCCCACCAG
	R: GACAGGGCTGTTACATTCAGG
Mus-HOMX1	F: AGGGTCAGGTGTCCAGAGAA
	R: GTTCTGCTTGTTGCGCTCTA
Mus-GAPDH	F: CATCCCAGAGCTGAACG
	R: CTGGTCCTCAGTGTAGCC

anti-Desmin (ab32362), rabbit anti-MYOD1 (ab203383), rabbit anti-MYF5 (ab125301), and rabbit anti-GAPDH. The blots were washed three times for 5 min with TBST and then incubated with horseradish peroxidase-labeled secondary antibody for 1 h at 37°C. Goat-anti-rabbit lgG (1:25000; Proteintech, USA) was used as the secondary antibody. After additional washes, the signal was detected using an ECL Chemiluminescence Substrate Kit (Biosharp, China). The protein signals were visualized by exposing the membranes in a Chemiluminescence Gel Imaging System (18200880; Alliance, UK). The level of expression of each protein was normalized to that of GAPDH. The results were quantified using ImageJ-win64 software (Rawak Software Inc., Stuttgart, Germany).

2.5. Gene expression from GEO database

To analyze the expression of oxidative stress related molecules in myogenic differentiation models, *HIF1-α*, *HIF1-β*, *VHL*, *LOX*, *EGLN1*, *P4HA1* and *HOMX1* were screened with GEO profiles database.

2.6. Statistical analysis

The results are presented as mean ± standard error of the mean (SEM). Statistical comparisons were made with a one-way ANOVA and the Tukey multiple comparison test using GraphPad Prism software, version 7.0 (GraphPad Software Inc., San Diego, CA, USA) to identify significant differences. P-values < 0.05 were considered statistically significant ([*] represents $P < 0.05$, [**] represents $P < 0.01$, [***] represents $P < 0.001$, and [****] represents $P < 0.0001$). All experiments were performed at least three times.

3. Results

3.1. Construction of myoblast differentiation model of C2C12 cells

We used Giemsa dyeing and expression of myoblast related genes to investigate whether the model of myoblast differentiation was successfully constructed. In the process of differentiation, the number of myotubes increased in the field of vision (Figure 1). As shown by western blotting and qPCR, the expression of MYOD1, MYF5 and Desmin gradually increased over seven days during the process of C2C12 myogenic differentiation (Figure 2). These results indicate that the myoblast differentiation model of C2C12 cells was established successfully.

3.2. Expression of oxidative stress related molecules in myoblast differentiation

The mRNA expression of oxidative stress related molecules at different time periods of myogenic differentiation of C2C12 cells are shown in Figure 3. With myogenic differentiation, the relative expression of *HIF1-α*, *HIF1-β*, *VHL, Lox*, *P4HA1*, and *EGLN1* genes increased. The expression of *HOMX1*, however, showed the opposite trend, with the highest expression seen prior to induction, and the lowest expression on day seven.

Through online analysis in GEO repository, GSE5447 and GSE55034 were selected for data mining analysis. The GSE5447 dataset included 6 samples of gene expression analysis during the 0 h, 6 h, and 24 h process of differentiation and after the addition of deltaNP73α which is an inhibitor in C2C12 cells. The GSE55034 dataset contained gene expression analysis

Figure 1. Giemsa staining of C2C12 during myogenic differentiation under the induction of 2% horse serum. (A) before induction. **(B)** induction for 3 days. **(C)** inudction for 5 days. **(D)** induction for 7 days.
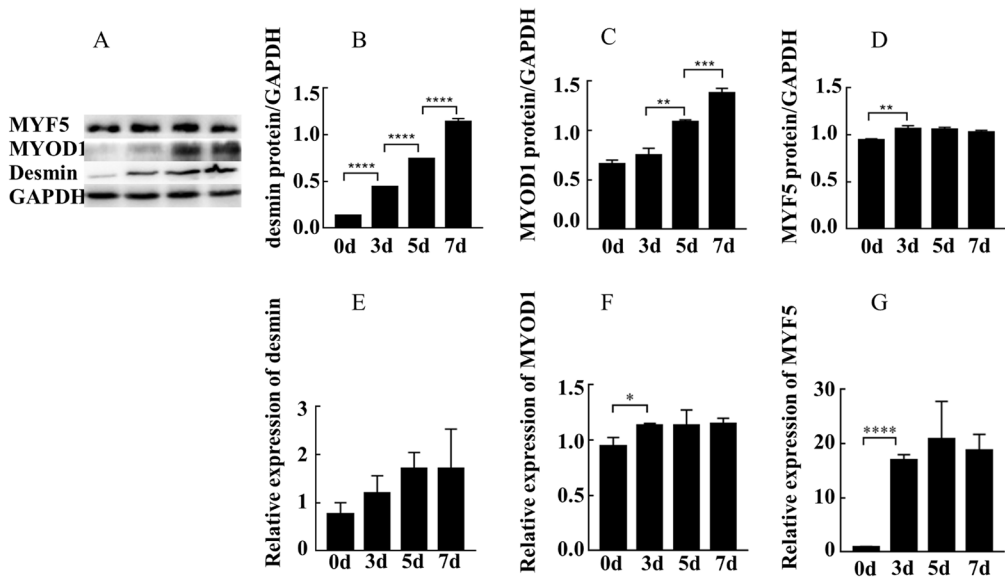
Figure 2. Expression of myogenic molecular markers. (A) The expression of MYF5, MYOD1 and Desmin protein during myogenic differentiation. **(B-D)** Gray scale analysis of Western Blot results. **(E-G)** The expression of *MYF5*, *MYOD1*, and *Desmin* mRNA during myogenic differentiation.
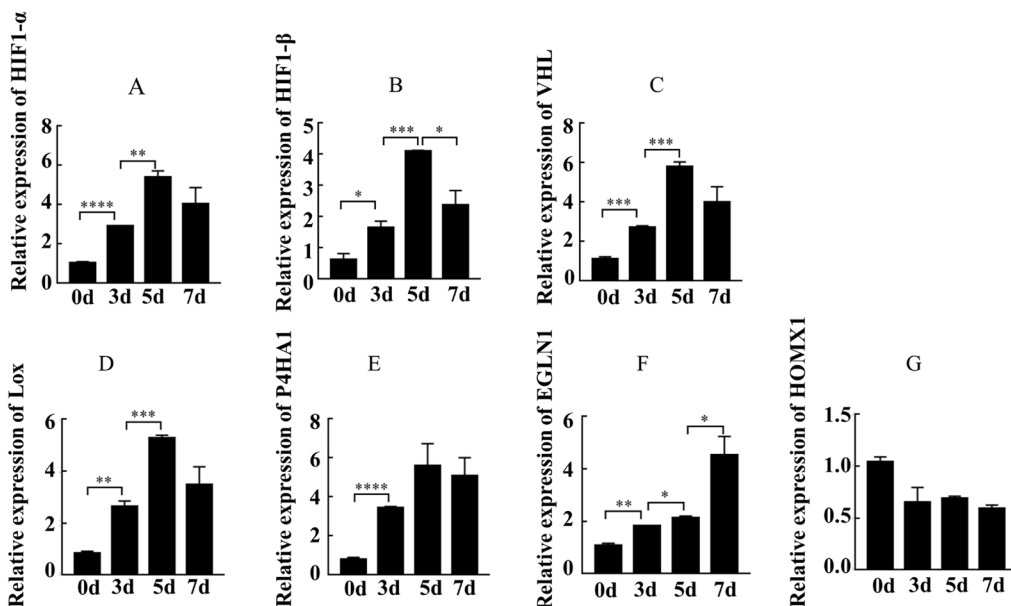
Figure 3. Expression of oxidative stress molecules at the mRNA level during myogenic differentiation. (A) *HIF1-α*, **(B)** *HIF1-β*, **(C)** *VHL*, **(D)** *Lox*, **(E)** *P4HA1*, **(F)** *EGLN1*, **(G)** *HOMX1*.

during myogenic differentiation in human cells with or without myogenic stimuli. *HIF1-α*, *HIF1-β*, *VHL*, *EGLN1*, *Lox*, and *P4HA1* were highly expressed during myogenic differentiation (Figure 4A-4F), and the expression of *HOMX1* decreased with differentiation (Figure 4G), which was consistent with the experimental results.

4. Discussion

Both GEO online analysis and experimental data showed that the expression of *HIF1-α*, *HIF1-β*, *VHL*, *LOX*, *P4HA1*, *EGLN1* genes were up-regulated at the mRNA level, while the expression of *HOMX1* was down-regulated during myogenic differentiation. Based on the above results, we highlight the possible relationship between ROS and myogenic differentiation as follows (Figure 5).

The mammalian *EGLN* family encodes proline hydroxylases, which is involved in the regulation of growth, differentiation and apoptosis of muscle cells, and the expression of EGLN1 is up-regulated in
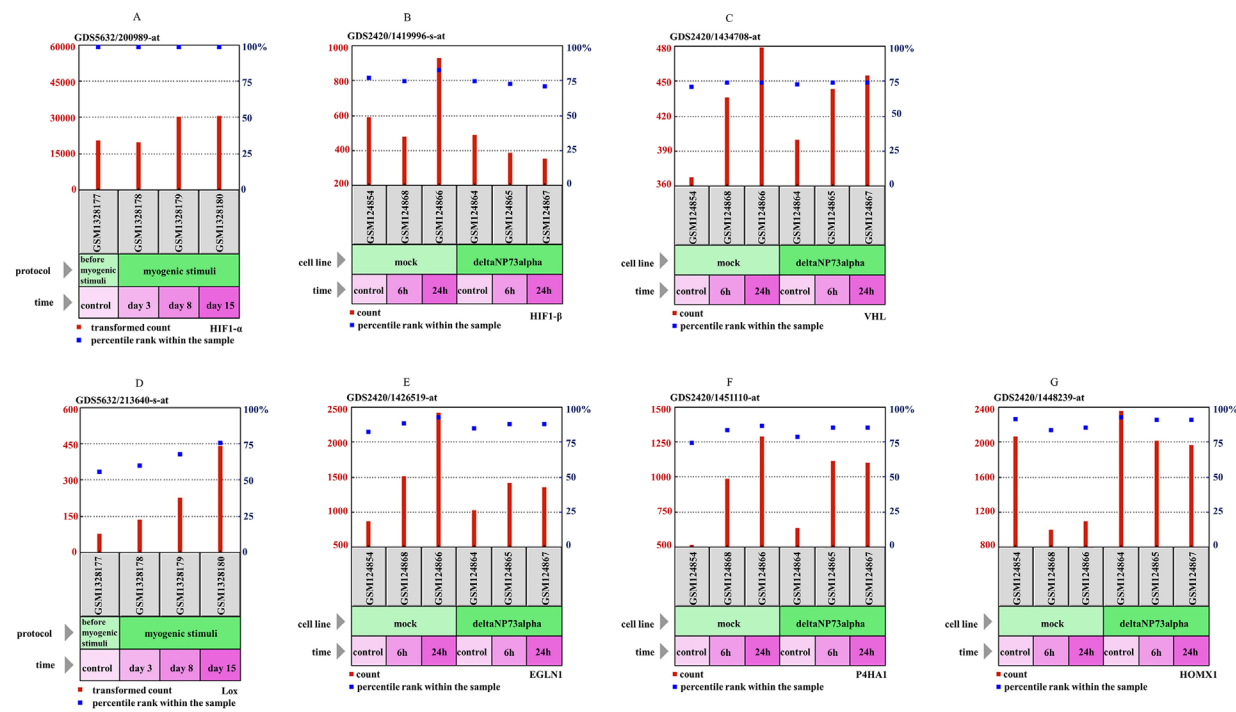
Figure 4. Expression of oxidative stress molecules during myogenic differentiation through bioinformatics prediction. (A) *HIF1-α,* **(B)** *HIF1-β,* **(C)** *VHL,* **(D)** *Lox,* **(E)** *P4HA1,* **(F)** *EGLN1,* **(G)** *HOMX1.*
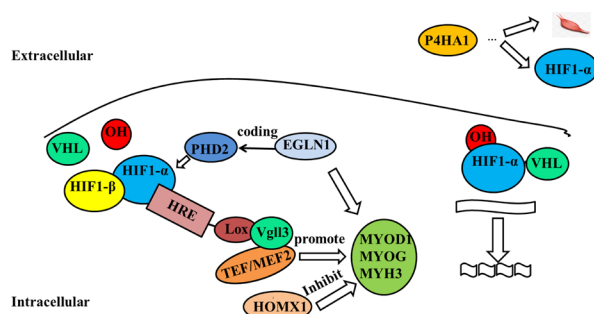
Figure 5. Schematic diagram showing the possible interacting mechanisms between myogenic differentiation and oxidative stress. Under hypoxia, HIF1-PHD2 axis promotes myogenic differentiation through HRE, leading to the expression of MYOD1, MYOG and MYH3. HOMX1 Inhibits myogenic differentiation.

induced vascular smooth muscle cells. The *EGLN1* gene mutation is associated with erythrocytosis and high-altitude hypoxia adaptation (*14,15*). Under hypoxia, the prolyl-4-hydroxylase2 (PHD2) protein encoded by the *EGLN1* gene inhibits hydroxylation of the proline of HIF1-α, HIF-α and β subunits preventing formation of a complete HIF dimer to initiate transcription, thereby increasing downstream target gene expression (*16*). Then HIF1-α binds to the hypoxia response element (HRE) of Lox, promoting the transcription and expression of Lox. Lox combines with vestigial-like family member 3 (VGLL3) co-activator and this conjugate binds with transcriptional enhancer factor/myocyte enhancer factor-2 (TEF/MEF2) to promote the subsequent

expression of MYOD1, myogenin (MYOG), myosin heavy chain 3 (MYH3) genes, thereby stimulating differentiation (*17*). HMOX1, a cell-protective enzyme, is induced in response to oxidative stress, during which it protects tissues and mitigates damage (*18*). Studies have found that the rate-limiting enzyme HMOX1 in the heme degradation pathway effectively inhibits the differentiation of myoblasts by targeting Myomirs and the inhibition of c/EBPδ (*19*), through inhibiting the expression of the primary regulator MYOD1 (*5*). As a tumor suppressor, VHL hydrolyzes proteins through the ubiquitin-proteasome pathway in mammals. VHL can interacts with myogenin (*20*) or HIF1-α (*21*) to degrade it, but VHL down-regulates the expression of myogenin protein in a concentration-dependent manner (*22*). Additionally, P4HA1 is necessary for collagen synthesis and deposition (*23*). Mutation of the *P4HA1* gene causes a congenital connective tissue disease associated with tendon and muscle damage (*24*). In addition, biopsy of a 2-year-old patient with a P4HA1 gene mutation showed muscle fiber atrophy and decreased collagen immune response in the muscle basement membrane (*24*). Through unbiased gene co-expression analysis, the HIF-1 pathway was identified as a potential downstream target of *P4HA1* (*25*). So P4HA1 affects myoblast differentiation and oxidative stress, but the specific molecular mechanism is still unclear.

Therefore, we concluded that the myoblast differentiation of C2C12 cells may be related to oxidative stress and more studies are required to better understand the specific molecular mechanisms between them.

References

1. Jia L, Li YF, Wu GF, Lu HZ, Yang GS, Shi XE. Interference of Sema7A inhibits C2C12 myoblasts proliferation and differentiation. Chinese Journal of Biochemistry and Molecular Biology. 2014; 30:170-178. (in Chinese)

2. Braun T, Buschhausen-Denker G, Bober E, Tannich E, Arnold HH. A novel human muscle factor related to but distinct from MyoD1 induces myogenic conversion in 10T1/2 fibroblasts. EMBO J. 1989; 8:701-709.

3. Rudnicki MA, Schnegelsberg PN, Stead RH, Braun T, Arnold HH, Jaenisch R. MyoD or Myf-5 is required for the formation of skeletal muscle. Cell. 1993; 75:1351-1359.

4. Wright WE, Sassoon DA, Lin VK. Myogenin, a factor regulating myogenesis, has a domain homologous to MyoD. Cell. 1989; 56:607-617.

5. Chargé SB, Rudnicki MA. Cellular and molecular regulation of muscle regeneration. Physiol Rev. 2004; 84:209-238.

6. Parise G, O'Reilly CE, Rudnicki MA. Molecular regulation of myogenic progenitor populations. Appl Physiol Nutr Metab. 2006; 31:773-781.

7. Li R, Jia Z, Trush MA. Defining ROS in biology and medicine. React Oxyg Species (Apex). 2016; 1:9-21.

8. Musarò A, Fulle S, Fanò G. Oxidative stress and muscle homeostasis. Curr Opin Clin Nutr Metab Care. 2010; 13:236-242.

9. Powers SK, Smuder AJ, Criswell DS. Mechanistic links between oxidative stress and disuse muscle atrophy. Antioxid Redox Signal. 2011; 15:2519-2528.

10. Derbré F, Gratas-Delamarche A, Gómez-Cabrera MC, Viña J. Inactivity-induced oxidative stress: a central role in age-related sarcopenia? Eur J Sport Sci. 2014; 14 Suppl 1:S98-S108.

11. Sun QA, Hess DT, Nogueira L, Yong S, Bowles DE, Eu J, Laurita KR, Meissner G, Stamler JS. Oxygen-coupled redox regulation of the skeletal muscle ryanodine receptor-Ca^{2+} release channel by NADPH oxidase 4. Proc Natl Acad Sci U S A. 2011; 108:16098-16103.

12. Youm TH, Woo SH, Kwon ES, Park SS. NADPH Oxidase 4 Contributes to Myoblast Fusion and Skeletal Muscle Regeneration. Oxid Med Cell Longev. 2019; 2019:3585390.

13. Le Moal E, Pialoux V, Juban G, Groussard C, Zouhal H, Chazaud B, Mounier R. Redox control of skeletal muscle regeneration. Antioxid Redox Signal. 2017; 27:276-310.

14. Bonnin A, Gardie B, Girodon F, Airaud F, Garrec C, Bézieau S, Vignon G, Mottaz P, Labrousse J, Lellouche F. A new case of rare erythrocytosis due to EGLN1 mutation with review of the literature. Rev Med Interne. 2020; 41:196-199. (in French)

15. Simonson TS, Yang Y, Huff CD, Yun H, Qin G, Witherspoon DJ, Bai Z, Lorenzo FR, Xing J, Jorde LB, Prchal JT, Ge R. Genetic evidence for high-altitude adaptation in Tibet. Science. 2010; 329:72-75.

16. Zhou Y, Ouyang N, Liu L, Tian J, Huang X, Lu T. An EGLN1 mutation may regulate hypoxic response in cyanotic congenital heart disease through the PHD2/HIF-1A pathway. Genes Dis. 2018; 6:35-42.

17. Gabay Yehezkely R, Zaffryar-Eilot S, Kaganovsky A, Fainshtain Malka N, Aviram R, Livneh I, Hasson P. Intracellular role for the matrix-modifying enzyme lox in regulating transcription factor subcellular localization and activity in muscle regeneration. Dev Cell. 2020; 53:406-417.e405.

18. Xu XZ, He P. Heme oxygenase-1 and oxidative stress. Zhongguo Dang Dai Er Ke Za Zhi. 2009; 11:706-709. (in Chinese)

19. Kozakowska M, Ciesla M, Stefanska A, *et al.* Heme oxygenase-1 inhibits myoblast differentiation by targeting myomirs. Antioxid Redox Signal. 2012; 16:113-127.

20. Pickart CM. Back to the future with ubiquitin. Cell. 2004; 116:181-190.

21. Tarade D, Ohh M. The HIF and other quandaries in VHL disease. Oncogene. 2018; 37:139-147.

22. Fu J, Menzies K, Freeman RS, Taubman MB. EGLN3 prolyl hydroxylase regulates skeletal muscle differentiation and myogenin protein stability. J Biol Chem. 2007; 282:12410-12418.

23. Gilkes DM, Bajpai S, Chaturvedi P, Wirtz D, Semenza GL. Hypoxia-inducible factor 1 (HIF-1) promotes extracellular matrix remodeling under hypoxic conditions by inducing P4HA1, P4HA2, and PLOD2 expression in fibroblasts. J Biol Chem. 2013; 288:10819-10829.

24. Zou Y, Donkervoort S, Salo AM, *et al.* P4HA1 mutations cause a unique congenital disorder of connective tissue involving tendon, bone, muscle and the eye. Hum Mol Genet. 2017; 26:2207-2217.

25. Xu R. P4HA1 is a new regulator of the HIF-1 pathway in breast cancer. Cell Stress. 2019; 3:27-28.

*Address correspondence to:
Yanqin Lu and Jinxiang Han, Shandong First Medical University & Shandong Academy of Medical Sciences, # 6699 Qingdao Road, Ji'nan, Shandong250117, China.
E-mail: yqlu@sdfmu.edu.cn (YL), jxhan@sdfmu.edu.cn (JH)

Original Article

Rare and intractable fibrodysplasia ossificans progressiva shows different PBMC phenotype possibly modulated by ascorbic acid and propranolol treatment

Deborah Ribeiro Nascimento[1], Suzana Lopes Bomfim Balaniuc[1], Durval Batista Palhares[1], Adam Underwood[2], Marilene Garcia Palhares[1], Fabiana Alves[3,4], Francisco Oliveira Vieira[3,4], Elaine Maria Souza-Fagundes[3], Liane De Rosso Giuliani[1], Paula Cristhina Niz Xavier[1], Helen Lima Del Puerto[3], Robson Augusto Souza Santos[3], Amy Milsted[2], Jose Mauro Brum[5], Iandara Schettert Silva[1], Almir Sousa Martins[1,3,*]

[1] UFMS/ Faculty of Medicine, Campo Grande, MS, Brazil;
[2] Walsh University, Division of Mathematics and Sciences, North Canton, OH, USA;
[3] UFMG/ Department of Physiology and Biophysics, Belo Horizonte, MG, Brazil;
[4] Centro Universitário Metodista Izabela Hendrix- IMIH, Belo Horizonte, MG, Brazil;
[5] Procter & Gamble Health Care & Global Clinical Sciences, Mason, OH, USA.

SUMMARY   Fibrodysplasia Ossificans Progressiva (FOP) is a rare congenital intractable disease associated with a mutation in *ACVR1* gene, characterized by skeleton malformations. Ascorbic acid (AA) and propranolol (PP) in combination is reported to minimize flare-ups in patients. FOP leukocyte phenotype may possibly be modulated by AA and PP treatment. In this study, expression of 22 potential target genes was analyzed by RT-PCR in peripheral blood mononuclear cells culture (PBMC) from FOP patients and controls to determine effectiveness of the combination therapy. PBMC were treated with AA, PP and AA+PP combination. Basal expression of 12 of the 22 genes in FOP PBMC was statistically different from controls. *ACVR1*, *ADCY2*, *ADCY9* and *COL3* were downregulated while *COL1* was upregulated. *ADRB1*, *ADRB2*, *RUNX2*, *TNF-α* and *ACTB*, were all overexpressed in FOP PBMC. In control, AA upregulated *COL1*, *SVCT1*, *ACTB*, *AGTR2* and downregulated *ADCY2*. In FOP cells, AA upregulated *ACVR1*, *BMP4*, *COL1*, *COL3*, *TNF-α*, *ADCY2*, *ADCY9*, *AGTR2* and *MAS*, while downregulated *ADBR2*, *RUNX2*, *ADCY1*, *SVCT1* and *ACTB*. PP increased *ADBR1* and decreased *RUNX2, TNF-α, AGTR1, ACTB* and *CHRNA7* genes in treated control PBMC compared to untreated. PP upregulated *ADBR1*, *ADBR2* and *MAS*, and downregulated *TNF-α* and *ACTB* in treated FOP PBMC versus untreated. AA+PP augmented *ADRB1* and *ADRB2* expressions in control PBMC. In FOP PBMC, AA+PP augmented *ACVR1*, *COL1*, *COL3*, *ADBR1*, *AGTR2* and *MAS* expression and downregulated *ADBR2*, *RUNX2*, *ACTB* and *MRGD*. These data show distinct gene expression modulation in leukocytes from FOP patients when treated with AA and or PP.

Keywords   FOP, gene expression modulation, peripheral blood mononuclear cells, FOPCON

1. Introduction

Fibrodysplasia ossificans progressiva (FOP) is a rare intractable autosomal dominant disease affecting one in every two million individuals, characterized by congenital skeletal malformations and postnatal heterotopic ossification. In newborns FOP does not stimulate developmental skeletal deformation, except for hallux valgus (*1*). Classical FOP individuals have a heterozygous mutation (c.617G>A, p.R206H) in the *ACVR1* receptor gene, or *ALK2*, located on chromosome 2q23-24 (*2*). This mutation confers a gain of function, activating the signaling pathway of BMP [bone morphogenic protein] independent of ligand stimulation and also functions as a Type II receptor BMP independent. In addition, activin-A, a TGF-β-related cytokine, and BMP, competitive antagonist in wild *ACVR1*, is recognized as an agonist in *ACVR1* R206H (*1,3*).

FOP pathophysiology shows an impaired BMP signaling pathway that correlates to ontogeny defects in embryonic stage and to development and progress

of heterotopic ossification (HO) in postnatal life. This is often preceded by inflammatory processes induced or spontaneous (*1,2*), favored by a less perfused and acidic pH tissue microenvironment. Further, this aberrant process usually begins in the first decade of life and progresses with developmental maturation, leading to ankylosis of the major joints and chest fusion. Immune system neutrophils, macrophages and importantly mast cells are recruited, stimulating secretion of several cytokines. Muscle tissue and adjacent soft tissues are degraded and replaced by fibroproliferative cells that generate cartilage and subsequently ectopic bone (*4*).

Pathways of the autonomous nervous system (ANS) play important roles in neovascularization and in final osteoblast and osteoclasts differentiation (*5*). Gaps exist in knowledge of the role of adrenergic pathways and receptors in the algesia, inflammatory crises and in ectopic bone formation in FOP. Understanding of neural anti-inflammatory pathways functioning as important neuronal regulators of immune response need to be clarified (*6*). Imbalance of the two main axes of the renin-angiotensin system (RAS) has also been implicated in the pathogenesis of this and other inflammatory and fibrotic processes (*7*).

Curative therapy is currently not available, nor FOP medications completely free of side effects. FOP management aims to control flare-ups and symptoms by corticosteroids, mast cell inhibitors, non-steroidal anti-inflammatory drugs, cyclooxygenase inhibitors, bisphosphonates, muscle relaxants, bone marrow transplants, rosiglitazone, retinoic acid receptor agonists and commonly used treatments for pain, including narcotic analgesics (*1*). Clinical trials are being developed with anti-activin A antibodies/REGN2477 (phase 2), Rapamycin (phases 2, 3) and Palovarotene (phase 3). Results are promising, with adverse effects under study and carefully monitored (*3,8*). A wide range of molecular mechanisms is involved in the exacerbated activation of the mutated gene in FOP in addition to the aberrant BMP-Smad 1/5/8 signaling (*9*). It is relevant to consider the study of factors not yet explored in FOP.

In some patients, FOP symptoms are improved by ascorbic acid (AA). This antioxidant, anti-inflammatory and modulator of collagen synthesis is reported to reduce outbreaks, and transiently stabilize crisis, either used alone or in combination with disodium etidronate (*10*). Long studied and approved for various clinical indications, ascorbic acid is a therapeutic possibility for anti-growth and invasiveness of solid cancers, and is a useful therapeutic supplement in several angiogenic diseases (*11,12*). Despite many studies demonstrating the efficacy of AA in gene expression regulation, and genomic modulation and differentiation of embryonic stem cells (*11-14*), it has not been considered for regulation of FOP pathophysiology pathways.

Since AA may help in FOP treatment, and the nonspecific adrenergic β-blocker propranolol (PP)

has surfaced as an important treatment of infantile hemangioma with potential antiangiogenic effects (*15*), Palhares *et al.* (*10*), have suggested using propranolol with ascorbic acid (FOPCON) for continuous administration to FOP patients. However, the mechanisms by which AA+PP work are not yet clarified. The hypothesis of the work presented here is that transcription of genes directly or indirectly involved in heterotopic ossification is modulated by vitamin c and the β-blocker propranolol in a cell culture model of PBMC from FOP patients, compared to control individuals.

2. Materials and Methods

2.1. Samples

Peripheral blood mononuclear cells (PBMC) were cultured using peripheral whole blood samples collected by antecubital venipuncture from volunteers (FOP [*n* = 8] and healthy control subjects [*n* = 8]). Whole blood was collected in heparinized tubes, kept at 4°C for up to 24 hours prior to processing. Volunteer participants were informed and signed the consent form (ICF). This research was approved by Research Ethics Committee of the Federal University of Minas Gerais (document #403073/CAAE 17422113.3.0000.5149).

2.2. PBMC culture

PBMC method was performed as previously described (*16*) with some modification. Briefly, 15 mL heparinized blood was transferred to 50 mL Falcon tube containing Ficoll-diatrozoate mixture (Histopaque®-1077, Sigma® 10771), ratio 1:2 of Ficoll-diatrozoate/blood. The leukocyte ring obtained by ficoll density gradient by centrifugation 40 min/1.400 rpm/24°C, maximum acceleration specification and minimum braking at high-speed centrifuge (Heraeus Multifuge X3R Centrifuge - Thermo SCIENTIFIC®). Mononuclear cells were collected from plasma:Ficoll-diatrozoate interface, transferred to new tubes and washed 3× in culture medium, twice in sterile DEMEM medium (Gibco® pH, 7.2 to 7.4) and once in complete RPMI 1640 medium (10% fetal bovine serum + L-glutamine + gentamicin + streptomycin, pH 7.4) (Gibco® pH, 7.2 to 7.4). Cells washed at 1200rpm/7 min/4°C were resuspended in 1 mL complete RPMI Medium. Cell density was adjusted to desired concentration after counting in Newbauer Chamber with Trypan Blue. Required sterile procedures were performed in laminar flow hood (BIOSEG® 12, VECO Group). Cell culture was performed in a 24-well plate, with 640 or 800 microliters of the cell suspension (1.2×10^6 or 1.5×10^6 cells) cultured and stabilized for 24 hours in complete RPMI 1640 medium, maintained in a CO_2 incubator (5%) at 37°C (Thermo scientific® / Forma Series II Water Jacket CO_2 incubator).

2.3. Treatments of PBMC

Treatment with propranolol, ascorbic acid and propranolol plus ascorbic acid was performed after 24 hours of cell cultivation and stabilization, in triplicate for 96-well plate cell viability assessment at 3×10^5 cells per well and in 24-well plates, for 24 hours in CO_2, incubator at 1.2×10^6 or 1.5×10^6 cells for Real-time PCR. Ascorbic acid (L [+] - Ascorbinsaure Zur Analyze; Vitamin C C6H8O6 pro Analysis 13496OS Art. 127 pa Merck®) dosage used for the treatment was standardized, and optimal dosage (2 mM) was maintained (*16*). Propranolol (Propranolol HCL from CHANGZHOU YABANG® evaluated Quality Control by All Chemistry Laboratory under number ALL 46092-1) treatment dose was 15 µM (*17,18*). Ascorbic acid solution was prepared in complete RPMI 1640 Medium (AA, q.s.p 5 mL of medium), and pH adjusted to 7.4 with NaOH. Propranolol was also prepared in complete RPMI 1640 Medium (0.22 mg propranolol, q.s.p. 5 mL medium) but no pH adjustment was required. Both solutions were sterile filtered (SF; 22 µm) under laminar flow hood (BIOSEG® 12, VECO Group). Trypan blue stained cells were counted after 24 hours of treatment to analyze viability.

2.4. Total RNA extraction

Cultured 1.2×10^6 to 1.5×10^6 treated and untreated cells were transferred from plate to 1.5 mL microcentrifuge tubes, centrifuged immediately at 1,200 rpm (bench-top refrigerated centrifuge, 3K30 Sigma®) for 7 min, to concentrate cell pellet. Total RNA was extracted using Stat-60® reagent, according to manufacturer protocol. RNA was resuspended in 25 µL of DEPC water, quantified at 260 nm in a Denovix® DS-11 nanodrop. Total RNA was DNase I treated (TURBO DNA-free kit, Ambion Inc., Foster, California, USA), DNase I was inactivated with EDTA/75ºC/10 min according to manufacturer's protocol. Aliquots were re-quantified at 260 nm for later use in RT-PCR.

2.5. Oligonucleotide primers

Oligonucleotide primers, described in Table 1, for reverse transcription (RT) and real-time PCR (qPCR) were designed through GenBank sequences in BLASTn program analysis (*https://blast.ncbi.nlm.nih.gov/Blast. cgi*), synthesized by IDT (Integrated DNA technologies; *http://www.idtdna.com*), received lyophilized, resuspended in sterile filtered H_2O (0.22 µm; q.s.p. 100 pmol/µL) and stored as 10 pmol/µL at -20°C. S26 mRNA was the endogenous normalizer.

2.6. Reverse transcription (RT) and Real-time PCR (qPCR)

Single-stranded complementary DNA synthesis (sscDNA) was performed by RT. Briefly, 700 ng of RNA was pre-incubated at 70ºC for 10 min with 10 pmol of each reverse primer with 10 pmol of oligo dT18 primer (Invitrogen), followed by ice storage on the bench.

Table 1. Targeted genes and selected oligonucleotide primers

Gene	mRNA Description	Oligonucleotide primer sequences	Target (bp)
ACVR1	activin A receptor type 1	F<CTGCCTTCGAATAGTGCTGTCCAT>R<TAAATCTCGATGGGCAATGGCTGG	100
BMP4	bone morphogenetic protein 4	F<CAGGAGATGGTAGTAGAGGGATGT>R<AGTCTGTGTAGTGTGTGGGTGA	140
COL1	collagen type I α-1 chain	F<CAAAGGAGACACTGGTGCTAAG>R<CTCCTCGCTTTCCTTCCTCTC	89
COL3	collagen type III α-1 chain	F<AGCTGTTGAAGGAGGATGTTCCCA>R<TTTGGCATGGTTCTGGCTTCCA	77
ADRB1	Adrenoceptor β-1	F<TTCTACGTGCCCCCTGTGCATC>R<GATCTTCTTCACCTGCTTCTGG	78
ADRB2	adrenoceptor β-2	F<CTGTGCGTGATCGCAGTGGAT>R<CTTATTCTTGGTCAGGCTC	78
RUNX2	RUNX family trans. factor 2	F<CTTGACCATAACCGTCTTCAC>R<CGAGGTCCATCTACTGTAACT	81
TNF-α	tumor necrosis factor α	F<CCAGGGACCTCTCTCTAATCA>R<CTTTGCTACAACATGGGCTAC	95
ACTB	β-actin mRNA	F<TCACCCACACTGTGCCCATCTACGA>R<CAGCGGAACCGCTCATTGCCAATGG	295
ADCY1	adenylate cyclase 1	F<TGGTCACCTTCGTGTCCTATG>R<CTGTGACCAGCAAGTGCGACG	98
ADCY2	adenylate cyclase 2	F<GCCTTGTTGCCATGGGATACCT>R<TGAAGAGGAAGAACGATACCTG	81
ADCY7	adenylate cyclase 7	F<GTGTTCGACGCATGGACAAAG>R<GCTGAAGGGCAGTAGTGTGTA	96
ADCY9	adenylate cyclase 9	F<GCTACCGGGTCCTCAACGAG>R<ATGTACGTGGCTCCGATGGT	103
SVCT1	Sodium vit. C carrier type 1	F<ACTCTCCTCCGCATCCAGATCTTC>R<TGTCAAGGTCAGGACATAGCA	90
SVCT2	Sodium vit. C carrier type 2	F<TGCTCGAGCCATCCTGTCTTTAG>R<AGATGTGTTCTGTGTGCAACAG	98
AGTR1	angiotensin II receptor type 1	F<TTCAGCCAGCGTCAGTTTCA>R<GGCGGGACTTCATTGGGT	101
AGTR2	angiotensin II receptor type 2	F<TATGGCCTGTTTGTCCTCATTG>R<CCATTGGGCATATTTCTCAGGT	115
MAS	MAS1 proto-oncogene GPCR	F<GCTACAACACGGGCCTCTATCTG>R<TACTCCATGGTGGTCACCAAGC	160
MRGD	MAS related GPCR D	F<TCCCTGCCTCTGAGCATCTA>R<GAGAGGCGTGACAAGCTGAA	100
CHRNA7	Cholinergic α-7 subunit receptor	F<CTTTACAAGGAGCTGGTCAAGAAC>R<GCTCAGGGAGAAGTAGACGGTGA	90
IL10	interleukin 10	F<ATGAGCATTCAGACTGGGTAAAC>R<TTTTAGGGGCTAAGAAACGCAT	123
ALPL	alkaline phosphatase	F<TGTCATCATGTTCCTGGGAGATGG>R<CAGGGTTGTGGTGGAGCTGAC	86
S26	S26 ribosomal protein RNA	F<TGTGCTTCCCAAGCTGTATGTGAA>R<CGATTCCTGACTACTTTGCTGTG	75

(Bp) base pair; (F) forward sense (5′-3′); (R) reverse anti-sense (5′-3′).

Then, 40 U (11 µL) of reverse transcriptase enzyme mix in RT buffer (50 mM KCl, 20 mM Tris-HCl, pH 8.4) containing 2 µL of dNTP mix (10 mM each) were incubated at 45°C/1 hour, with RNA and primer solution. RT was terminated at 4°C and immediately used in qPCR, or frozen at -20°C, until qPCR. All reagents were from Invitrogen™ (SuperScript™ First-Strand Synthesis System for RT-PCR). sscDNA samples were used in qPCR performed on *QuantStudio 6 Flex Real-Time System*® (ThermoFisher Scientific,) using reaction protocol described by the SYBR Green PCR Master Mix Kit (Invitrogen Life Technologies, Carlsbad, CA, USA). Triplicate samples were applied to 384-well plates (ABI PRISM® 384-Well Optical Reaction Plate with Barcode, Invitrogen Life Technologies, Carlsbad, CA, USA), in a final reaction volume of 10 µL each. Aliquots of 0.8 µL of sscDNA from the samples were pipetted into each channel of the plate plus 9.2 µL of SYBR Mix (5 µL of the SYBR Green PCR Master Mix Kit, 0.6 µL of each primer (sense and antisense; 10 pmol/µL) and 3 µL sterile filtered water). The plate was sealed with optical adhesive (ABI PRISM® Optical Adhesive Covers, Invitrogen Life Technologies, Carlsbad, CA, USA). qPCR performed as: [stage 1] a 50°C / 2 min cycle; [stage 2] a cycle at 95°C/10 min; [stage 3] 40 cycles of 95°C/15 s, followed by a dissociation curve from 60°C.

Relative quantification of mRNA expressions determined by comparative analysis with endogenous control, using comparative CT method, as $2^{-\Delta\Delta CT}$ method for relative levels of gene expression was applied (*19*). Data were analyzed in *GraphPad Prism 5* program for statistics, and unpaired *t* test plus ANOVA were applied. Results were statistically significant for $p \leq 0.05$.

3. Results

3.1. PBMC viability

Viability was assessed by trypan blue staining. PBMC were viable after treatment with Propranolol and ascorbic acid at 15 µM and 2 mM, respectively, and used in experiments.

3.2. Phenotype profile

Phenotype profile differences were detected as observed (Figure 1, Table 2, Tables S2 and S4, http://www.irdrjournal.com/action/getSupplementalData.php?ID=74) by the variations in mRNA expression among PBMC of control individuals versus FOP PBMC. Twelve out of 22 genes (54.5%) showed significant expression differences, when baseline mRNA expression was compared to control cells. There was no significant difference of baseline mRNA expression for *BMP-4*, *ADCY7*, *SVCT2*, *AGTR1*, *AGTR2*, *MAS*, *MRGD*, *CHRNA7*, *IL-10* and *ALPL* genes (Figure 1, Table 2).

3.3. Ascorbic acid effect on gene expression

Expression data demonstrated gene modulation by AA in both patient and control PBMC in culture (Table 2 and Table S1, *www.irdrjournal.com/action/getSupplementalData.php?ID=74*). AA treatment of normal PBMC modulated five out of 22 genes (22.7%), with *COL1*, *ACTB*, *SVCT1* and *AGTR2* upregulated and *ADCY2* downregulated, while significant upregulation of *ACVR1*, *BMP4*, *COL1*, *COL3*, *ADRB1*, *TNF-α*, *AGTR2* and *MAS* occurred in FOP PBMC. When AA treated FOP PBMC was compared to untreated FOP PBMC, there was downregulation of *ADRB2*, *RUNX2*, *ACTB* and *ADCY1* genes (Table 2 and Table S3, *www.irdrjournal.com/action/getSupplementalData.php?ID=74*). Further, downregulation was observed in *MAS* and *MRGD* genes, in controls (Tables 2 and Table S1, *www.irdrjournal.com/action/getSupplementalData.php?ID=74*), at both baseline and after treatment. *ADCY1*, *2*, *7* and *9*, *SVCT1* and *SVCT2* coding genes, were here checked only for AA. All *ADCY*, but 7, were altered in FOP PBMC
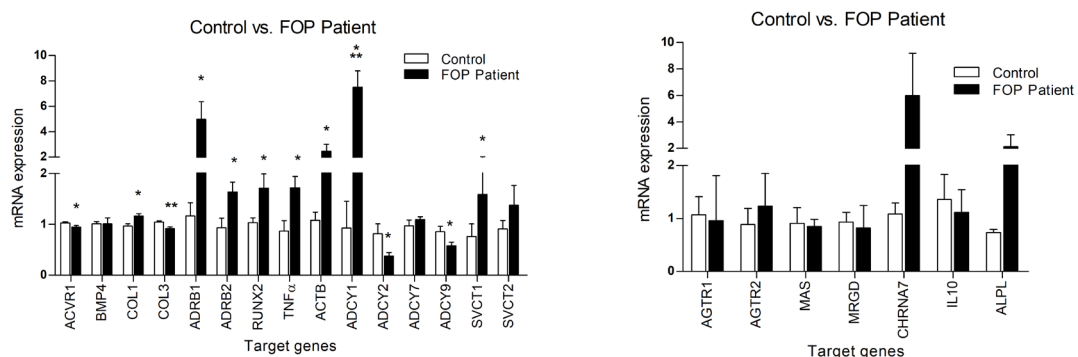
Figure 1. Distinct gene expression profiles between FOP peripheral blood mononuclear cells versus control cells. FOP PBMC basal profile gene expressions were statistically different compared to controls (*$p < 0.05$; **$p < 0.01$; ***$p < 0.001$). *ACVR1*, *ADCY2*, *ADCY9* and *COL3* showed downregulated and *COL1* upregulated. *ADRB1* and *2*, *RUNX2*, *TNF-α* and *ACTB*, were most overexpressed in FOP PBMC among evaluated mRNAs. There was no significant difference of baseline mRNA expression for *BMP-4*, *ADCY7*, *SVCT2*, *AGTR1*, *AGTR2*, *MAS*, *MRGD*, *CHRNA7*, *IL-10* and *ALPL* genes.

Table 2. Illustration of gene modulation in FOP PBMC and groups control in response to *in vitro* treatments with ascorbic acid (AA), propranolol (PP) and propranolol combined with ascorbic acid (PPAA) and comparisons

Genes	FOP X Control	Cont. AA X Cont.	FOP AA X FOP	FOP AA X Contr.	FOP AA X Contr. AA	Contr. PP X Contr.	FOP PP X FOP	FOP PP X Contr.	FOP PP X Contr. PP	Contr. PPAA X Contr.	FOP PPAA X FOP	FOP PPAA X Contr.	FOP PPAA X Contr. PPAA
ACVR1	↓	-	↑	↑↑	↑↑	-	-	-	-	-	↑	↑	↑↑
BMP4	-	-	↑↑	↑	↑↑	-	-	-	↑	-	-	-	-
COL1	↑	↑	↑↑	↑↑↑	↑↑	-	-	-	-	-	↑	↑↑	-
COL3	↓↓	-	↑	↑↑	↑↑	-	-	-	-	-	↑	↑	-
ADRB1	↑	-	↑	↑	↑	↑	↑	↑↑	↑	↑↑	↑	↑	-
ADRB2	↑	-	↓	-	↓	-	↑	↑	↑	↑	↓	-	-
RUNX2	↑	-	↓	-	↓	↓	-	-	↑	-	↓	-	-
TNF-α	↑	-	↑	↑	↑	↓	↓	-	↑	-	-	↑	↑
ACTB	↑	↑	↓	-	↓	↓↓	↓↓	↓↓	-	-	↓	-	↓
ADCY1	↑↑↑	-	↓↓	-	N	N	N	N	N	N	N	N	N
ADCY2	↓	↓	↑	-	N	N	N	N	N	N	N	N	N
ADCY7	-	-	-	-	N	N	N	N	N	N	N	N	N
ADCY9	↓	-	↑↑↑	-	N	N	N	N	N	N	N	N	N
SVCT1	↑	↑	↓	-	N	N	N	N	N	N	N	N	N
SVCT2	-	-	-	-	N	N	N	N	N	N	N	N	N
AGTR1	-	-	-	-	-	↓	-	↓	-	-	-	-	↓
AGTR2	-	↑	↑↑	↑↑↑	-	-	-	↑	↑	-	↑	↑	↑
MAS	-	-	↑	↑	↑	-	↑	↑	↑	-	↑	↑↑	↑
MRGD	-	-	-	↓↓	↓↓	-	-	↓↓	↓	-	-	↓↓	↓↓↓
CHRNA7	-	-	-	↓↓	↓↓	↓	-	-	-	-	-	↓↓	↓
IL-10	-	-	-	-	↓	-	-	-	-	-	-	-	-
ALPL	-	-	-	↑	-	-	-	-	-	-	-	-	-

Modulation (arrows); (-) not significant; ↑/↓ = up/downregulation ($p \leq 0{,}05$); ↑↑/↓↓ = up/downregulation ($p = 0{,}001$ to $\leq 0{,}01$); ↑↑↑/↓↓↓ = up/downregulation ($p < 0{,}001$); (N) not experimented.

compared to normal PBMC base line expressions. When FOP PBMC were treated with AA, *ADCY 1*, *2* and *9* were reversed, that is, upregulated *ADCY 1* showed a reduction in expression, while downregulated *9* and *2*, were increased. However, the final expression of all *ADCY* analyzed were brought to physiological mRNA expression levels, similar to control PBMC (Table 2).

3.4. Propranolol effects

In PBMC of normal individuals PP modulated 37.5% (6/16) of genes. It increased *ADBR1* and decreased *RUNX2*, *TNF-α*, *AGTR1*, *ACTB* and *CHRNA7* genes in control PBMC, compared to untreated control (Table 2). FOP PBMC responded to PP by modulating 31.2% (5/16) genes by increasing *ADRB1*, *ADRB2* and *MAS*, while decreasing *TNF-α* and *ACTB* when compared to baselines of untreated FOP PBMC (Table 2 and Table S3, *www.irdrjournal.com/action/getSupplementalData.php?ID=74*). PP treated FOP PBMC compared to untreated control PBMC, kept increased *ADBR1* and *ADBR2*, while showing significant downregulation of *AGTR1*, *MRGD* and *CHRNA7*, and upregulation of *AGTR2* and *MAS* in FOP cells in response to treatment with propranolol (Table 2 and Table S2, *www.irdrjournal. com/action/getSupplementalData.php?ID=74*).

3.5. Ascorbic acid and propranolol (AA+PP) combination effects on gene expression

In normal control PBMC, the combination of AA with PP resulted in the modulation of only two out of 16 genes (12.5%) studied, up regulation of *ADBR1* and *ADBR2* (Table 2 and Table S1, *www.irdrjournal.com/ action/getSupplementalData.php?ID=74*). However, the effect of AA+PP over PBMC of FOP carriers, compared to normal control PBMC, resulted in a statistically significant modulation of FOP gene profile, by upregulating *ACVR1*, increasing *COL1*, reversing *COL3* from down to upregulation, kept same profile for *ADRB1* but normalized *ADBR2*, counter-regulatory modulations in the expression of *ACVR1*, *COL3*, *ADRB2*, *RUNX2* and *ACTB* in relation to the baseline state of FOP PBMC, while increasing *AGTR2* and *MAS* genes, AA+PP downregulated *ADRB2*, *RUNX2* and normalized *ACTB* (Table 2 and Table S2, *www.irdrjournal.com/ action/getSupplementalData.php?ID=74*). *MRGD* and *CHRNA7* mRNA expressions were significantly downregulated by AA+PP, when FOP PBMC were compared to normal control group and after treatment. An overview of summarized data is shown in Table 2 and Figure 2.

4. Discussion

The study of FOP is hindered by tissue sample restrictions inherent to deep connective tissues traumas which trigger HO. Cellular models, including Epstein-Barr transformed lymphoblast cell lines, dental pulp
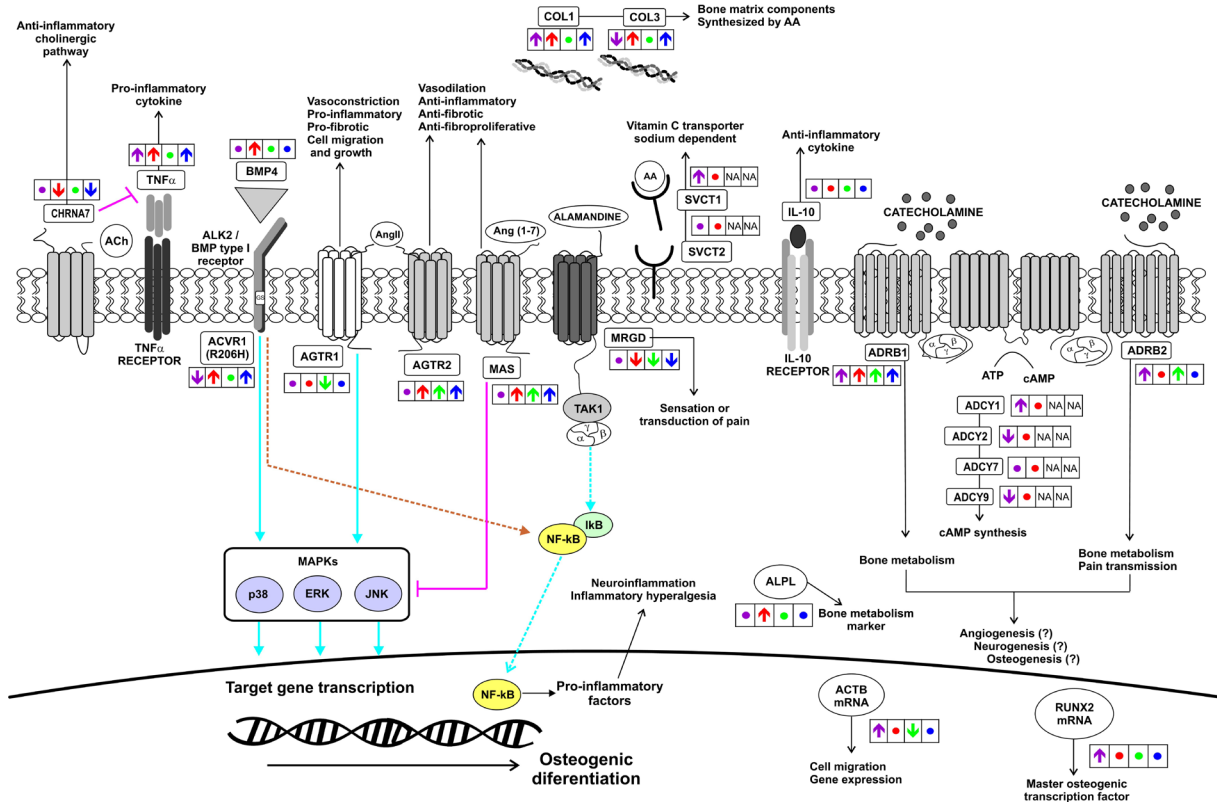
Figure 2. Proposed mode of ascorbic acid + propranolol effect on the expression of downstream targets modulating fibrodysplasia ossificans progressiva peripheral blood mononuclear cells compared to normal PBMC. FOP PBMC mRNA expressions compared to normal control PBMC at basal (**Purple**), AA treatment (**Red**), PP treatment (**Green**) and AA+PP treatment (**Blue**); (●) equal to control or unchanged; (**NA**) not experimented. FOP PBMC basal mRNA expression was statistically significant ($p \leq 0.05$) (Figure 1) when compared to controls. *ACVR1*, *ADCY2*, *ADCY9* and *COL3* showed downregulated and *COL1* upregulated. AA upregulated *ACVR1*, *BMP4*, *COL1*, *COL3*, *TNF-α*, *ADCY2*, *ADCY9*, *AGTR2* and *MAS*, while downregulating *ADBR2*, *RUNX2*, *ADCY1*, *SVCT1* and *ACTB*. PP upregulated *ADBR1*, *ADBR2* and *MAS*, while downregulating *TNF-α* and *ACTB*. The combination of AA+PP augmented expressions of *ACVR1*, *COL1*, *COL3*, *ADBR1*, *AGTR2* and *MAS* but downregulated *ADBR2*, *RUNX2*, *ACTB* and *MRGD* genes, when compared to untreated (OBS: the graph map molecules are only representative designs, but without complex structural biochemical purpose).

stem cells from FOP children (*20*), and induced stem cells from dermal fibroblasts from skin biopsy (*21*), are important tools, yet of limited access. We evaluated cultured FOP PBMC and data points to a prone unbalanced inflammatory phenotypic profile state of gene expressions in FOP cells. FOP cells showed an altered basal gene expression profile. Renin-angiotensin system receptor genes did not comprise the mRNA profile of FOP, yet they were clearly regulated in response to proposed treatments. AA and PP alone or in combination, are shown to modulate anti-inflammatory gene effects. Dose results used were consistent with literature of different cell cultures (*13,17,18,22*).

Half of the genes evaluated from FOP PBMC were sensitive to treatments, in contrast to ~13% of genes in control PBMC. PP alone modulated eight genes in FOP PBMC and six in normal PBMC, among 16 genes studied. AA and PP combination changed expressions of ~63% of FOP PBMC analyzed genes, while only two genes were regulated in the control group. These data show that the PBMC model may useful while

elucidating the broader impact of the *ACVR1* gene mutation in concert with the other FOP-related genes not yet included in pathophysiology pathways. AA may modulate genes epigenetically as verified in other studies (*13,23*).

There are few reports on AA+PP pharmacokinetics interactions. AA may influence PP absorption and first-pass metabolism in healthy young humans, slightly reducing plasma PP availability and decreasing its urinary excretion, but elimination rate is not changed (*24*). Apart from this, AA+PP may contribute to the beneficial effects of beta-blockers that minimize human atrial fibrillation (*25*). The interaction of AA+PP *in vivo* as well as *in vitro* remains to be clarified. AA shows Na+ dependent high affinity to transporters SVCT1 and SVCT2 proteins after digestion. SVCT1 expression has been shown to occur in intestine and kidney, transporting AA into and from the blood. However, it remains unclear if SVCT1 is an AA receptor and therefore how AA is transported in pathological conditions (*13*). Membrane bound SVCT2 allows intracellular AA to exceed

extracellular concentration (*13,23*). Our data showed *SVCT2* gene expression is stable, with no alteration of expression in both FOP and control cells. Yet, *SVCT1* was overexpressed in FOP PBMC and sensitive to the AA downregulation effect in FOP PBMC.

PBMC adenylate cyclase coding genes *(ADCY) 1*, *2*, *7* and *9*, were also checked for AA modulation. *ADCY 1*, *2* and *9* expressions were altered in FOP PBMC, yet AA reversed this and brings expression back to physiological levels. Additionally, using Northern blot and qPCR analysis, others have reported *ADCY1*, *ADCY7* and *ADCY9* are highly expressed while *ADCY2* is downregulated in peripheral blood leukocyte cells (*26*). AA modulation of *ADCY* genes shows a new approach to target pathophysiology of FOP. Given that AA is a competitive inhibitor of ADCY, it may suppress genes under control of cAMP-dependent pathways (*13*), changing intracellular cAMP concentrations, thus inhibiting peripheral myelin protein-22 (PMP22) by suppressing *PMP22* gene expression (*13,27*). Intracellular cAMP favors ubiquitous expression of proinflammatory mediators such as TNFα and IL-10 (*26,28*). AA's role in modulation of ADCY genes demonstrates the importance of specific receptors coupled to heterotrimeric G proteins (*29*). The abnormal *ADCY* profile in FOP PBMC may be involved in the molecular unbalance of FOP and *ADCY7* is likely linked to this disorder, though expressed, was not modulated or impacted by AA.

FOP involves complex pathophysiological pathways in which signaling and response of immunoinflammatory factors differ greatly from normal defensive inflammatory mechanisms. ADRB1 and ADRB2, and possibly others receptors, seem to participate in the sympathetic regulation of HO stages, such as angiogenesis, neurogenesis and osteogenesis (*5,6*). Reports demonstrate catecholamines and additional signaling cascades of the sympathetic nervous system (SNS) and immune system interact through cytokine production in lymphocytes, dependent on β2 adrenergic receptors density in PBMC (*30*). A cause-effect relationship of ADCY system dysregulation and β-adrenergic receptors downregulation in lymphocytes suggests impairment of β-adrenergic transmembrane signaling in septic patients, linking ADCY to β-adrenergic pathways (*31*). In this regard, it is noteworthy to highlight the fact that unspecific adrenoreceptor antagonists are not well studied in FOP.

Togari (*32*) studying bone resorption processes, observed SNS modulation of osteoclast differentiation and osteoclastogenesis inhibiting factors produced by osteoblast/stromal cells with adrenergic and neuropeptide receptors. Furthermore, deletion of *ADRB1*, *2*, or both, leads to altered bone phenotypes. While ADRB1 signaling is shown to regulate anabolic bone responses, ADRB2 regulates bone remodeling through the expression of tumor necrosis factor TNFSF11(RANKL) in osteoblasts (*33*). The role of PBMC signaling in HO is not clear. Genes *ADRB1* and *2* were overexpressed in

FOP PBMC before treatment. AA+PP downregulated *ADRB2*, suggesting *ADRB2* receptor as putative candidate in a FOP pathophysiological pathway and its response to AA+PP may benefit FOP as suggested by Palhares *et al.* (*10*). These results may provide possible routes to be explored in pharmacotherapy studies of FOP and HO. There is evidence that ADRB are expressed in human macrophages and monocytes to generate anti- and pro-inflammatory effects, hinged on how they are activated or inhibited, possibly showing that receptor responsiveness changes during cell differentiation (*34*).

Post-translationally modified type III pre-procollagen is a main component of bone matrix, contributing to proper maintenance, physiology, and coordination of post-injury repair; all processes dependent on L-ascorbic acid (*12,35*) and is a regulator of type I and II collagen fibril diameter (*36*). AA stimulates the synthesis of types I and III collagen in fibroblasts *in vitro*, where it stabilizes and upregulates its mRNA expression, without altering the cellular protein presentations (*37*). AA treatment of FOP (*38*) was originally based on the hypothesis that AA possibly modulates collagen gene expression and deposition (*13,38*). *COL3* downregulation in FOP PBMC may be fundamental in FOP pathophysiology. Low *COL3* could lead to weakened endochondral tissue, facilitating infiltration and establishment of local inflammatory processes during flare-ups. AA or AA+PP *COL3* upregulation may improve tissue resistance by favoring anti-inflammatory environment. Additionally, AA positive influence on type-I and -III collagen synthesis could contribute to a reduction in new bone deposition based on angiostatic effects (*12,39,40*). Nevertheless, overexpression of *COL1* found in FOP PBMC should be further investigated, in view that type I collagen largely coats some blood vessels in developing bone, possibly secreted from osteoblasts and endothelial cells (*41*), noting that PP alone did not show effects on the collagen mRNA.

ALPL (Alkaline Phosphatase, Liver/Bone/Kidney) activity in muscle satellite cells is induced by ACVR1 (R206H), inhibiting antagonists and increasing BMP4 for osteoblasts formation (*2,42*). FOP patients may show increased serum ALPL, especially in flare-ups (*43*), however, FOP PBMC *in vitro* showed no *ALPL* expression differences when compared to PBMC controls in stabilized cultures. It seems, though, that FOP *ALPL* increases seen *in vivo* depend on multifactorial compounds for final HO. The RUNX2 transcription factor, a major regulator of osteoblast differentiation *via* SMAD1 signaling and involved in the final ossification process, requires local BMP production. The combined expression of BMPs and RUNX2 stimulates osteoblastic gene expression in FOP primary teeth isolated cells (SHED). These SHED have been shown to mineralizes faster than control cells with high expression of *ALPL* (*20*). In our study FOP PBMC showed increased *RUNX2* expression.

Treatment with AA or AA+PP decreased *RUNX2* expression levels while not altering expression of *ALPL*. Recent studies have shown AA dose-dependent modulation of osteogenic gene expression in human osteosarcoma G292 cells and high doses of AA leads to downregulation of *RUNX2* and *ALPL* expression (*44*). This suggests that AA treatment may inhibit osteoblast maturation. High doses of AA can act as a pro-oxidant that drives ALPL activity increases after osteogenic induction by BMP2 facilitated by oxidative stress (*10,44*). Indeed, downregulation of *RUNX2* may benefit FOP clinical conditions by minimizing HO.

Despite the striking flare-up process preceding HO, targeted studies on inflammatory genes in FOP are crucial, for example, TNF-α role in HO is paradoxical. The transient inhibition of RUNX2 function during skeletogenesis, due to the activity of Twist proteins (-1 and -2), whose gene expression is induced by TNF-α (*45*), needs to be clarified. For instance in *Nfactc1-Cre/caAcvr1fl/wt* mice, a genetic model similar to FOP, TNF-α serum levels are elevated and also histologically located in HO anlagen cartilaginous formation areas (*46*). However, studies exploring cytokine modulation of FOP demonstrate that plasma TNF-α levels are above average in patients undergoing flare-up (*4*), while IL-10 plasma levels are significantly increased in FOP subjects with no flare-up (*47*).

AA supplementation modulated various genes in a PBMC microarray study, from healthy individuals, mainly under inflammatory stimulation by LPS. TNF-α and pro-inflammatory cytokines were activated and released in fresh PBMC before and after AA supplementation, but IL-10 was released only after supplementation (*48*). Similarly, we found overexpression of *TNF-α* in FOP PBMC in stabilized cell culture, which was further increased by AA. TNF-α may participate as an important inflammatory cytokine modulator of ossification during flare-up in FOP. Down regulation of *IL-10* did not suggest PBMC signaling involvement in FOP conditions. *In vivo* studies suggest that in the bone, the induction of osteoprotegerin levels and the suppression of RANKL mediated by TNF-α may represent an interrelated mechanism to prevent excessive loss of bone mass, assuming that TNF-α plays a role in the central regulation of bone mass in pathological conditions (*49*).

Inflammatory response to tissue damage is also regulated by the ANS through inflammatory reflex and signaling of the anti-inflammatory cholinergic pathway through vagus nerve, acetylcholine and CHRNA7 located in macrophages, dendritic cells, T and B lymphocytes, mast cells and basophils (*6,50,51*). In our study, ADBR2 blockade *in vitro* led to the downregulation of *CHRNA7* and increase of *TNF-α* , consistent with this path and consistent with earlier reports (*49*) looking like a paradoxical inflammatory regulation by TNF-α. Considering FOP

PBMC in a prone inflammatory state (*47,52*), it is reasonable to assume TNF-α as a protagonist in the inflammatory process. However, reported benefits of AA+PP (FOPCON) for FOP patients (*10*), may suggest a balance of neuro-inflammatory equilibrium by ANS. Yet, control of *TNF-α* gene expression through CHRNA7 signaling of anti-inflammatory cholinergic pathway remains a question in the context of FOP.

For the first time, the main receptors of the RAS were investigated in FOP PBMC, due to the potential inflammatory and algesia involvement in various pathologies (*53*). *AGTR1*, *AGTR2*, *MAS* and *MRGD* genes were not shown to be FOP PBMC phenotypic markers, nevertheless, the interrelationship between β-adrenergic function and angiotensin axes is evident (*7*). PP downregulated *AGTR1* gene expression in FOP and control PBMC. Interestingly, AA+PP augmented expressions of *AGTR2* and *MAS* and downregulated *MRGD* and *AGTR1* genes in FOP PBMC, favoring the anti-inflammatory RAS axis. PP inhibits angiogenesis through downregulation of vascular endothelial growth factor (VEGF) expression in hemangioma-derived stem cells (*18*), thus it would do the same to HO, possibly by means of RAS regulation *via* beta-adrenergic antagonism. PP would lead to renin reduction and RAS axis, reducing vascular supply (*15*). It seems that increase of *AGTR2* and *MAS* and decrease of *AGTR1* genes in FOP PBMC affect inflammatory paths towards HO, reducing angiogenesis. Responses in FOP PBMC AA+PP may explain much of the mechanism of FOPCON in benefit FOP patients. However, the RAS cascade extends well beyond the two main counterbalancing axes. The angiotensin converting enzymes *ACE1* and *ACE2* genes might be directly involved in the process yet to be investigated in FOP (*7,15*). However, *MRGD* showed significant downregulation in PBMC FOP in response to all treatments. Alamandine peptide binds to *MRGD* receptor towards vasodilation (*7*), which might favor HO, but the hypothesis of MRGD participation in FOP may link mainly to its role in the algesia mechanism, which is not yet studied in FOP. This speculation is not verified yet, but *MRGD* downregulation in FOP PBMC by AA+PP may be linked to vasoconstriction and pain relief (*10*), must be considered in the rationale of future research. Modulation of RAS pathways should be considered in the control of inflammation, fibrogenesis and angiogenesis in FOP.

The main aspect of the present work is that FOP leukocyte phenotype is possibly modulated by AA and PP treatment. Interestingly, we present for the first time that, *ACTB* is expressed in FOP PBMC and FOP leads to an upregulation that is significantly sensitive to AA and PP treatment. β-actin, besides involvement with inflammation, must modulate structural aspects of the cellular framework, perhaps to promote diapedesis and control leukocyte migration, a function that will need to be better clarified (*54*). ACTB protein has been shown

to activate endothelial nitric oxide synthase (eNOS) to form Nitric oxide (NO), a pro-inflammatory signaling molecule, mediator in inflammation pathogenesis, that induces inflammation due to over production in abnormal situations. A clarification of the NO path hole is needed for FOP.

In conclusion, FOP is an intractable disease due to the ACVR1 mutation. The destination is an imbalance of interconnected complex molecular cascades with inflammatory consequences, culminating in outbreaks and abnormal bone formation. It becomes impossible to treat this disease just by targeting a pathway or blocking a receptor, because a complex imbalance of many genes, such as a poorly governed molecular seesaw, makes it difficult to balance or harmonize physiologically. Any attempt at a therapeutic target disrupts the rest of the molecular pathways. Achieving fine-tuning of the various key targets is necessary, but extremely difficult, making this disease so far devoid of effective treatment. A future attempt to treat FOP should consider a multi-target cocktail.

Acknowledgements

Conflict of Interest: The authors have no conflicts of interest to disclose.

References

1. Kaplan FS, Pignolo RJ, Al Mukaddam MM, Shore EM. Hard targets for a second skeleton: therapeutic horizons for fibrodysplasia ossificans progressiva (FOP). Expert Opin Orphan Drugs. 2017; 5:291-294.

2. Shore EM, Xu M, Feldman GJ, *et al.* A recurrent mutation in the BMP type I receptor ACVR1 causes inherited and sporadic fibrodysplasia ossificans progressiva. Nat Genet. 2006; 38:525-527.

3. Hino K, Horigome K, Nishio M, Komura S, Nagata S, Zhao C, Jin Y, Kawakami K, Yamada Y, Ohta A, Toguchida J, Ikeya M. Activin-A enhances mTOR signaling to promote aberrant chondrogenesis in fibrodysplasia ossificans progressiva. J Clin Invest. 2017; 127:3339-3352.

4. Hildebrand L, Gaber T, Kühnen P, Morhart R, Unterbörsch H, Schomburg L, Seemann P. Trace element and cytokine concentrations in patients with Fibrodysplasia Ossificans Progressiva (FOP): A case control study. J Trace Elem Med Biol. 2017; 39:186-192.

5. Salisbury E, Sonnet C, Heggeness M, Davis AR, Olmsted-Davis E. Heterotopic ossification has some nerve. Crit Rev Eukaryot Gene Expr. 2010; 20:313-324.

6. Rosas-Ballina M, Tracey KJ. Cholinergic control of inflammation. J Intern Med. 2009; 265:663-679.

7. Santos RAS, Sampaio WO, Alzamora AC, Motta-Santos D, Alenina N, Bader M, Campagnole-Santos MJ. The ACE2/Angiotensin-(1-7)/MAS axis of the renin-angiotensin system: focus on Angiotensin-(1-7). Physiol Rev. 2018; 98:505-553.

8. Wentworth KL, Masharani U, Hsiao EC. Therapeutic advances for blocking heterotopic ossification in fibrodysplasia ossificans progressiva. Br J Clin Pharmacol. 2019; 85:1180-1187.

9. Haupt J, Xu M, Shore EM. Variable signaling activity by FOP ACVR1 mutations. Bone. 2018; 109:232-240.

10. Palhares DB, Nascimento DR, Palhares MG, Balaniuc SLB, Giuliani LR, Xavier PCN, Brum JMG, Alves F, Vieira FO, Souza-Fagundes EM, Underwood A, Milsted A, Santos RAS, Martins AS. Propranolol and ascorbic acid in control of fibrodysplasia ossificans progressiva flare-ups due to accidental falls. Intractable Rare Dis Res. 2019; 8:24-28.

11. Arrigoni O, De Tullio MC. Ascorbic acid: much more than just an antioxidant. Biochim Biophys Acta. 2002; 1569:1-9.

12. Ashino H, Shimamura M, Nakajima H, Dombou M, Kawanaka S, Oikawa T, Iwaguchi T, Kawashima S. Novel function of ascorbic acid as an angiostatic factor. Angiogenesis. 2003; 6:259-269.

13. Belin S, Kaya F, Burtey S, Fontes M. Ascorbic acid and gene expression: another example of regulation of gene expression by small molecules? Curr Genomics. 2010; 11:52-57.

14. Fernandes G, Barone AW, Dziak R. The effect of ascorbic acid on bone cancer cells *in vitro*. Cogent Biol. 2017; 3:1288335.

15. Stiles JM, Amaya C, Rains S, Diaz D, Pham R, Battiste J, Modiano JF, Kokta V, Boucheron LE, Mitchell DC, Bryan BA. Targeting of beta adrenergic receptors results in therapeutic efficacy against models of hemangioendothelioma and angiosarcoma. PLoS One. 2013; 8:e60021.

16. Nascimento DR, Giuliani LR, Palhares MG, Alves F, Martins SF, Vieira FO, Brum JMG, Giuliani LR, Palhares MG, Underwood A, Souza-Fagundes EM, Milsted A, Santos RAS, Martins AS. Ascorbic acid modulates the expression of genes involved in heterotopic ossification. NBC-Periódico Científico do Núcleo Biociências. 2017; 7:81-97.

17. Hajighasemi F, Mirshafiey A. Propranolol effect on proliferation and vascular endothelial growth factor secretion in human immunocompetent cells. J Clin Immunol Immunopathol Res. 2010; 2:22-27.

18. Zhang L, Mai HM, Zheng J, Zheng JW, Wang YA, Qin ZP, Li KL. Propranolol inhibits angiogenesis *via* down-regulating the expression of vascular endothelial growth factor in hemangioma derived stem cell. Int J Clin Exp Pathol. 2013; 7:48-55.

19. Livak KJ, Schmittgen TD. Analysis of relative gene expression data using real-time quantitative PCR and the $2^{-\Delta\Delta C_T}$ method. Methods. 2001; 25:402-408.

20. Billings PC, Fiori JL, Bentwood JL, O'Connell MP, Jiao X, Nussbaum B, Caron RJ, Shore EM, Kaplan FS. Dysregulated BMP signaling and enhanced osteogenic differentiation of connective tissue progenitor cells from

patients with fibrodysplasia ossificans progressiva (FOP). J Bone Miner Res. 2008; 23:305-313.

21. Micha D, Voermans E, Eekhoff MEW, van Essen HW, Zandieh-Doulabi B, Netelenbos C, Rustemeyer T, Sistermans EA, Pals G, Bravenboer N. Inhibition of TGFβ signaling decreases osteogenic differentiation of fibrodysplasia ossificans progressiva fibroblasts in a novel *in vitro* model of the disease. Bone. 2016; 84:169-180.

22. Chen Q, Espey MG, Krishna MC, Mitchell JB, Corpe CP, Buettner GR, Shacter E, Levine M. Pharmacologic ascorbic acid concentrations selectively kill cancer cells: action as a pro-drug to deliver hydrogen peroxide to tissues. Proc Natl Acad Sci. 2005; 102:13604-9.

23. Padayatty SJ, Levine M. Vitamin C physiology: the know and the unknown and Goldilocks. Oral Dis. 2016; 22:463-493.

24. Gonzalez JP, Calvo R, Rodríguez-Sasiaín JM, Jimenez R, Aguirre C, Valdivieso A, du Souich P. Influence of vitamin C on the absorption and first pass metabolism of propranolol. Eur J Clin Pharmacol. 1995; 48:295-297.

25. Eslami M, Badkoubeh RS, Mousavi M, Radmehr H, Salehi M, Tavakoli N, Avadi MR. Oral ascorbic acid in combination with beta-blockers is more effective than beta-blockers alone in the prevention of atrial fibrillation after coronary artery bypass grafting. Tex Heart Inst J. 2007; 34:268-274.

26. Ludwig M-G, Seuwen K. Characterization of the human adenylyl cyclase gene family: cDNA, gene structure, and tissue distribution of the nine isoforms. J Recept Signal Transduct Res. 2002; 22:79-110.

27. Passage E, Norreel JC, Noack-Fraissignes P, Sanguedolce V, Pizant J, Thirion X, Robaglia-Schlupp A, Pellissier JF, Fontés M. Ascorbic acid treatment corrects the phenotype of a mouse model of Charcot-Marie-Tooth disease. Nat Med. 2004; 10:396-401.

28. Risøe PK, Wang Y, Stuestøl JF, Aasen AO, Wang JE, Dahle MK. Lipopolysaccharide attenuates mRNA levels of several adenylyl cyclase isoforms *in vivo*. Biochim Biophys Acta. 2007; 1772:32-39.

29. Premont RT, Matsuoka I, Mattei MG, Pouille Y, Defer N, Hanoune J. Identification and characterization of a widely expressed form of adenylyl cyclase. J Biol Chem. 1996; 271:13900-13907.

30. Wahle M, Neumann RP, Moritz F, Krause A, Buttgereit F, Baerwald CGO. Beta 2-adrenergic receptors mediate the differential effects of catecholamines on cytokine production of PBMC. J Interferon Cytokine Res. 2005; 25:384-394.

31. Bernardin G, Kisoka RL, Delporte C, Robberecht P, Vincent J-L. Impairment of beta-adrenergic signaling in healthy peripheral blood mononuclear cells exposed to serum from patients with septic shock: involvement of the inhibitory pathway of adenylyl cyclase stimulation. Shock. 2003; 19:108-112.

32. Togari A. Adrenergic regulation of bone metabolism: possible involvement of sympathetic innervation of osteoblastic and osteoclastic cells. Microsc Res Tech. 2002; 58:77-84.

33. Pierroz DD, Bonnet N, Bianchi EN, Bouxsein ML, Baldock PA, Rizzoli R, Ferrari SL. Deletion of β-adrenergic receptor 1, 2, or both leads to different bone phenotypes and response to mechanical stimulation. J Bone Miner Res. 2012; 27:1252-1262.

34. Scanzano A, Cosentino M. Adrenergic regulation of innate immunity: a review. Front Pharmacol. 2015; 6:171.

35. Volk SW, Shah SR, Cohen AJ, Wang Y, Brisson BK, Vogel LK, Hankenson KD, Adams SL. Type III collagen regulates osteoblastogenesis and the quantity of trabecular bone. Calcif Tissue Int. 2014; 94:621-631.

36. Kuivaniemi H, Tromp G. Type III collagen (COL3A1): Gene and protein structure, tissue distribution, and associated diseases. Gene. 2019; 707:151-171.

37. Nusgens BV, Humbert P, Rougier A, Colige AC, Haftek M, Lambert CA, Richard A, Creidi P, Lapière CM. Topically applied vitamin C enhances the mRNA level of collagens I and III, their processing enzymes and tissue inhibitor of matrix metalloproteinase 1 in the human dermis. J Invest Dermatol. 2001; 116:853-859.

38. Palhares DB. Myositis ossificans progressive. Calcif Tissue Int. 1997; 60:394.

39. Olmsted-Davis E, Gannon FH, Ozen M, Ittmann MM, Gugala Z, Hipp JA, Moran KM, Fouletier-Dilling CM, Schumara-Martin S, Lindsey RW, Heggeness MH, Brenner MK, Davis AR. Hypoxic adipocytes pattern early heterotopic bone formation. Am J Pathol. 2007; 170:620-632.

40. Wang Y, Wan C, Deng L, Liu X, Cao X, Gilbert SR, Bouxsein ML, Faugere MC, Guldberg RE, Gerstenfeld LC, Haase VH, Johnson RS, Schipani E, Clemens TL. The hypoxia-inducible factor α pathway couples angiogenesis to osteogenesis during skeletal development. J Clin Invest. 2007; 117:1616-1626.

41. Ben Shoham A, Rot C, Stern T, Krief S, Akiva A, Dadosh T, Sabany H, Lu Y, Kadler KE, Zelzer E. Deposition of collagen type I onto skeletal endothelium reveals a new role for blood vessels in regulating bone morphology. Development. 2016; 143:3933-3943.

42. Akiyama S, Katagiri T, Namiki M, Yamaji N, Yamamoto N, Miyama K, Shibuya H, Ueno N, Wozney JM, Suda T. Constitutively active BMP type I receptors transduce BMP-2 signals without the ligand in C2C12 myoblasts. Exp Cell Res. 1997; 235:362-369.

43. Pignolo RJ, Shore EM, Kaplan FS. Fibrodysplasia ossificans progressiva: diagnosis, management, and therapeutic horizons. Pediatr Endocrinol Rev. 2013;10 Suppl 2:437-448.

44. Ferrazzo PC, Niccoli S, Khaper N, Rathbone CR, Lees SJ. Ascorbic acid diminishes bone morphogenetic protein 2-induced osteogenic differentiation of muscle precursor cells. Muscle Nerve. 2019; 59:501-508.

45. Bialek P, Kern B, Yang X, Schrock M, Sosic D, Hong N, Wu H, Yu K, Ornitz DM, Olson EN, Justice MJ, Karsenty G. A twist code determines the onset of osteoblast differentiation. Dev Cell. 2004; 6:423-435.

46. Agarwal S, Loder SJ, Brownley C, Eboda O, Peterson JR, Hayano S, Wu B, Zhao B, Kaartinen V, Wong VC, Mishina Y, Levi B. BMP signaling mediated by constitutively active activin type 1 receptor (ACVR1) results in ectopic bone formation localized to distal extremity joints. Dev Biol. 2015; 400:202-209.

47. Barruet E, Morales BM, Cain CJ, Ton AN, Wentworth KL, Chan TV, Moody TA, Haks MC, Ottenhoff THM, Hellman J, Nakamura MC, Hsiao EC. NF-κB/MAPK activation underlies ACVR1-mediated inflammation in human heterotopic ossification. JCI insight. 2018; 3:e122958.

48. Canali R, Natarelli L, Leoni G, Azzini E, Comitato R, Sancak O, Barella L, Virgili F. Vitamin C supplementation modulates gene expression in peripheral blood mononuclear cells specifically upon an inflammatory

stimulus: A pilot study in healthy subjects. Genes Nutr. 2014; 9:390.

49. Mito K, Sato Y, Kobayashi T, Miyamoto K, Nitta E, Iwama A, Matsumoto M, Nakamura M, Sato K, Miyamoto T. The nicotinic acetylcholine receptor α7 subunit is an essential negative regulator of bone mass. Sci Rep. 2017; 7:45597.

50. Zdanowski R, Krzyzowska M, Ujazdowska D, Lewicka A, Lewicki S. Role of α7 nicotinic receptor in the immune system and intracellular signaling pathways. Cent Eur J Immunol. 2015; 40:373-379.

51. Olofsson PS, Rosas-Ballina M, Levine YA, Tracey KJ. Rethinking inflammation: neural circuits in the regulation of immunity. Immunol Rev. 2012; 248:188-204.

52. Del Zotto G, Antonini F, Azzari I, Ortolani C, Tripodi G, Giacopelli F, Cappato S, Moretta L, Ravazzolo R, Bocciardi R. Peripheral blood mononuclear cell immunophenotyping in fibrodysplasia ossificans progressiva patients: evidence for monocyte DNAM1 up-regulation. Cytometry B Clin Cytom. 2018; 94:613-622.

53. Lan L, Xu M, Li J, Liu L, Xu M, Zhou C, Shen L, Tang Z, Wan F. Mas-related G protein-coupled receptor D participates in inflammatory pain by promoting NF-κB activation through interaction with TAK1 and IKK complex. Cell Signal. 2020; 76:109813.

54. Kondrikov D, Fonseca FV, Elms S, Fulton D, Black SM, Block ER, Su Y. β-actin association with endothelial nitric-oxide synthase modulates nitric oxide and superoxide generation from the enzyme. J Biol Chem. 2010; 285:4319-4327.

*Address correspondence to:
Almir Sousa Martins, UFMG/ Department of Physiology and Biophysics, Av Antonio Carlos, 6627, A4-256, Belo Horizonte, MG, Brasil - 31.270-900.
E-mail: alisbetermster@gmail.com; asm2011@ufmg.br

Original Article

The usage of enzyme replacement treatments, economic burden, and quality of life of patients with four lysosomal storage diseases in Shanghai, China

Jiahao Hu[1,§], Lin Zhu[1,§], Jiangjiang He[1], Dingguo Li[2], Qi Kang[1,*], Chunlin Jin[1,*]

[1] Shanghai Health Development Research Center (Shanghai Medical Information Research Center), Shanghai, China;
[2] Shanghai Foundation for Rare Disease, Shanghai, China.

SUMMARY   Lysosomal storage diseases (LSDs) are a group of rare diseases that cause progressive physical dysfunction and organ failure, which significantly affected patients' quality of life. The objective of this study was to explore the characteristics and usage of Enzyme Replacement Treatments (ERTs), which is the only specific therapy for LSDs, of patients with the four different LSDs (Gaucher, Fabry, Pompe disease and Mucopolysaccharidosis) in Shanghai, and then evaluate the economic burden and quality of life of these patients. A total of 31patients, involving 5, 14, 4 and 8 patients with Gaucher, Fabry, Pompe disease and Mucopolysaccharidosis, respectively, were included in analysis. The result showed that only five Gaucher disease (GD) patients in Shanghai used Imiglucerase in 2019, while the other 26 patients with the other three LSDs did not receive ERTs. The total health expenditure of GD patients was 2,273,000CNY on average mainly resulted by the high cost of Imiglucerase. The total health expenditure of the other 26 patients was 37,765CNY on average. Though the cost-sharing mechanism between basic medical insurance, charity fund and patients had been explored for Gaucher disease in Shanghai, the out-of-pocket part, which was 164,301 CNY, still laid a heavy economic burden on the patients and their families. The mean EQ-VAS score of GD patients was 76.4 ± 15.5, which was higher than that of the other three LSDs. It is recommended that the scope of drug reimbursement list and the reimbursement level should be further expanded and raised to help improve the living conditions of patients with LSDs.

Keywords   Rare diseases, lysosomal storage diseases, enzyme replacement treatment, patient survey, quality of life, disease burden, Shanghai

1. Introduction

Lysosomal storage diseases (LSDs) are a group of diseases caused by defects in single genes. Enzyme defects cause nearly seventy percent of the LSDs, and the rest are defects in enzyme activator or associated proteins (*1*). A deficit in any of these enzymes will result in progressive accumulation of materials in affected organs and tissues, which will result in an increase in the size and number of these organelles and finally in cellular dysfunction and organ failure (*2*). Though as a group, LSDs are with an estimated incidence of 1/5,000 to 1/5,500, one single LSD is usually recognized as a rare disease with estimated incidences ranging from 1/50,000 to 1/250,000 live births (*2*).There is currently no systematic epidemiology study nor patient registry for LSDs in China.

There are 16 different approved therapies for 7

LSDs in the world (*3*), while there are only altogether 8 available therapies (seven of them are ERTs) in China for 5 LSDs, which are Gaucher disease (GD), Fabry Disease (FD), Mucopolysaccharidosis (MPS), Pompe Disease (PD), and Niemann-Pick disease (NP), according to the National Rare Diseases List (NRDL). However, only Miglustat for NP type C is now included in the National Drug Reimbursement List (NDRL), while the other seven ERTs are not. See Table 1 for the details. The newly updated NDRL (2020 version) did not contain these extremely expensive drugs for rare diseases (*4*). Theoretically, there are no healthcare security measures on the national level in China for patients with the mentioned four LSDs, which are GD, PD, FD and MPS.

Current studies regarding LSDs patients in China are mainly from the clinical aspect, while only few are not. Chen *et al.* introduced the demographic characteristics and distribution of all 322 diagnosed patients with

Table 1. Marketed and reimbursed drugs for LSDs in China

NRDL code	Disease	Approved name	Brand name	Approved date in China	Included in NDRL
27	Fabry disease	Agalsidase beta[a]	Fabra-zyme	2009/12	No
		Agalsidase alfa	Replagal	2020/8	No
31	Gaucher disease	Imiglucerase	Cerezyme	2008/11	No
		Velag-lucerase[a]	Vpriv	No	—
		Taliglucerase[a]	Elelyso	No	—
		Miglusta	Zavesca	No	—
		Eliglustat[a]	Cerdelga	No	—
35	Pompe disease	Alglucosidase alfa	Myozyme	2017/12	No
		Migalastat[a]	Galafpld	No	—
73	MPS				
	Type I	Laronidase[a]	Aldulra-zyme	2020/6	No
	Type II	Idursulfase[a]	Elaprase	2020/9	No
	Type IVA	Elosulfase[a]	Vimizim	2019/6	No
	Type VI	Galsulfase	Naglazyme	No	—
82	Niemann-Pick disease type C	Miglustat	Zavesca	2017/9	Yes
	Wolman disease	Sebelipase	Kanuma	No	—
	Neuronal ceroid lipofuscinosis type 2 (CLN2)	Cerliponase	Brineura	No	—

[a], Drugs included in the List of Urgently Needed New Drugs from Overseas for Clinical Use.

LSDs in Eastern China (*5*). Zhao *et al.* studied the characteristics of 59 Chinese PD patients from the Pompe Registry (*6*). Yang *et al.* described the cost-sharing mechanism for Imiglucerase in Qingdao, Shandong province (*7*). Except for the mentioned three literatures, there are some large-scale surveys focusing on living conditions of patients with rare disease in China. Some surveys on LSDs did report the cost of illness while health resources utilization and quality of life of those patients remained unknown (*8-11*).

In 2011, Shanghai Children's Hospitalization Assistance Fund, managed by the Red Cross Society of China Shanghai Branch decided to reimburse the ERTs for patients with the mentioned four LSDs, with a maximum reimbursement amount of 100,000CNY per patient per year (*12*). In 2013, Imiglucerase could be paid by the basic medical insurance in Shanghai and reimbursement level was ranging from 80%-85% depending on the dosage. In 2017, the Shanghai Foundation for Rare Disease established a special assistance fund for LSD patients supported by enterprises (*13*). The assistant amount was decided based on the income level of patients, ranging from 70% to 100% of the out-of-pocket (OOP) expenditure part, who were receiving ERTs treatments. The consequential outcomes of these policies on patients with LSDs in Shanghai are still little known.

Our study aimed to explore the characteristic and usage of ERTs of patients with GD, PD, FD and MPS in Shanghai and then evaluated the economic burden and quality of life (QoL) of these patients.

2. Materials and Methods

2.1. Study design

This study focusing on patients with 4 LSDs was based on a large survey of living conditions of patients with rare diseases in Shanghai. The survey used a self-designed questionnaire based on a literature review and interviews with several doctors, health economists and government officials in the field of rare diseases. Snowballing sampling method was adopted due to that there was no epidemiological data nor patient registry of patients with rare diseases in Shanghai. The electronic questionnaire was administered using the Wenjuanxing software (Changsha Ranxing Information Technology Co. LTD) and filled out online by patients with rare diseases or their primary caregivers. The participants recruitment process was conducted through online and offline platforms and networks. The doctors from hospitals in Shanghai, which act as members of the National Rare Disease Diagnosis and Treatment Network, helped to invite their diagnosed patients with rare diseases to participate in the survey. Several patient organizations of rare diseases also called on patients to involve in the investigation. The whole process of data collection was done from April to August 2020.

2.2. Inclusion criteria

The patients would only be included in the survey when they met the following conditions: *i*) The disease they were diagnosed with was recognized as rare disease on the list of NRDL or Orphanet (*14*); *ii*) They paid their Basic Medical Insurance premium in Shanghai, including urban employee and urban resident basic medical insurance; *iii*) The patients or their primary caregivers were willing to participate in the survey and were able to complete the online questionnaire.

2.3. Quality control

The follow-up telephone calls of each participant

were made to ensure the quality of data. The follow-up interviews could correct the obvious mistakes participants made and refill in the blanks they left. The follow-up visits were performed by four postgraduates majoring in health policy or health management research, who had been strictly and systematically trained before.

2.4. Data extraction

The information of patients diagnosed with GD, PD, FD and MPS were extracted from the whole dataset. A total of 31 patients were enrolled, including 5 GD patients, 4 PD patients, 14 FD patients and 8 MPS patients, in this study. 18 patients answered the questionnaire themselves and the rest 13 patients' conditions were reported by their caregivers due to reasons like "the patient cannot read".

Several important variables were chosen from the long questionnaire, including socio-demographic information (birthday, gender, education, marriage, occupation, personal annual income, annual household income, and *etc.*), economic burden caused by the disease (direct medical costs, direct non-medical costs and indirect cost in 2019), the treatments received (usage of drugs, numbers of outpatients visits and days of hospitalization) and health states (quality of life measured by EQ-5D-Y and EQ-5D-3L for different age groups).

2.5. Data analysis

Since the included participants were too little ($n = 31$), descriptive statistics were mainly used for the analysis. The economic burden is defined as the sum of direct medical costs, direct non-medical costs, and indirect costs from the patient's perspective (*4*). The EQ-5D Visual Analogue Scale (VAS) scores and problems reported in 5 dimensions (mobility, self-care, usual activities, pain/discomfort, and anxiety/depression) were used to evaluate the patients' QoL. Statistical analysis was performed using SPSS 26.0 software.

2.6. Ethical statements

Informed consents were attained by all the participants before the formal survey started. The participants' privacy, including any individual information they provided in the survey, would be protected. This study was approved by the Medical Ethics Committee of Shanghai Health Development Research Center (No. 2020004).

3. Results

3.1. General characteristics

Table 2 demonstrates the characteristics of patients with

4 LSDs in Shanghai. Seventeen of the included patients were male (54.8%). Ten were non-adult among the 31 patients and eight of them were boys (80.0%). The mean age of the sample was 29.8 ± 14.4 years. Five patients failed to complete their education as they suffered from the diseases. Only 12 of the 21 adult patients (57.1%) were employed in 2019. Thirteen of the 21 adult participants were married. Only 1 of the married adults had not given birth to a child. Altogether 16 participants had urban resident basic medical insurance and 15 participants had urban employee basic medical insurance. Additionally, two patients purchased commercial health insurances. The mean personal and household annual incomes were 57,218 CNY and 184,987 CNY (1 USD≈6.8 CNY), respectively.

3.2. Usage of ERTs and other medical services utilizations

The FD patients paid outpatient visits for the most times, which was 8.1 times on average in 2019, while the PD patients visited the outpatient clinics for 0.5 times on average, which was the least. The GD patients was hospitalized for the longest time on average, which took them 27.8 days on average. The patients with MPS were hospitalized for only 1.1 days on average. Only the 5 patients with GD were treated with ERTs in 2019. Each of them used 151 bottles of Imiglucerase on average. None of the other 26 patients with LSDs used ERTs in 2019. The details are shown in Table 3.

3.3. Health expenditure

The mean total health expenditure of patients with GD was 2,273,100 CNY in 2019 while that of patients with the other 3 LSDs (PD, FD and MPS) was 37,765 CNY. The higher percent of OOP cost in outpatient expenditure among GD patients was caused by one GD patient who received a spine surgery and paid follow-up visits in outpatient clinics. The inpatient expenditure contributed 2,234,400 CNY, which was over 98.3% of the total cost of GD. Notably, the cost for Imiglucerase accounted for 99.9% of the total inpatient cost, and of which 79.0% could be covered by basic medical insurance and 15.6% was funded by Shanghai Foundation for Rare Disease. The GD patients also needed to pay the rest 5.4% by themselves, which was still 121,200 CNY in average. The medical cost of the other 3 LSDs, including 68.9% outpatient cost and 13.4% inpatient cost could be covered by basic medical insurance. The mean out-of-pocket expenditure for patients with the other 3 LSDs was 21,367 CNY in total. The mean cost happened outside of hospital (which includes cost for drugs and medical devices purchased from retail pharmacies) was similar for GD patients (4,300 CNY) and patients with the other 3 LSDs (4,700 CNY). However, expenditure happened outside of hospital should be self-paid. See Table 4 for details.

Table 2. The socio-demographic characteristics of patients with 4 LSDs

Characteristics	Overall (*n* = 31)		Non-adult (*n* = 10)		Adult (*n* = 21)	
	n	%	*n*	%	*n*	%
Gender						
Male	17	54.8	8	80.0	9	42.9
Female	14	45.2	2	20.0	12	57.1
Mean age (x ± S)	29.8 ± 14.4		12.4 ± 3.3		38.1 ± 9.5	
Educational level						
No education	4	12.9	4	40.0	0	0.0
Primary school	2	6.5	1	10.0	1	5.0
Middle school	7	22.6	5	50.0	2	9.5
High school	4	12.9	0	0.0	6	28.6
College or higher	14	45.2	0	0.0	12	57.1
Employment status						
Employed	—	—	—	—	12	57.1
Unemployed	—	—	—	—	8	38.1
Retired	—	—	—	—	1	4.8
Marriage						
Married	—	—	—	—	13	61.9
Single	—	—	—	—	6	28.6
Divorced	—	—	—	—	2	9.5
Fertility						
No	—	—	—	—	9	42.9
Yes	—	—	—	—	12	57.1
Medical Insurance						
Urban Employee Basic Medical Insurance	15	48.4	0	0.0	15	71.4
Urban Resident Basic Medical Insurance	16	51.6	10	100.0	6	28.6
Additional commercial insurance	2	6.5	0	0.0	2	9.5
Personal income per year(CNY, 1 USD≈6.8 CNY)						
0	—	—	—	—	4	19.0
10,000-49,999	—	—	—	—	5	23.8
50,000-99,999	—	—	—	—	2	9.5
100,000-199,999	—	—	—	—	8	38.1
200,000-299,999	—	—	—	—	2	9.5
Household annual income (CNY, 1 USD≈6.8 CNY)						
10,000-49,999	1	3.2	1	10.0	0	0.0
50,000-99,999	6	19.4	1	10.0	5	23.8
100,000-199,999	9	29.0	4	40.0	5	23.8
200,000-299,999	12	38.7	4	40.0	8	38.1
Above 300,000	3	9.7	0	0.0	3	14.2

Table 3. Usage of ERTs and other medical services utilization among patients with 4 LSDs in 2019

Health Resources Used	GD		PD		FD		MPS	
	Mean(SD)	Median	Mean(SD)	Median	Mean(SD)	Median	Mean(SD)	Median
Numbers of outpatient visits	6.6 (10.1)	0	0.5 (0.5)	0.5	8.1 (11.6)	5.5	7.9 (10.4)	0
Days of hospitalizations	27.8 (3.6)	26	3.5 (6.1)	0	5.1 (8.3)	0	1.1 (2.6)	0
Quantities of ERTs used	151 (47.7)[*]	130[*]	—	—	—	—	—	—

[*]The strength of Imiglucerase is 400U/bottle.

3.4. Economic burden of patients

The average economic burden of patients caused by GD was 164,301 CNY, while the average economic burden of patients with PD, FD and MPS was 58,352 CNY in 2019. Direct medical cost was the majority of the disease burden, which contributed 97.1% and 60.5% of the total disease burden for GD patients and patients with the other three LSDs, respectively. The indirect cost of patients with PD, FD and MPS was 21,860 CNY, which was higher than that of GD patients. The details are shown in Table 5.

3.5. Quality of life

The QoL of patients with individual LSD was shown in Table 6. The mean EQ-VAS scores of patients with GD, FD, PD and MPS were 76.4, 55.0, 52.0, and 46.0, respectively. The mean EQ-VAS score of GD patients was the highest. Most patients with LSDs reported

Table 4. Health expenditure of patients with 4 LSDs in 2019

Cost (CNY)	GD (*n* = 5)		PD, FD and MPS (*n* = 26)	
	Mean (SD)	Median	Mean (SD)	Median
Total	2,273,000 (820,670)	1,648,000	37,765 (110,490)	4,700
Outpatient				
Total	34,400 (46,482)	4,000	13,088 (29,797)	2,450
Basic medical insurance	300 (600)	0	9,017 (24,931)	1,400
Out-of-pocket	34,100 (46,682)	2,500	4,071 (6,896)	750
Inpatient				
Total	2,234,400 (795541)	1,612,000	19,977 (82,313)	0
Basic medical insurance	1,764,244 (593,872)	0	2,681 (5,516)	0
Charity	348,956 (135,764)	262,080	0 (0)	0
Out-of-pocket	121,200 (71,639)	100,000	17,296 (82,559)	0
Outside the hospital	4,300 (8,600)	0	4,700 (9,162)	1,000

Table 5. Economic burden of patients with 4 LSDs in 2019

Cost (CNY)	GD (*n* = 5)			PD, FD and MPS (*n* = 26)		
	Mean (SD)	Median	%	Mean (SD)	Median	%
Total economic burden	164,301 (113,267)	112,500	100.0	58,352 (113,675)	7,000	100.0
Direct medical cost	159,600 (111,062)	102,500	97.1	35,321 (92,353)	4,000	60.5
Direct non-medical cost	2,361 (2,212)	2,000	1.4	1,171 (2,218)	50	2.0
Indirect cost	2,340 (2,396)	2,200	1.4	21,860 (49,503)	0	37.5

Table 6. The QoL of patients with 4 LSDs in 2019

EQ-5D-3L Dimension	Problems	Total *n* (%)	GD *n* (%)	FD *n* (%))	PD *n* (%)	MPS *n* (%)
EQ-VAS(Mean ± SD)		31 (100)	76.4 ± 15.5	55.0 ± 19.7	52.0 ± 12.9	46.0 ± 28.6
Mobility	No	16 (51.6)	5 (100)	9 (64.3)	0 (0)	2 (25.0)
	Yes	15 (48.4)	0 (0)	5 (35.7)	4 (100)	6 (75.0)
Self-care	No	23 (74.2)	5 (100)	14 (100)	2 (50.0)	2 (25.0)
	Yes	8 (25.8)	0 (0)	0 (0)	2 (50.0)	6 (75.0)
Usual activities	No	13 (41.9)	4 (80.0)	7 (50.0)	1 (25.0)	1 (12.5)
	Yes	18 (58.1)	1 (20.0)	7 (50.0)	3 (75.0)	7 (87.5)
Pain/discomfort	No	6 (19.4)	2 (40.0)	1 (7.1)	1 (25.0)	2 (25.0)
	Yes	25 (80.6)	3 (60.0)	13 (92.9)	3 (75.0)	6 (75.0)
Anxiety/depression	No	8 (25.8)	3 (60.0)	2 (14.3)	1 (25.0)	2 (25.0)
	Yes	23 (74.2)	2 (40.0)	12 (85.7)	3 (75.0)	6 (75.0)

problems in Pain/discomfort and Anxiety/depression dimensions, accounts for 80.6% and 74.2%. All the GD patients reported no problems in Mobility, while 35.7%, 100% and 75% of patients with FD, PD, and MPS reported problems in such dimension. GD patients also had better performance than patients with PD and MPS in Self-care dimension.

4. Discussion

This is the first study focusing on the usage of all the available ERTs for LSDs in China, as well as the disease burden and QoL of patients with GD, FD, PD and MPS, respectively. The study revealed that the patients using ERTs in Shanghai were still the minority, which was 5 (16.1%) patients with GD, which might

be related to the high costs of available ERTs. Until now, there has been no healthcare security policies for patients with any LSDs on the national level in China, and Shanghai basic medical insurance only reimburses Imiglucerase for GD patients while ERTs for the other three LSDs are not reimbursed. Thus, in the absence of reimbursement, patients with LSDs rarely can afford the expensive cost of ERTs.

Based on foreign experience, a national policy framework, especially reimbursement policies, for patients with rare diseases is necessary (*15-18*). For instance, the Australian government developed the Life Saving Drug Plan to reimburse expensive and life-saving drugs for life threatening and rare diseases, including GD, FD, PD, MPS type I, type II, type IVA, type VI, and neuronal ceroid lipofuscinosis type 2

(CLN2), which are LSDs (*19*). In UK, Eliglustat and Migalastat for GD type1 and FD, respectively, was recommended to use in the National Health System *via* a health technology assessment process called Highly Specialized Technology appraisal for new and existing highly specialized medicines and treatments (*20,21*). Nevertheless, the National Healthcare Security Administration recently claimed that it had basically included all the drugs for rare diseases meeting certain criteria and could not further include orphan drugs with extremely high cost into the NRDL due to the poor affordability (*22*). Therefore, the current situation in China is that only some of ERTs are reimbursed in some areas, which to a certain extent increase the accessibility for ERTs, but this causes the inequities of healthcare among different areas and different diseases.

The premise is that ERTs are reimbursed, but our study found whether patients actually used ERTs also depended on the reimbursement level. Though the basic medical insurance in Shanghai started to reimburse Imiglucerase from 2013, our interviews with the 5 GD patients reported that none of them started to use it until the Shanghai Foundation for Rare Disease established the special assistance fund for LSD patients in 2017 (*13*). The reason was that, unlike common drugs, the OOP part after reimbursement remained still unaffordable to the patients. It was estimated to be 300,000-400,000 CNY per patient per year, while the annual disposable income per capital in Shanghai was 69,442CNY in 2019 (*23*). The Shanghai Foundation for Rare Disease reimbursed the patients depending on their personal income levels, which meant the lower their personal income is, the more reimbursement they would get. However, our study found that the average OOP health expenditure of the 5 patients with GD was still 121,200 CNY in 2019, which was almost 2 times of the annual disposable income per capital of Shanghai residents. The relatively low reimbursement rate in Shanghai also caused inadequate dosage among the patients with GD. Based on our interview, a few patients' dosage of Imiglucerase were lower than the dosage recommended by their physicians according to patients' age, weight, and disease severity. As a result, the economic burden of LSD patients in our study may be underestimated.

The OOP expenditure in Shanghai was found to be higher than that of GD patients from Qingdao City, Shangdong Province and Zhengjiang Province through comparison between different areas. The Qingdao government established a supplementary medical insurance to cover 80% of the cost for Imiglucerase. The donations from the enterprises and civil assistance for low-income families would cover some of the rest part as well (*24*). Another study reported 8 GD patients' average OOP expenditure for Imiglucerase was 82,700 CNY in Qingdao in 2017 (*7*). The Zhejiang government settled a special fund for rare diseases in 2020, especially for the expensive drugs. The fund reimburses three drugs for LSDs, which are Imiglucerase for GD, Agalsidase alfa for PD, and Agalsidase beta for FD, respectively (*25*). These patients need to pay no more than 10,0000 CNY per year by themselves in Zhejiang (*26*).

Regarding QoL, LSDs usually cause progressive damage in connective tissue, skeletal structure and various organs (*27*), pain and physical discomfort were the most frequently mentioned symptoms by patients, which was also reported in our study. The EQ-VAS scores of patients with all the four included LSDs were lower than the Chinese population norm of 80.4 (*28*), revealing the impaired QoL in patients with LSDs. Among the 4 LSDs, GD patients receiving ERTs had highest mean EQ-VAS score (76.4), which was quite close to the norm. The mobility and self-care ability of GD patients in our study were significantly better than patients with FD, PD and MPS as well. With the better health status, eighty percent of the GD patients worked as normal people did, while only 50% (8/16) of the adult patients with the other three LSDs could go to work. Most GD patients didn't need others to take care of them, which may be the reason why the indirect cost of GD patients (2,340 CNY) was much lower than that of the patients with the other three LSDs (21,860 CNY). Though previous study has confirmed that receiving ERTs is meaningful to the patients and could improve their QoL (*29*), the data analyzed in this study were cross-sectional, providing no evidence of a causal association between ERTs and QOL.

Our study has several limitations as well. Firstly, the sample size was notably small, but similar with other studies among the patients with LSDs and could be acceptable considering that the study was only conducted in a single city (*30,31*). Our study included around 50.8% (31/61) of the total samples based on our preliminary interviews with doctors and rare diseases organizations. It was believed altogether 61 alive patients with the four mentioned LSDs were in Shanghai right now. The treatment patterns of patients with LSDs, who did not participate in our study, were the same as that of patients included. Thus, we believe the results in our study could represent the actual situation that patients with LSDs in Shanghai are faced with. Secondly, the quality-of-life data could only be presented in the form of EQ-5D VAS scores rather than utility values as there are no EQ-5D-Y value set available in the world. Besides, our study only reported the current impaired QOL of patients with 4 LSDs. However, the causal relation between ERTs and the QOL of patients with LSDs could not be explained explicitly in the cross-sectional design, which needs to be further explored based on a randomized controlled trial, or panel data. Finally, with the inaccessibility of the hospital information systems, we adopted the online survey approach, which brought the general limitations of recall bias and preference bias. We added a round of quality control in the form of telephone interview to improve the quality.

5. Conclusions

Based on the current polices in Shanghai and our study on the patients with four LSDs, few patients with LSDs in Shanghai could have access to available ERTs without a high reimbursement level. Though the cost-sharing mechanism of basic medical insurance, charity fund and patients had been explored for Gaucher disease in Shanghai, the OOP part still laid a heavy economic burden on the patients and their families. The healthcare security system should pay more attention to LSDs patients, who need to be treated with extremely expensive ERTs. The scope of drug reimbursement list and the reimbursement level should be further expanded and raised to help improve the quality of life of patients with LSDs. Furthermore, considering the genetic background of LSDs and the high disease burden caused by LSDs, the preventive approach should be recommended by subsidizing the cost of gene tests during pregnancy.

References

1. Ferns JM, Halpern SH. Lysosomal storage diseases. In: Consults in Obstetric Anesthesiology. Springer, Cham, New York City, US, 2020; pp. 1-34.
2. Khatiwada B, Pokharel A. Lysosomal storage disease. JNMA J Nepal Med Assoc. 2009; 48:242-245.
3. Beck M. Treatment strategies for lysosomal storage disorders. Dev Med Child Neurol. 2018; 60:13-18.
4. National Healthcare Security Administration, Ministry of Human Resource and Social Security. Notice on the issuance of "National Basic Medical Insurance, Working Injury Insurance and Maternity Insurance Drug List (2020)". *http://www.nhsa.gov.cn/art/2020/12/28/ art_37_4220.html* (accessed July 5, 2021). (in Chinese)
5. Chen X, Qiu W, Ye J, Han L, Gu X, Zhang H. Demographic characteristics and distribution of lysosomal storage disorder subtypes in Eastern China. J Hum Genet. 2016; 61:345-349.
6. Zhao Y, Wang Z, Lu J, Gu X, Huang Y, Qiu Z, Wei Y, Yan C. Characteristics of Pompe disease in China: A report from the Pompe registry. Orphanet J Rare Dis. 2019; 14:78.
7. Yang Y, He JJ, Wang YQ, Kang Q, Hu SL. Study feasibility of multi-payment for drugs for rare diseases-taking Gaucher's disease in Qingdao as example. China Pharmacy. 2019; 30:2593-2597. (in Chinese)
8. China News. Report on patients with MPS: diagnosis and treatment facing multiple difficulties. *https://news.sina. cn/2020-05-15/detail-iirczymk1742021.d.html* (accessed July 19, 2021). (in Chinese)
9. People's Daily Online. Long-term living condition of patients with Gaucher disease (2019). *http://health.people. com.cn/n1/2019/0228/c14739-30908140.html* (accessed July 19, 2021). (in Chinese)
10. Xinhua Net. "2018 China Rare Disease Research Report" released, 30% doctors said they did not know about rare diseases. *http://www.xinhuanet.com/gongyi/2018-02/28/ c_129819383.htm* (accessed July 19, 2021). (in Chinese)
11. CN-Health. The first phase of the "Comprehensive Social Survey of Rare Diseases in China 2019" released, a sociological perspective on the real survival of rare patients. *https://www.sohu.com/a/348406469_139908* (accessed July 19, 2021). (in Chinese)
12. Red Cross Society of China, Shanghai Branch. Including disease-specific therapies for LSDs in the payment range of Shanghai Children's Hospitalization Assistance Fund. *http://www.redcross-sha.org/Home/View.aspx?id=5570* (accessed July 5, 2021). (in Chinese)
13. Shanghai Foundation for Rare Disease. To establish special assistance fund for LSDs. *http://www.hjbjjh.org/ Reception/GuidanceInfo.aspx?id=565&mid=0* (accessed July 5, 2021). (in Chinese)
14. Orphanet. The portal for rare diseases and orphan drugs. *https://www.orpha.net/consor/cgi-bin/index.php* (accessed July 5, 2021).
15. Wyatt K, Henley W, Anderson L, Anderson R, Nikolaou V, Stein K, Klinger L, Hughes D, Waldek S, Lachmann R, Mehta A, Vellodi A, Logan S. The effectiveness and cost-effectiveness of enzyme and substrate replacement therapies: A longitudinal cohort study of people with lysosomal storage disorders. Health Technol Assess. 2012; 16:1-543.
16. Kanters TA, Redekop WK, Hakkaart L. International differences in patient access to ultra-orphan drugs. Health Policy Technol. 2018; 7:57-64.
17. Herder M. What is the purpose of the orphan drug act? PLoS Med. 2017; 14:e1002191.
18. Commission of the European Communities. Communication from the Commission to the European Parliament, the Council, the European Economic and Social Committee and the Committee of the Regions. *http://www.europlanproject.eu/Resources/docs/ ECCommunication_COM-2008-679final.pdf* (accessed July 5, 2021).
19. The Department of Health. Life Saving Drugs Program - Information for patients, prescribers and pharmacists. *https://www.health.gov.au/initiatives-and-programs/life-saving-drugs-program?utm_source=health.gov.au&utm_ medium=callout-auto-custom&utm_campaign=digital_ transformation* (accessed July 5, 2021).
20. National Institute for Health and Care Excellence. Eliglustat for treating type 1 Gaucher disease. *https:// www.nice.org.uk/guidance/hst5/chapter/5-Consideration-*

of-the-evidence (accessed July 5, 2021).

21. National Institute for Health and Care Excellence. Migalastat for treating Fabry disease: Evidence submissions. *https://www.nice.org.uk/guidance/hst4/chapter/4-Evidence-submissions* (accessed July 5, 2021).

22. National Healthcare Security Administration. Letter from the National Healthcare Security Administration on the reply to the proposal No. 4482 of the Third Session of the 13th National Committee of the CPPCC. *http://www.nhsa.gov.cn/art/2020/12/23/art_26_4178.html* (accessed July 19, 2021). (in Chinese)

23. Shanghai Statistical Bureau. Disposable income and consumption expenditure per capita of Shanghai residents in 2019. *http://tjj.sh.gov.cn/ydsj71/20200121/0014-1004407.html* (accessed July 5, 2021). (in Chinese)

24. Qingdao Municipal Bureau of Human Resources and Social Security, Qingdao Finance Bureau. Notice on the Implementation of Universal Supplementary Medical Insurance in Qingdao. *https://m12333.cn/policy/swff.html* (accessed July 19, 2021). (in Chinese)

25. Zhejiang Healthcare Security Administration. Announcement on the publication of the outcome of negotiations on special drugs for rare diseases. *http://ybj.zj.gov.cn/art/2020/6/24/art_1615797_48765290.html* (accessed July 5, 2021). (in Chinese)

26. Zhejiang Healthcare Security Administration, Zhejiang Provincial Department of Finance, Zhejiang Health Commission. Notice on the establishment of medication security mechanism for rare diseases in Zhejiang Province. *http://ybj.zj.gov.cn/art/2019/12/31/art_1229113757_601196.html* (accessed July 5, 2021). (in Chinese)

27. Ratko TA, Marbella A, Sarah Godfrey M, Naomi Aronson M. Technical Brief 12 - Enzyme-Replacement Therapies for Lysosomal Storage Diseases. Blue Cross and Blue Shield Association Technology Evaluation Center Evidence-based Practice Center, 2013; pp. 1-107.

28. Szende A, Janssen B, Cabasese J. Self-Reported Population Health: An International Perspective based on EQ-5D. In: PharmacoEconomics & Outcomes News. Springer, Dordrecht, Dordrecht, the Netherlands, 2014; pp. 1-210.

29. Dams D, Briers Y. Therapeutic Enzymes: Function and Clinical Implications. In: Advances in Experimental Medicine and Biology. Springer Singapore, Singapore, 2019; pp. 233-253.

30. Conner T, Cook F, Fernandez V, Rangel-Miller V. An online survey of burden of illness in families with mucopolysaccharidosis type II children in the United States. Mol Genet Metab Rep. 2019; 21:100499.

31. Péntek M, Gulácsi L, Brodszky V, *et al*. Social/economic costs and health-related quality of life of mucopolysaccharidosis patients and their caregivers in Europe. Eur J Health Econ. 2016; 17 Suppl 1:89-98.

[§]These authors contributed equally to this work.
Address correspondence to:
Chunlin Jin and Qi Kang, Shanghai Health Development Research Center, Shanghai Medical Information Center, Shanghai 200040, China.
E-mail: kangqi@shdrc.org (Q.K.), jinchunlin@shdrc.org (CL.J.).

Brief Report

One-year follow-up of thyroid function in 23 infants with Prader-Willi syndrome at a single center in China

Min Yang[1,2], Jun Ye[1], Lianshu Han[1], Wenjuan Qiu[1], Yongguo Yu[1], Xuefan Gu[1], Huiwen Zhang[1,*]

[1] Department of Pediatric Endocrinology/Genetics, Xinhua Hospital, Shanghai JiaoTong University School of Medicine, Shanghai Institute for Pediatric Research, Shanghai, China;
[2] Department of Pediatrics, Shengjing Hospital of China Medical University, Shenyang, Liaoning, China.

SUMMARY   Endocrine disorders are common in patients with Prader-Willi syndrome (PWS). Whether hypothyroidism is present in patients with PWS, and especially infants and young children, remains unclear. The aims of this study were to evaluate thyroid function in patients with PWS, to assess the prevalence of thyroid dysfunction, and to evaluate the effect of growth hormone on thyroid function. Subjects were 23 patients with PWS ages 3 months to 3 years who were followed for up to one year. Four patients were lost to follow-up after the first visit. The remaining 19 patients were treated with recombinant human growth hormone (rhGH). PWS was diagnosed based on a genetic analysis. Free thyroxine (FT4), free triiodothyronine (FT3), and thyroid-stimulating hormone (TSH) levels were evaluated before and after growth hormone treatment. A total of 9 patients (9/23 = 39.1%) developed abnormal thyroid function. Five out of 23 patients (21.7%) had abnormal thyroid function before growth hormone treatment. Four patients developed thyroid dysfunction during the 3- to 9-month period of rhGH treatment. Of the 9 patients with abnormal thyroid function, 7 (5 boys, 2 girls) had central hypothyroidism, and the other 2 patients had subclinical hypothyroidism. TSH levels were higher in patients with PWS due to maternal uniparental disomy (UPD) than in patients with PWS due to a 15q11-q13 deletion. The prevalence of hypothyroidism was high in infants and young children with PWS. Thyroid function should be regularly monitored in patients with PWS at both diagnosis and follow-up.

Keywords   Prader-Willi syndrome, thyroid function, growth hormone, hypothyroidism

1. Introduction

Prader-Willi syndrome (PWS) is a complex genomic imprinting disorder in which afflicted individuals experience physical and behavioral abnormalities. PWS is caused by the loss of expression of paternally transcribed genes in a highly imprinted region of chromosome 15q11-q13 (*1*). The most common molecular alteration is deletion of the paternal copy of the gene locus (70%), and the remaining cases result from maternal uniparental disomy (28%) and imprinting defects (2%) (*2*).

Abnormalities of the hypothalamo-pituitary axis are present in PWS (*3*). Magnetic resonance imaging studies have revealed hypothalamic-pituitary abnormalities, including anterior pituitary hypoplasia and an absent, small, or ectopic posterior pituitary gland, in more than 50% of patients with PWS (*4,5*). Whether hypothyroidism is present and whether it should be treated in PWS remains unclear, and this is especially true in infants and young children (*6-8*). This is an important question because hypothyroidism can contribute to delayed psychomotor development when present early in life and left untreated. Several studies have investigated thyroid function in children with PWS, and central hypothyroidism has been found in 20-30% of patients with PWS (*9,10*). However, thyroid function in patients with PWS needs to be further explored in infants and young children.

The current study retrospectively analyzed thyroid function in 23 patients with PWS between the ages of 3 months and 3 years from August 2014 to January 2019, and it investigated the effect of growth hormone on thyroid function by comparing the results before and 3 and 6 months after treatment with recombinant human growth hormone (rhGH).

2. Patients and Methods

2.1. Patients and blood samples

Potential subjects were 23 patients with PWS ages 3 months to 3 years. All of patients were regularly followed up at Xinhua Hospital in Shanghai, China. Height (or length) and weight were measured with the patient wearing light clothing without shoes. Height was measured to the nearest 0.1 cm with a wall-mounted stadiometer. Body weight was measured to the nearest 0.1 kg. Body mass index (BMI) was calculated as the weight in kg/height in meters squared. All of the patients had a normal thyroid-stimulating hormone (TSH) level at neonatal screening for congenital hypothyroidism. A group of 22 healthy children ages 1-3 years were served as the control group. This study was approved by the Ethics Committee of this hospital. Due to the retrospective nature of the study, informed consent was waived.

An automated chemiluminescent immunoassay was used to measure thyroid hormone levels. The reference values were 3.5-6.5 pmol/L for free triiodothyronine (FT3), 11.5-22.7 pmol/L for free thyroxine (FT4), and 0.55-4.78 μIU/mL for TSH. Thyroid function was classified as euthyroidism (normal FT4 level and TSH level ≤ 5 μIU/mL), hypothyroidism (low FT4 level and TSH level ≥ 10 μIU/mL), central hypothyroidism (low FT4 level and TSH level ≤ 5 μIU/mL), or subclinical hypothyroidism (normal FT4 level and TSH level > 5 μIU/mL).

2.2. Statistical analysis

Data were processed and statistically analyzed using SPSS 13.0 (SPSS, Chicago, IL, USA). Normally distributed data are reported as the mean ± SD, and skewed data are presented as medians. Between-group comparisons were performed using the Mann-Whitney *U*-test and Fisher's exact test for differences in proportions. $P < 0.05$ indicated a statistically significant difference.

3. Results and Discussion

Potential subjects were 23 patients with PWS (12 boys, 11 girls) ages 3 months to 3 years. The diagnosis of PWS was genetically confirmed in all of the patients. PWS was due to a 15q11-q13 deletion in 17 subjects (73.9%) and by uniparental disomy (UPD) in 6 subjects (26.1%). Four of the 23 patients (17.4%) were born prematurely, and seven patients (30.4%) were small for gestational age (SGA). The mean birth weight and length were 2.6 kg ± 0.43 kg (-2.02 ± 1.37 SD) and 48.71 cm ± 1.64 cm (-0.8 ± 0.99 SD), respectively. Patients with PWS had a median (IQR) age of 0.67 years (0.25-2.67 years). At diagnosis, the mean and SD of length and weight in patients with PWS were -1.42 ±1.51 SD and -0.8 ± 0.99 SD, respectively. Patients

with PWS often had a low birth weight and were SGA (30.4%). This finding is consistent with the results of previous studies. Diene *et al.* studied 142 children with PWS (age 0.2-18.8 years) and found that the median birth weight was 2.65 kg (1.16-3.9), corresponding to -1.2 SD (-3.5 to +3.8). Thirty-seven out of 142 (30%) patients were born SGA (*10*). Mean maternal age was 30.3 ± 4.1 years. Mean paternal age was 32.3 ± 5 years. Most patients exhibited hypotonia, feeding difficulties, growth retardation, and microphallus. All boys had cryptorchidism, which had been surgically treated. One boy had congenital bilateral hip dislocation.

In contrast to several previous studies (*11-13*), the current findings revealed a relatively high prevalence of abnormal thyroid function in 5 out of 23 patients (21.7%) on the first test of thyroid function, with a higher frequency in males (4/5, 80%). The five patients were receiving substitutive therapy with L-thyroxine (Table 1, Patient 1 to Patient 5). A large population study found that 13.6% of patients (46/339) had abnormal thyroid function at subject recruitment, and abnormal thyroid function was also more common in males (27/46, 58.7%) (*7*). Another study reported that thyroid function was normal in newborn screening of infants with PWS (*14*). Moreover, that study found hypothyroidism in only one out of 21 older children (ages < 2 years) with PWS. However, the prevalence of hypothyroidism was higher in other studies. Diene *et al.* reported that 31 out of 127 subjects (24.4%) with PWS in France were diagnosed with hypothyroidism (*10*). In addition, a study of 18 patients with PWS conducted during the first 2 years of life reported that the prevalence of hypothyroidism (serum total thyroxine and/or FT4 levels below the 25th percentile of the reference population) was 72% (*15*). Studies of adult patients with PWS have reported that the frequency of hypothyroidism is 2.12% (1/47), which is similar to its frequency in the general population (*16*). Overall, thyroid function needs to be monitored when caring for infants and young children with PWS.

Four patients (Patient 6 to Patient 9, Table 1) had abnormal thyroid function during rhGH therapy for 3 to 9 months. In the current study, abnormal thyroid function was most often central hypothyroidism (7/9), suggesting that hypothalamic-pituitary-thyroid axis dysfunction might be a common feature in infants with PWS. This finding agrees with the results of most of the previous studies. Lorenzo *et al.* studied 339 patients with PWS (ages 0.2 to 50 years) and noted central hypothyroidism in 23 patients (*7*). Of those patients, 14 were under the age of 2 years. The highest prevalence of central hypothyroidism was reported by Vaiani *et al.*, with a rate of 72.2% (13/18) in a group of 18 infants with PWS (ages 0.16-2 years) (*15*). These findings indicate that there is a high incidence of transient or definitive hypothalamic-pituitary-thyroid axis dysfunction in patients with PWS.

Table 1. Abnormal thyroid function in patients with PWS before and after GH treatment

Patient no.	Status	Sex	Age (yrs)	FT3	FT4	TSH	Diagnosis	Mutation
1	Baseline	F	0.83	5.2	11.36	2.11	CEH	UPD
2	Baseline	M	0.94	4.32	10.21	2.47	CEH	DEL
3	Baseline	M	0.37	4.18	8.81	2.64	CEH	DEL
4	Baseline	M	1	2.88	9.91	2.13	CEH	DEL
5	Baseline	M	0.46	6.06	14.61	5.25	SH	DEL
6	3 months	M	1.08	4.08	8.56	3.17	CEH	DEL
7	3 months	M	0.56	5.68	14.34	5.29	SH	DEL
8	3 months	F	0.5	4.54	10.94	0.46	CEH	DEL
9	3 months	F	1.17	3.71	10.38	0.28	CEH	DEL

CEH, central hypothyroidism; DEL, 15q11-q13 deletion; F, female; FT3: free triiodothyronine; FT4, free thyroxine; M, male; SH, subclinical hypothyroidism; TSH, thyroid-stimulating hormone; UPD, uniparental disomy.

Table 2. Comparison of thyroid hormone levels in different groups of patients with PWS

Variables	PWS ($n = 23$)	CON ($n = 22$)	Boys ($n = 12$)	Girls ($n = 11$)	DEL ($n = 17$)	UPD ($n = 6$)	Baseline ($n = 9$)	3 months	Baseline ($n = 4$)	6 months
FT3 (pmol/L)	5.45 ± 0.95	5.88 ± 0.73	5.48 ± 1.152	5.42 ± 0.73	5.41 ± 1.08	5.58 ± 0.45	5.9 ± 0.75	5.77 ± 0.77	6.09 ± 0.47	6.15 ± 0.55
FT4 (pmol/L)	12.96 ± 1.92	15.91 ± 2.63	13.12 ± 2.32	12.8 ± 1.44	12.73 ± 2	13.63 ± 1.63	13.03 ± 1.17	13.09 ± 2.05	14.54 ± 1.87	14.24 ± 2.89
TSH (uIU/L)	2.066 ± 0.96	2.07 ± 0.9	2.56 ± 1.23	1.89 ± 0.64	2.01 ± 1.13	2.19 ± 0.29[*]	1.16 ± 0.39	1.45 ± 0.148	1.67 ± 0.39	1.45 ± 0.148

[*]$P < 0.05$ ($P = 0.0353$). Baseline, before growth hormone treatment; PWS, Prader-Willi syndrome; 3 months, 3 months of growth hormone treatment; 6 months, 6 months of growth hormone treatment.

Table 3. Comparison of the prevalence of thyroid dysfunction in different groups of patients with PWS

Variables	Boys ($n = 12$)	Girls ($n = 11$)	DEL ($n = 17$)	UPD ($n = 6$)
Prevalence of Thyroid Dysfunction	3/12 (25%)	2/11 (11.2%)	4/17 (23.5%)	1/5 (20%)
Prevalence of Normal Thyroid Function	9/12 (75%)	9/11 (81.8%)	13/17 (76.5%)	4/5 (80%)
P	0.54	0.54	0.61	0.61

Although abnormal thyroid function seemed to be more common in boys than girls, there were no differences in thyroid hormone between the two groups (Table 2), and this finding was similar to the results of previous reports (*16*). Likewise, there were no differences in the proportion of patients with thyroid dysfunction by gender or cause of PWS (Table 3). Only TSH levels were found to be higher in patients with PWS due to UPD than in patients with PWS due to a 15q11-q13 deletion. However, the mean levels of TSH were within the reference range, and there were no differences in FT3 and FT4 levels between those two groups. Thus, the clinical significance of higher TSH levels in PWS due to UPD is unclear and needs to be studied further.

All children were naive to GH treatment at the start of the study. They received a dose of 0.5 mg-1 mg rhGH/m2/day. Four patients were lost to follow-up after the first visit. After 3 months of GH treatment, 3 patients (21.4%, 3/14) developed abnormal thyroid function. Two of the three (1 boy and 1 girl) had central hypothyroidism, and the third (1 boy) had subclinical

hypothyroidism. Another boy was diagnosed with central hypothyroidism after rhGH treatment for 9 months (Table 1). Daily doses of rhGH in these four patients were 0.5 mg-0.6 mg/m2/day. There were no differences in thyroid hormone levels between subjects with normal thyroid function before and 3 months and 6 months after rhGH treatment (Table 2).

A few studies have reported the effects of GH treatment on thyroid function in patients with a GH deficiency and hypopituitarism (*17-19*). GH may increase the serum FT3 level and decrease the serum FT4 level by up-regulating type 2 iodothyronine deiodinase expression (*20*). In a study of thyroid function in 75 children (ages between 6 months and 16 years) with PWS receiving rhGH therapy at a dose of 1 mg/m2/day for 1 year, 25% of the patients with PWS were found to have central hypothyroidism with significantly lower FT4 levels while TSH levels were normal (*12*). This suggests that patients with PWS were likely to suffer from hypothyroidism during GH treatment.

In conclusion, the prevalence of hypothyroidism is high in infants and young children with PWS. Thyroid

function should be regularly monitored in patients with PWS at both diagnosis and follow-up.

Funding: None.

Conflict of Interest: The authors have no conflicts of interest to disclose.

References

1. Butler MG. Prader-Willi Syndrome: Obesity due to genomic imprinting. Curr Genomics. 2011; 12:204-215.
2. Cassidy SB, Schwartz S, Miller JL, Driscoll DJ. Prader-Willi syndrome. Genet Med. 2012; 14:10-26.
3. Harris RM, Stafford DEJ. Prader Willi syndrome: Endocrine updates and new medical therapies. Curr Opin Endocrinol Diabetes Obes. 2020; 27:56-62.
4. Iughetti L, Bosio L, Corrias A, Gargantini L, Ragusa L, Livieri C, Predieri B, Bruzzi P, Caselli G, Grugni G. Pituitary height and neuroradiological alterations in patients with Prader-Labhart-Willi syndrome. Eur J Pediatr. 2008; 167:701-702.
5. Emerick JE, Vogt KS. Endocrine manifestations and management of Prader-Willi syndrome. Int J Pediatr Endocrinol. 2013; 2013:14.
6. Konishi A, Ida S, Shoji Y, Etani Y, Kawai M. Central hypothyroidism improves with age in very young children with Prader-Willi syndrome. Clin Endocrinol (Oxf). 2021; 94:384-391.
7. Iughetti L, Vivi G, Balsamo A, *et al.* Thyroid function in patients with Prader-Willi syndrome: An Italian multicenter study of 339 patients. J Pediatr Endocrinol Metab. 2019; 32:159-165.
8. Oto Y, Murakami N, Matsubara K, Saima S, Ogata H, Ihara H, Nagai T, Matsubara T. Effects of growth hormone treatment on thyroid function in pediatric patients with Prader-Willi syndrome. Am J Med Genet A. 2020; 182:659-663.
9. Miller JL, Goldstone AP, Couch JA, Shuster J, He G, Driscoll DJ, Liu Y, Schmalfuss IM. Pituitary abnormalities in Prader-Willi syndrome and early onset morbid obesity. Am J Med Genet A. 2008; 146A:570-577.
10. Diene G, Mimoun E, Feigerlova E, Caula S, Molinas C, Grandjean H, Tauber M; French Reference Centre for PWS. Endocrine disorders in children with Prader-Willi syndrome – Data from 142 children of the French database. Horm Res Paediatr. 2010; 74:121-128.
11. Butler MG, Smith BK, Lee J, Gibson C, Schmoll C, Moore WV, Donnelly JE. Effects of growth hormone treatment in adults with Prader-Willi syndrome. Growth Horm IGF Res. 2013; 23:81-87.
12. Festen DA, Visser TJ, Otten BJ, Wit JM, Duivenvoorden HJ, Hokken-Koelega AC. Thyroid hormone levels in children with Prader-Willi syndrome before and during growth hormone treatment. Clin Endocrinol (Oxf). 2007; 67:449-456.
13. Tauber M, Barbeau C, Jouret B, Pienkowski C, Malzac P, Moncla A, Rochiccioli P. Auxological and endocrine evolution of 28 children with Prader-Willi syndrome: Effect of GH therapy in 14 children. Horm Res. 2000; 53:279-287.
14. Sharkia M, Michaud S, Berthier MT, Giguère Y, Stewart L, Deladoëy J, Deal C, Van Vliet G, Chanoine JP. Thyroid function from birth to adolescence in Prader-Willi syndrome. J Pediatr. 2013; 163:800-805.
15. Vaiani E, Herzovich V, Chaler E, Chertkoff L, Rivarola MA, Torrado M, Belgorosky A. Thyroid axis dysfunction in patients with Prader-Willi syndrome during the first 2 years of life. Clin Endocrinol (Oxf). 2010; 73:546-550.
16. Butler MG, Theodoro M, Skouse JD. Thyroid function studies in Prader-Willi syndrome. Am J Med Genet A. 2007; 143A:488-492.
17. Giavoli C, Profka E, Rodari G, Lania A, Beck-Peccoz P. Focus on GH deficiency and thyroid function. Best Pract Res Clin Endocrinol Metab. 2017; 31:71-78.
18. Ebuchi Y, Kubo T, Furujo M, Higuchi Y, Fujinaga S, Tsuchiya H, Urata N, Ochi M, Namba T, Hara N, Kishi M. Effect of growth hormone therapy on thyroid function in isolated growth hormone deficient and short small for gestational age children: A two-year study, including on assessment of the usefulness of the thyrotropin-releasing hormone (TRH) stimulation test. J Pediatr Endocrinol Metab. 2020; 33:1417-1423.
19. Agha A, Walker D, Perry L, Drake WM, Chew SL, Jenkins PJ, Grossman AB, Monson JP. Unmasking of central hypothyroidism following growth hormone replacement in adult hypopituitary patients. Clin Endocrinol (Oxf). 2007; 66:72-77.
20. Yamauchi I, Sakane Y, Yamashita T, Hirota K, Ueda Y, Kanai Y, Yamashita Y, Kondo E, Fujii T, Taura D, Sone M, Yasoda A, Inagaki N. Effects of growth hormone on thyroid function are mediated by type 2 iodothyronine deiodinase in humans. Endocrine. 2018; 59:353-363.

Address correspondence to:
Huiwen Zhang, Department of Pediatric Endocrinology/ Genetics, Xinhua Hospital, Shanghai JiaoTong University School of Medicine, Shanghai Institute for Pediatric Research, Shanghai 200092, China.
E-mail: zhanghuiwen@xinhuamed.com.cn

The coincidence of two ultra-rare hereditary eye diseases: gyrate atrophy and Kjer optic atrophy - a surprising diagnosis based on next-generation sequencing

Anna Skorczyk-Werner[1,*], Dorota Raczynska[2], Anna Wawrocka[1], Dinara Zholdybayeva[3], Nurgul Yakhiyayeva[3], Maciej Robert Krawczynski[1,4]

[1] Department of Medical Genetics, Poznan University of Medical Sciences, Poznan, Poland;
[2] Department of Ophthalmology, Gdansk Medical University, Gdansk, Poland;
[3] West Kazakhstan Marat Ospanow Medical University and 'Koz Zharygy' Center, Aktobe, Kazakhstan;
[4] Centers for Medical Genetics 'Genesis', Poznan, Poland.

SUMMARY Genetically determined ophthalmic diseases form a numerous and heterogenic group of disorders. Making the accurate clinical diagnosis of genetic eye disease is often a challenge for an ophthalmologist. In many cases, only genetic testing enables the establishment of the proper clinical diagnosis. Here we describe two ultra-rare diseases: gyrate atrophy of the choroid and retina (GACR) and Kjer-type optic atrophy coexisting in a 39-year-old Polish patient with severe visual impairment including a significant reduction of visual acuity and night blindness. Atrophic pigmented changes with large pigment deposits and chorioretinal atrophy with the retina's disturbed structure (with atrophic scarring changes and the epiretinal membrane) of both eyes were observed. Electroretinography (ERG) revealed extinguished responses. A Next-Generation Sequencing (NGS) panel comprising 275 retinal genes revealed a presence of potentially pathogenic variants in two genes: a homozygous variant c.1058G>A (p.Gly353Asp) in the *OAT* gene and a heterozygous variant c.1886C>G (p.Ser629Ter) in the *OPA1* gene. The diagnosis established based on NGS is surprising because initially, several different diagnoses have been made, including high degenerative myopia, choroideremia, Leber congenital amaurosis, and severe, atypical retinitis pigmentosa. This report provides the unquestioned diagnostic value of the combination of chorioretinal imaging and the NGS technique. To our knowledge, this is the first and the only description of the coincidence of gyrate atrophy and Kjer-type optic atrophy.

Keywords gyrate atrophy of the choroid and retina (GACR), Kjer-type optic atrophy, Next-Generation Sequencing (NGS)

1. Introduction

Gyrate atrophy of the choroid and retina (OMIM#258870, GACR) is an ultra-rare genetic condition inherited in an autosomal recessive manner. The disorder primarily affects the ocular tissues. Symptoms include night blindness, visual field constriction, and myopia, usually starting in the first decade of life, followed by progressive vision loss due to macular affection and cataract formation in the second decade (*1*). The global incidence of GACR is unknown, but the theoretical global incidence is approximately 1 in 1,500,000 births (*2*). The highest prevalence is observed in Finland, with about 1 in 50,000 individuals (*3*). Retinal features of patients with GACR involve sharply demarcated, circular areas of chorioretinal atrophy that start in

the mid-peripheral retina in the first decade and spread centrally to the macular region (*1*). It may lead to blindness, at the latest by 40-60 years (*4*). Other symptoms that may occur are neonatal blood hyperammonemia and type II muscle fiber atrophy with tubular aggregates' formation (*5*). Patients with gyrate atrophy generally have normal intelligence. However, minor central nervous system (CNS) abnormalities: degenerative changes in brain magnetic resonance imaging (MRI) and nonspecific electroencephalogram (EEG) abnormalities suggest that the CNS is involved, although no clear clinical correlates have been reported (*6*). Moreover, it was reported that peripheral nervous system abnormalities could also be observed in some gyrate atrophy patients. More than 50% of patients with GA were revealed to have electrophysiologic signs

of peripheral neuropathy. Most of them had mild or no symptoms, but 10% have symptomatic peripheral neuropathy, which was never disabling (*7*).

The disease is caused by a homozygous or compound heterozygous mutation in the *OAT* gene encoding an enzyme: ornithine delta-aminotransferase. OAT is a mitochondrial matrix enzyme that catalyzes ornithine's reversible transamination to glutamate semialdehyde (*8*), which plays a pivotal role in cellular detoxification (*9*). The OAT enzyme binds pyridoxal 5'-phosphate: a derivative of vitamin B6, as a cofactor (*2*). Mutations in the *OAT* gene result in a decrease or absence of the OAT enzyme activity. Deficiency of the OAT enzyme results in a 10 to 20 times increase in the plasma level of the amino acid ornithine, which is toxic to RPE and choroid (*4*). The *OAT* gene is located on chromosome 10q26.13 (*10*). It contains 11 exons and spans over 21 kb (*11*).

Optic atrophy type 1 (OMIM#165500, OPA1, Kjer-type optic atrophy), also known as autosomal dominant optic atrophy (ADOA), is a neuro-ophthalmic condition characterized by bilateral optic nerve pallor associated with an insidious decrease in visual acuity in early childhood, visual field defects, and color vision defects. The most typical symptoms are centrocoecal visual field scotoma found in the vast majority of patients affected with OPA1 and tritanopia (*12,13*). The disease causes bilateral degeneration of the optic nerves affecting primarily the retinal ganglion cells (RGC) and their axons forming the optic nerve (*14,15*). It leads to a moderate to severe loss of visual acuity. A considerable degree of inter- and intra-familial phenotypic variability was observed in ADOA (*12*). Moreover, the disease shows incomplete penetrance. It was reported to be as low as 43% (*16*). The clinical picture of optic atrophy type 1 may also include (in 20% of patients) some extraocular symptoms (s.c. ADOA plus syndrome, OMIM#125250), such as auditory neuropathy resulting in sensorineural hearing loss, mild peripheral myopathy, neuropathy, or less commonly: progressive external ophthalmoplegia, spastic paraparesis and multiple sclerosis-like illness (*13,15,17*).

Kjer-type optic atrophy is inherited in an autosomal dominant manner, and is caused by heterozygous variants in the *OPA1* gene. The prevalence of ADOA is 1:30,000-1:50,000 births and is much higher in Denmark (1:10,000 births) (*15*). The *OPA1* gene encodes ubiquitously expressed mitochondrial dynamin-like GTPase. The protein is associated with the inner mitochondrial membrane. It is required to maintain cristae integrity and play an essential role in mitochondrial fusion and maintaining mitochondrial DNA stability. It controls many processes, including energy metabolism and apoptosis (*14,15*). The *OPA1* gene is located on chromosome 3q28. It contains 31 exons, including the alternatively spliced exons: 4, 4b, 5b, and spans more than 100 kb (*14*).

2. Patient and Methods

2.1. Clinical data and analysis

A 39-year-old man of Polish origin was referred to a genetic clinic in 2019, due to severe visual impairment, including a significant reduction of visual acuity and night blindness. Initially, several differential diagnoses have been made in the proband including high degenerative myopia, choroideremia, Leber congenital amaurosis, and severe, atypical retinitis pigmentosa. Written informed consent was obtained from all subjects: the patient, his healthy mother and son, the patient's sister showing ADOA symptoms, and her three sons. This study was conducted in accordance with the tenets of the Declaration of Helsinki and the Association for Research in Vision and Ophthalmology (ARVO) statement on human subjects.

The patient was born at term from an uneventful pregnancy. His psychomotor development was normal. The parents were unrelated. The mother is still healthy and shows normal vision, but the father died at 37 due to a heart attack, and there is no information regarding his ophthalmological status. The patient has two older sisters and a younger brother. One sister and her son show ADOA symptoms (Figure 1).

Severe visual impairment has been observed in the patient since childhood. When the subject was 4-years-old, his parents noticed his low visual acuity and night blindness. At the age of 8, the patient's visual acuity
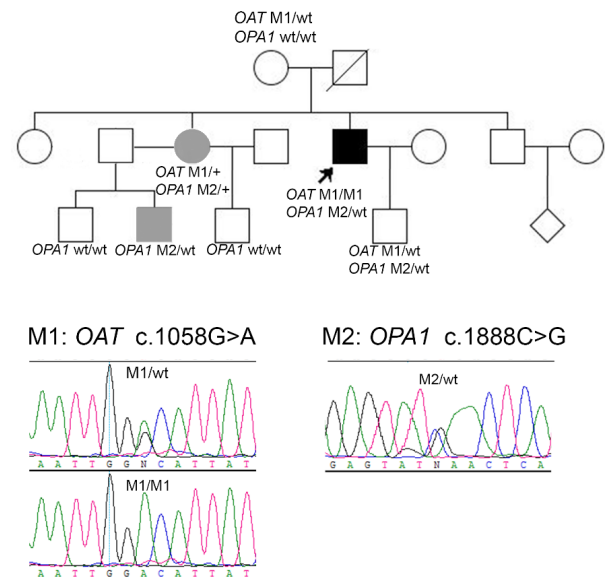

Figure 1. Pedigree of the examined family together with the segregation analysis results, and chromatograms of the identified variants. The upper panel shows the pedigree. Symbols filled with grey indicate individuals affected with optic atrophy type 1, the proband (affected with GA and ADOA) is marked with an arrow and a square filled with black. Unfilled symbols indicate unaffected individuals. A slash indicates a deceased person. The bottom panel shows chromatograms of the identified variants.

was 0.3, and he had high myopia (-11,0 D). In 2010, at the age of 29, the patient underwent bilateral cataract extraction with posterior chamber intraocular lens implantation. In the next years, biodegradation and subluxation of intraocular lenses (IOLs) to the vitreal cavity were noted. In 2017 the pars plana vitrectomy with removal of both IOLs was done at the age of 36. A significant deterioration of vision has been observed. Presently, the best-corrected (+6.0 D) visual acuity is reduced to 0.05 and 0.063 in the right and left eye, respectively. The patient is aphakic now and shows massive keratopathy. No extraocular symptoms were observed.

The patient underwent ophthalmological examinations, including visual acuity testing, fundus photography, spectral optical coherent tomography (SOCT), fundus autofluorescence (FAF), and electroretinography (ERG).

2.2. Molecular analysis

Blood samples from the patient were obtained for genetic examination. Later, blood samples were also obtained from his healthy mother and son, the sister showing ADOA symptoms, and her three sons (Figure 1). Genomic DNA was extracted from peripheral blood leukocytes using standard protocols. Due to the clinical suspicion of Leber congenital amaurosis NGS (Next Generation Sequencing), a diagnostic panel for 20 LCA genes (Asper Biogene, Asper Biotech Ltd., Tartu, Estonia) was firstly performed on the patient. The names of the genes analyzed in the LCA panel are listed in Supplementary material 1a (*http://www.irdrjournal.com/action/getSupplementalData.php?ID=75*). The analysis results have not revealed any potentially pathogenic variants in the analyzed genes, so the patient's DNA sample was subjected to panel NGS of 275 inherited retinal disease-associated genes (Genomed, Warsaw, Poland). The names of the genes analyzed in the retinal panel are listed in Supplementary material 1b (*http://www.irdrjournal.com/action/getSupplementalData.php?ID=75*). The NGS analysis was performed using SeqCap EZ HyperCap protocol and molecular probes NimbleGen SeqCap EZ (Roche) on a NextSeq 500 Illumina sequencing system.

3. Results and Discussion

Here we report an unusual case of a Polish patient with ocular symptoms of atypical severe retinal dystrophy and night blindness. The patient underwent ophthalmological examinations, including visual field testing, fundus photography, spectral optical coherent tomography (SOCT), fundus autofluorescence (FAF), and electroretinography (ERG). Retinal changes: atrophic pigmented changes with large pigment deposits and chorioretinal atrophy were present in both eyes'
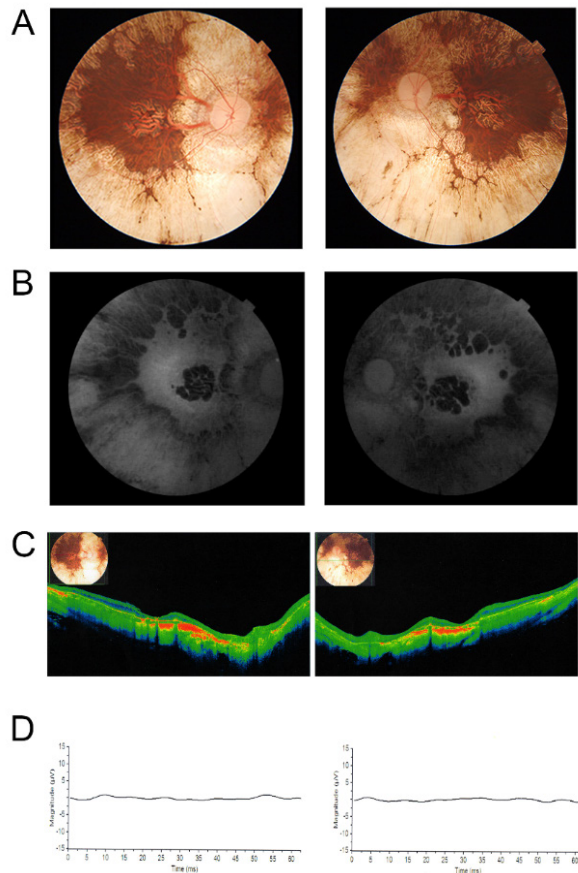

Figure 2. Retinal features of the patient. Right eye photographs are shown on the left and left eye - on the right. (A) Eye fundus photographs; **(B)** Eye fundus autofluorescence; **(C)** SOCT macular scan of the eye; **(D)** Photopic ERG.

retinas. SOCT revealed a totally disturbed structure of the retina with atrophic scarring changes and the epiretinal membrane. Pattern VEP showed no responses. Full-field ERG revealed totally extinguished photopic responses. Figure 2 shows the results of funduscopy (Fig.2A), fundus autofluorescence imaging (Fig.2B), SOCT (Fig.2C), and ERG (Fig.2D).

NGS on the retinal panel revealed presence of potentially pathogenic variants in two genes: a homozygous variant c.1058G>A (p.Gly353Asp) in the *OAT* gene (NM_000274.4) and a heterozygous variant c.1886C>G (p.Ser629Ter) in *OPA1* gene (NM_130837.3). Both variants are classified as pathogenic according to ACMG (American College of Medical Genetics and Genomics). Moreover, the *in silico* predictions of the (p.Gly353Asp) substitution potential pathogenicity with the use of SIFT (Sorting Intolerant from Tolerant, *https://sift.bii.a-star.edu.sg*) and Poly-Phen-2 (Polymorphism Phenotyping v.2, *http://genetics.bwh.harvard.edu/pph2*) indicated that the variant is probably damaging (the score 1.0 for PolyPhen-2 and 0.00 for SIFT). These results indicate a coincidence of two ultra-rare hereditary eye diseases: gyrate atrophy of the choroid and retina (GACR) and optic atrophy type 1 (Kjer-type optic atrophy). Segregation analysis for the

presence and independent inheritance of two identified altered alleles with Sanger sequencing of the appropriate *OAT* (exon 9), and *OPA1* (exon 20) gene fragments was performed. The primers used for amplification and sequencing as well as the Polymerase Chain Reaction (PCR) conditions are available upon request. The PCR products were bidirectionally sequenced using dye-terminator chemistry (v3.1BigDye® Terminator, Life Technologies). The sequencing products were separated on an ABI 3130xl capillary sequencer (Applied Biosystems). The segregation analysis revealed the presence of the heterozygous c.1886C>G *OPA1* variant in the patient's 40-year-old sister and her 8-year-old son, which confirmed the Kjer optic atrophy diagnosed in these individuals. The substitution was also identified in the patient's 10-year-old, asymptomatic son. The c.1058G>A variant in the *OAT* gene was tested in the patient's mother, the sister affected with Kjer optic atrophy, and the patient's son. The variant was identified in a heterozygous state in all these three patient's relatives. The segregation analysis results together with the pedigree of the family and chromatograms of the identified variants are shown in Figure 1.

The c.1058G>A (p.Gly353Asp) variant identified in the *OAT* gene was a previously reported rare variant (*18*) and it was identified as a heterozygous variant in GnomAD Browser (*19*) in 10 out of 113,298 analyzed alleles in healthy individuals. Based on *in silico* predictions of potential pathogenicity, the c.1058G>A variant is predicted to be damaging. Moreover, it causes a substitution of conserved glycine to aspartic acid at the amino acid position 353, localized within the C-terminal domain. The C-terminal domain and the N-terminal segment contribute to generating the gateway to the enzyme's active site (*2,9*). The OAT enzyme is expressed in most tissues, but the harmful consequences are confined mainly to the visual system. Our patient doesn't present any non-ocular symptoms or muscle fiber atrophy that can be observed in some gyrate atrophy patients.

The heterozygous variant c.1886C>G in the *OPA1* gene results in an introduction of the premature stop codon (p.Ser629Ter) in the protein's dynamin central region. It has been suggested that haploinsufficiency rather than the truncated protein's improper function may represent a major pathomechanism for dominant optic atrophy (*20*). The segregation analysis performed in the affected family revealed the p.Ser629Ter variant in the proband's sister and her son, showing symptoms of optic atrophy type 1, which was previously not confirmed by genetic diagnosis. The patient's mother, who has no ophthalmological problems, does not carry the mutation. Still, there is no information about the patient's father's vision, who died at 37 due to a heart attack. We cannot exclude the possibility that he also carried the *OPA1* variant, especially considering the high phenotypic variability of the ADOA and incomplete penetrance of

the gene.

The diagnosis made based on the NGS retinal panel is surprising because several different diagnoses have been previously suggested. Moreover, the clinical picture of the visual impairment observed in our patient did not allow us to diagnose any of these two identified diseases due to overlap of their symptoms. In the GACR, the pace of vision deterioration is not so fast as in our patient, while patients suffering from ADOA do not show retinal changes observed in the proband.

The appropriate molecular diagnosis in patients with genetic eye diseases is crucial, considering that the possibility of treatment with gene therapy has recently emerged for some of these disorders (*21*). In patients with GACR, pharmacological treatment may help to moderate the rate of chorioretinal atrophy progression. The treatment includes a low-protein, arginine-restricted diet, which may slow the progression of the disease (*22*) and administration of vitamin B6 (pyridoxine) - the precursor of the OAT cofactor that may help to reduce by 50% the level of serum ornithine in a subset of patients and slow down the chorioretinal atrophy (*2*). Proper genetic counseling also plays a crucial role, especially from the point of view of family planning.

4. Conclusion

To our knowledge, this is the first and the only description of the coincidence of gyrate atrophy and Kjer-type optic atrophy. The cooperation between ophthalmologists and geneticists is indispensable in making an accurate clinical diagnosis and planning treatment. The use of the NGS technique is beneficial, especially in unique, unclear cases. In most cases, the use of NGS panels enables a proper diagnosis, which is the basis of genetic counseling, and nowadays, in some cases, it gives a chance for an effective treatment. This report provides the unquestioned diagnostic value of the combination of retinal imaging and the NGS technique.

Acknowledgements

References

1. Elnahry AG, Tripathy K. Gyrate atrophy of the choroid

and retina. *https://www.ncbi.nlm.nih.gov/books/NBK557759* (accessed March 27, 2021).

2. Montioli R, Bellezza I, Desbats MA, Borri Voltattorni C, Salviati L, Cellini B. Deficit of human ornithine aminotransferase in gyrate atrophy: Molecular, cellular, and clinical aspects. Biochim Biophys Acta Proteins Proteom. 2021; 1869:140555.

3. Mäntyjärvi M, Tuppurainen K. Colour vision in gyrate atrophy. Vision Res. 1998; 38:3409-3412.

4. Takki KK, Milton RC. The natural history of gyrate atrophy of the choroid and retina. Ophthalmology. 1981; 88:292-301.

5. Kaiser-Kupfer MI, Kuwabara T, Askanas V, Brody L, Takki K, Dvoretzky I, Engel WK. Systemic manifestations of gyrate atrophy of the choroid and retina. Ophthalmology. 1981; 88:302-306.

6. Valtonen M, Näntö-Salonen K, Jääskeläinen S, Heinänen K, Alanen A, Heinonen OJ, Lundbom N, Erkintalo M, Simell O. Central nervous system involvement in gyrate atrophy of the choroid and retina with hyperornithinaemia. J Inherit Metab Dis. 1999; 22:855-866.

7. Peltola KE, Jääskeläinen S, Heinonen OJ, Falck B, Näntö-Salonen K, Heinänen K, Simell O. Peripheral nervous system in gyrate atrophy of the choroid and retina with hyperornithinemia. Neurology. 2002; 59:735-740.

8. Valle D, Simell O. The hyperornithinemias. In: Stanbury JB, Wyngaarden JB, Fredrickson DS, Goldstein JL, Brown MS. (eds.): The Metabolic Basis of Inherited Disease. (5th ed.) New York: McGraw-Hill (pub.) 1983; pp. 382-401.

9. Shen BW, Hennig M, Hohenester E, Jansonius JN, Schirmer T. Crystal structure of human recombinant ornithine aminotransferase. J Mol Biol. 1998; 277:81-102.

10. Barrett DJ, Bateman JB, Sparkes RS, Mohandas T, Klisak I, Inana G. Chromosomal localization of human ornithine aminotransferase gene sequences to 10q26 and Xp11.2. Invest Ophthalmol Vis Sci. 1987; 28:1037-1042.

11. Mitchell GA, Looney JE, Brody LC, Steel G, Suchanek M, Engelhardt JF, Willard HF, Valle D. Human ornithine-delta-aminotransferase: cDNA cloning and analysis of the structural gene. J Biol Chem. 1988; 263:14288-14295.

12. Votruba M, Fitzke FW, Holder GE, Carter A, Bhattacharya SS, Moore AT. Clinical features in affected individuals from 21 pedigrees with dominant optic atrophy. Arch Ophthalmol. 1998; 116:351-358.

13. Delettre-Cribaillet C, Hamel CP, Lenaers G. Optic Atrophy Type 1. 2007 Jul 13 [updated 2015 Nov 12]. In: Adam MP, Ardinger HH, Pagon RA, Wallace SE, Bean LJH, Stephens K, Amemiya A, editors. GeneReviews® [Internet]. Seattle (WA): University of Washington, Seattle; 1993-2020.

14. Lenaers G, Reynier P, Elachouri G, Soukkarieh C, Olichon A, Belenguer P, Baricault L, Ducommun B, Hamel C, Delettre C. OPA1 functions in mitochondria and dysfunctions in optic nerve. Int J Biochem Cell Biol. 2009; 41:1866-1874.

15. Lenaers G, Hamel C, Delettre C, Amati-Bonneau P, Procaccio V, Bonneau D, Reynier P, Milea D. Dominant optic atrophy. Orphanet J Rare Dis. 2012; 7:46.

16. Toomes C, Marchbank NJ, Mackey DA, Craig JE, Newbury-Ecob RA, Bennett CP, Vize CJ, Desai SP, Black GC, Patel N, Teimory M, Markham AF, Inglehearn CF, Churchill AJ. Spectrum, frequency and penetrance of OPA1 mutations in dominant optic atrophy. Hum Mol Genet. 2001; 13:1369-1378.

17. Yu-Wai-Man P, Griffiths PG, Gorman GS, *et al.* Multi-system neurological disease is common in patients with OPA1 mutations. Brain. 2010; 133:771-786.

18. Brody LC, Mitchell GA, Obie C, Michaud J, Steel G, Fontaine G, Robert MF, Sipila I, Kaiser-Kupfer M, Valle D. Ornithine delta-aminotransferase mutations in gyrate atrophy. Allelic heterogeneity and functional consequences. J Biol Chem. 1992; 267:3302-3307.

19. Genome aggregation database (gnomAD browser). Search for an OAT gene. *https://gnomad.broadinstitute.org* (accessed March 27, 2021).

20. Delettre C, Griffoin JM, Kaplan J, Dollfus H, Lorenz B, Faivre L, Lenaers G, Belenguer P, Hamel CP. Mutation spectrum and splicing variants in the OPA1 gene. Hum Genet. 2001; 109:584-591.

21. Garafalo AV, Cideciyan AV, Héon E, Sheplock R, Pearson A, WeiYang Yu C, Sumaroka A, Aguirre GD, Jacobson SG. Progress in treating inherited retinal diseases: Early subretinal gene therapy clinical trials and candidates for future initiatives. Prog Retin Eye Res. 2020; 77:100827.

22. Kaiser-Kupfer MI, de Monasterio FM, Valle D, Walser M, Brusilow S. Gyrate atrophy of the choroid and retina: improved visual function following reduction of plasma ornithine by diet. Science. 1980; 210:1128-1131.

Address correspondence to:
Anna Skorczyk-Werner, Department of Medical Genetics, Poznan University of Medical Sciences, 8 Rokietnicka St. 60-806 Poznan, Poland.
E-mail: aniaskorczyk@poczta.onet.pl

Brief Report

Familial SDHB gene mutation in disseminated non-hypoxia-related malignant paraganglioma treated with [^{90}Y]Y/[^{177}Lu]Lu-DOTATATE

Izabela Łoń[1], Jolanta Kunikowska[2], Piotr Jędrusik[1,*], Jarosław Góra[1], Sadegh Toutounchi[3], Grzegorz Placha[1], Zbigniew Gaciong[1]

[1] Department of Internal Medicine, Hypertension and Vascular Diseases, Medical University of Warsaw, Warsaw, Poland;
[2] Department of Nuclear Medicine, Medical University of Warsaw, Warsaw, Poland;
[3] Department of General and Endocrine Surgery, Medical University of Warsaw, Warsaw, Poland.

SUMMARY   Familial paraganglioma may be related to mutations in succinate dehydrogenase (SDH) enzyme complex genes. Among patients with hereditary paraganglioma, SDH subunit B (SDHB) gene mutations are associated with the highest morbidity and mortality related to a higher malignancy rate. We report a family with the c.689G>A (p.Arg230His) mutation in the SDHB gene identified in two family members, a father and his daughter. While the 14-year-old daughter had no evidence of clinical disease, recurrent and later disseminated [^{131}I]metaiodobenzylguanidine uptake-negative head and neck paraganglioma with multiple bone metastases developed in the father who underwent peptide receptor radionuclide therapy with [^{90}Y]Y/[^{177}Lu]Lu-dodecane tetraacetic acid octreotate (DOTATATE) at the time of the genetic diagnosis. This treatment was repeated 6 years later due to disease progression and the patient, who is currently 49 years old, remains alive and in good overall clinical condition at 8 years of follow-up after the original presentation at our unit. The growing armamentarium of imaging methods available for such patients may inform decision making regarding choice of the optimal treatment approach, potentially contributing to improved outcomes.

Keywords   somatostatin receptor imaging, succinate dehydrogenase, catecholamine-producing tumor, positron emission tomography/computed tomography

1. Introduction

Paragangliomas, along with pheochromocytomas, are rare catecholamine-producing neuroendocrine tumors originating from cells derived from the neural crest. According to the World Health Organization (WHO) classification, pheochromocytomas occur in the adrenal medulla, while paragangliomas are extraadrenal tumors of sympathetic or parasympathetic origin, which can occur in the paravertebral ganglia, mediastinum, abdomen, pelvis, head or neck.

They typically present as painless, gradually enlarging masses with slow growth and no specific clinical features until symptoms of catecholamine overproduction or a mass effect. In addition to variable location, they can be solitary or multiple, sporadic or hereditary, and benign or malignant. They may be of sympathetic or parasympathetic origin, and secreting or non-secreting hormones. Multiple tumors are more common in hereditary compared to sporadic cases.

Location in the upper part of the body above the diaphragm, particularly within the neck or head, is typical for parasympathetic paragangliomas. These tumors may also have specific names related to their site, including glomus jugulare for jugular location, glomus tympanicum for tympanic paraganglia and chemodectoma for carotid body paraganglia. Most of them are benign but sometimes they have a malignant nature with multiple distant metastases, usually to the cervical lymph nodes, lungs, bones, and liver.

The estimated combined annual incidence of pheochromocytoma/paraganglioma is 0.8 per 100,000 person-years, with approximately 500 to 1,600 cases annually in the United States (*1*). The prevalence of pheochromocytoma/paraganglioma among hypertensives in general outpatient clinics is 0.2-0.6%. Pheochromocytoma is found in nearly 5% of patients with an incidentally discovered adrenal mass on imaging (*2*).

In most reports that included large groups of patients, about 30% or more of paragangliomas were hereditary

(*3,4*). They are associated with germ-line or more rarely somatic mutations of one of five succinate dehydrogenase (SDH) enzyme complex genes, functioning as tumor suppressor genes, or occur as part of multineoplasm syndromes including von Hippel-Lindau disease (VHL), neurofibromatosis type 1, multiple endocrine neoplasia type 2A and 2B, and rare Carney-Stratakis triad. More recently, Myc-associated factor X (MAX) gene, hypoxia-inducible factor (HIF)-2α gene, and *TMEM127* gene mutations were also identified in individuals with paragangliomas (*5*). An autosomal dominant inheritance with incomplete penetrance and variable expression is typical for the hereditary forms (*1*).

The most common genetic defects in patients with paragangliomas are mutations of SDH complex genes. Depending on the specific gene, there are 5 types of paraganglioma syndromes (PGL1 to 5 syndromes), which have been linked to mutations of various complex SDH genes. The most commonly mutated gene in patients with familial paraganglioma syndromes is the one coding for SDH subunit D (SDHD).

Malignancy in paragangliomas is rather rare, as only about 10% of paragangliomas are malignant but this rate is higher in hereditary compared to sporadic cases and it is closely related to the specific mutated gene. The highest morbidity and mortality has been reported, related to a higher (21-79%) malignancy rate, in carriers of SDH subunit B (SDHB) gene mutations (*3,6*).

Despite great progress, imaging of paragangliomas may remain challenging. Detection of distant metastases is crucial for the diagnosis of a malignant form and leads to a change in the therapeutic strategy.

In the present study, we present the clinical course and imaging study results that formed our decision making regarding the choice of the optimal treatment approach in a male patient with the hereditary, malignant form of paraganglioma associated with the Arg230His mutation in the SDHB gene (PGL4 syndrome).

2. Materials and Methods

2.1. The patient

A Caucasian male, currently 49 years old, presented first at the age of 25 years with right carotid paraganglioma. He was treated surgically in 1996, and a local recurrence was diagnosed 12 years later. For that reason, he was operated on again in 2008 and paraganglioma was again confirmed in the histopathological diagnosis. In October 2012, a large tumor was found in the right temporal region and the patient underwent right temporal craniectomy. The pathology report described a 5 × 4 × 1 cm tumor with an adherent dura mater area sized 5 × 3 cm, in the cross-section appearing creamy-brown, partly calcified, and invading the dura mater, with the Ki-67 index of 10%, corresponding to the WHO G2 grade. Immunohistochemical staining was positive for chromogranin A (CgA), protein S100 and synaptophysin, confirming the neuroendocrine nature of the tumor cells.

In November 2012, the patient was admitted for further evaluation to the Department of Internal Diseases, Hypertension and Angiology, Medical University of Warsaw. He did not have any symptoms suggesting catecholamine overproduction. Physical examination revealed paleness, tachycardia, and systolic murmur at the base of the heart. Blood pressure was normal with no orthostatic hypotension. Laboratory tests showed mild microcytic anemia with low serum iron concentration. Transferrin and ferritin levels were in the normal range, as were thyroid hormones and thyroid-stimulating hormone. Echocardiography showed no abnormalities. Ambulatory blood pressure monitoring showed normotension with preserved normal circadian rhythm. Neck ultrasonography revealed focal recurrence.

Catecholamine testing showed elevated 24-hour urinary unfractionated metanephrines (1,326 µg/24h, reference range 100-1,000 µg/24h), while 24-hour urinary excretion of norepinephrine (70 µg/24h, reference range 23-105 µg/24h), epinephrine (6.9 µg/24h, reference range 4-20 µg/24h) and dopamine (307 µg/24h, reference range below 450 µg/24h) was within the normal range. Plasma CgA level was elevated more than 6-fold above the upper reference limit (641.6 ng/mL, reference range 0-94 ng/mL).

2.2. Genetic testing

Genomic DNA was extracted from venous blood and polymerase chain reaction (PCR) was used to amplify the eight exons of the SDHB gene, four exons of the SDHD gene, three exons of the VHL gene, and exons 10, 11, 13, 14, 15, 16 of the RET gene. Primer sequences and PCR conditions are listed in Table 1. PCR products were purified with NucleoFast 96 PCR kit (Macherey-Nagel, Düren, Germany). The sequencing of PCR products was conducted using BigDye 3.1 chemistry and ABI3130 genetic analyzer (Applied Biosystems, Foster City, CA, USA) according to the manufacturer's protocol.

3. Results and Discussion

We found the c.689G>A (p.Arg230His) mutation in exon 7 of the SDHB gene (reference sequence NM_003000.2) in the patient and in one of his two daughters who was 14 years old at that time. The affected daughter was asymptomatic, had no tumors found in whole body magnetic resonance imaging (MRI) performed in January 2014, and her catecholamine testing results were normal. There was no family history of neoplasms and carotid body tumors.

Somatostatin receptor imaging with [68Ga]Ga-dodecane tetraacetic acid octreotate (DOTATATE)

Table 1. Primer sequences and polymerase chain reaction (PCR) conditions for the genetic analysis.

Set of primers for PCR amplification of the evaluated gene exons

SDHD			
SDHD1F	GTTCACCCAGCATTTCCTCTTC	SDHD1R	GTCCTCACTTCCATCCCCTTC
SDHD2F	CAGTAACCCCAGTGAAATAGATGC	SDHD2R	TAGAGCCCAGAAAGCAGCAG
SDHD3F	TGTAGGCATTGAGATACCCTTG	SDHD3R	CACAGCAAACAAACTGAGCA
SDHD4F	GTGGAGTGGCAAATGGAGACAT	SDHD4R	CTGTGGATGCAATGGACACCTA
		SDHD4R2*	GCAGAGGCAAAGAGGCATACAT
SDHB			
SDHB_1F	GCCTTGCCCTATGCTTCCTC	SDHB_1R	CTGAAAGTCGCCCTGCCTCT
SDHB_2F	CAAGGATGTGAAAAGCATGTCC	SDHB_2R	TGTGCCAGCAAAATGGAATTATC
SDHB_3F	GCATTTACCCAAGAAAAGGAAT	SDHB_3R	CATCCAGGTGTCTCCGATTA
SDHB_4F	GCAAATAAAAACAAAACCAGAGAG	SDHB_4R	GAAGGGAGAAAAGCCAACAGG
SDHB_5F	TTCACGGGTTCACACTACTCAC	SDHB_5R	TCCAAGAAATGGGGTAAATAAAGC
SDHB_6F	TTACCCTGTTTGGACTGGATGG	SDHB_6R	ATCACCCCTTGGATTTTGCTA
SDHB_7F	GTTGCTCTCTGCCAATCACCTC	SDHB_7R	ATACAGTCCCTGCCTTCACCAA
SDHB_8F	GACTCCTGGCACCTTCACATTC	SDHB_8R	TGGGTTTTCCCTTTCAGTTTCA
RET			
RETY10F	CCTATGCTTGCGACACCAGTT	RETY10R	CCCTTGTTGGGACCTCAGATG
RETY11F	AGGGGGCAGTAAATGGCAGTA	RETY11R	CTATGGAAATGGGGGCAGAAC
RETY13F	AAGCCTCAAGCAGCATCGTCT	RETY13R	GGAGCAGTAGGGAAAGGGAGAA
RETY14F	GGCAGAGAGCAAGTGGTTCAAG	RETY14R	GGGCTAGAGTGTGGCATGGT
RETY15F	CACCCCTCTGCTGGTCACAC	RETY15R	GCTCCACTAATCTTCGGTATCTTCC
RETY16F	CTCAGCAATCCACAGGAGGTTC	RETY16R	CCACCCCAAGAGAGCAACAC
VHL			
VHL1F	GATGATTGGGTGTTCCCGTGT	VHL1R	GGCTTCAGACCGTGCTATCGT
VHL1F2*	GTGGAAATACAGTAACGAGTTGGC		
VHL2F	CGGTGTGGCTCTTTAACAACC	VHL2R	TGAGAACTGGGCTTAATTTTTCAA
VHL3F	GCCTCTTGTTCGTTCCTTGTA	VHL3R	ATTTTGTGATGTTTGCCCCTAA

*nested (internal) sequencing primer. Polymerase chain reaction (PCR) conditions: first denaturation step at 95°C for 5 minutes was followed by 42 cycles of denaturation (94°C for 30 seconds), annealing (60°C for 30 seconds) and extension (72°C for 50 seconds), with the final extension at 72°C for 10 minutes.
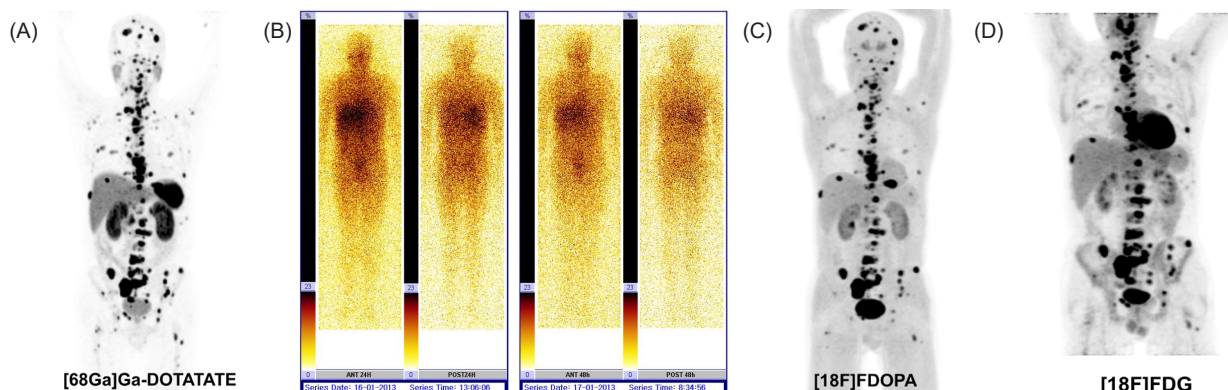

Figure 1. Imaging studies before treatment. (A) Somatostatin receptor imaging with [68Ga]Ga-DOTATATE demonstrating an increased uptake in the right neck and regional lymph nodes as well disseminated foci in bones. **(B)** [131I]mIBG whole body scintigraphy scan revealed no uptake at the site of metastases. **(C)** Positron emission tomography/computed tomography (PET/CT) imaging with [18F]FDOPA. **(D)** PET/CT imaging with [18F]FDG.

positron emission tomography/computed tomography (PET/CT) demonstrated an increased uptake in the right neck and regional lymph nodes as well disseminated foci in bones with high somatostatin receptor overexpression (maximum standardized uptake values [SUVmax] up to 57) (Figure 1A).

Due to poor results of chemotherapy in paraganglioma cases, radionuclide therapy was considered. Both peptide receptor radionuclide therapy (PRRT) with radiolabelled somatostatin analogues and [131I]metaiodobenzylguanidine (mIBG) therapy have become established methods for the treatment of disseminated paraganglioma. To choose the best

treatment option, [131I]mIBG scan was performed but it showed no uptake at the site of metastases (Figure 1B).

On the basis of several studies in the literature that have shown that [18F]F-dihydroxyphenylalanine ([18F]FDOPA) PET/CT is an excellent imaging tool in head and neck paragangliomas with the sensitivity approaching 100% (7), [18F]FDOPA PET/CT was performed to exclude metastases without somatostatin expression and it showed uptake in the same sites as [68Ga]Ga-DOTATATE PET/CT (Figure 1C).

Due to the high somatostatin receptor expression on [68Ga]Ga-DOTATATE PET/CT, a multidisciplinary team consisting of an oncologist, a nuclear medicine

physician, and a cardiologist opted for PRRT. Grading of paragangliomas and neuroendocrine tumors is based on primary tumors, but metastatic lesions could have higher Ki-67 values. For prognostication and evaluation of tumor metabolic activity before PRRT, PET/CT with [^{18}F]-fluorodeoxyglucose ([^{18}F]FDG) was performed, showing an increased uptake in all foci with SUVmax up to 24, matched with [^{68}Ga]Ga-DOTATATE PET/CT findings, with no additional foci shown (Figure 1D).

Before therapy, hemoglobin level was 10.2 g/dL, and other laboratory test results including kidney function tests were in the normal range.

The therapy was approved by the ethics committee at the Medical University of Warsaw and the patient gave a written informed consent. As a preparation for the therapy, the patient received a prophylactic low dose of doxazosin. Iron deficiency was also corrected.

Mixed amino-acid (1,000 mL of Vamin 18, Fresenius Kabi) and Ringer's solutions (500 mL) were infused over 8 hours for kidney protection, with infusion of 200 mL directly prior to treatment administration. Before administration of the radiopharmaceutical, ondansetron (8 mg, Zofran, Glaxo Wellcome) was injected intravenously to prevent nausea and vomiting.

Overall, 4 PRRT treatment sessions with tandem isotope [^{90}Y]Y/[^{177}Lu]Lu-DOTATATE (50% of the activity as [^{90}Y]Y-DOTATATE and 50% as [^{177}Lu]Lu-DOTATATE) were performed. The total injected activity was 14.8 GBq (400 mCi), with 3.7 GBq (100 mCi) per session.

PRRT was initiated in February 2013. Six weeks later, the patient began to feel increasing sensory abnormalities and weakness within the lower extremities. Repeated history taking revealed that in fact, the patient felt a slight numbness in the feet already four months earlier. MRI revealed an absolute stenosis of the spinal canal at the Th7 and Th8 vertebrae, with myelopathy at this level, due to two epidural tumors inside the spinal canal, associated with metastases involving the posterior vertebrae elements. Tumor embolization attempt was ineffective, and laminectomy involving Th7, Th8, and partially Th6, with removal of two tumors and spinal decompression was successfully performed. Neurological symptoms resolved completely following the surgery and rehabilitation. During hospitalization in the Department of Neurosurgery, anemia was observed with hemoglobin level of 8.9 g/dL and hematocrit of 26.6%.

After the surgery and Th7/Th8 stabilization, PRRT was continued, with the last treatment session in September 2013. The radionuclide therapy was well tolerated by the patient. Following PRRT, hemoglobin level was 12.7 g/dL and stable during further follow-up. Liver and kidney function tests were normal, as were other laboratory test results. Plasma CgA level decreased gradually from 641.6 ng/mL initially to 414.9 ng/mL at 3 months, 339.8 ng/mL at 6 months, and 262.6 ng/mL at 12 months.

In follow-up [^{68}Ga]Ga-DOTATATE PET/CT at 3, 6 and 12 months after the therapy, stable disease was observed with decreasing SUVmax up to 38, with no new metastatic foci. The patient was able to resume work.

The disease was stable in follow-up imaging until July 2017 but in February 2019, follow-up [^{68}Ga]Ga-DOTATATE PET/CT scanning revealed multiple small new foci in bones, including the skull, ribs, spine (Th9, L2 and L4 vertebrae), pelvis, and femurs, mostly of mixed osteolytic-osteosclerotic nature on CT. Two additional PRRT treatment sessions with [^{90}Y]Y/[^{177}Lu]Lu -DOTATATE were performed in March and June 2019, with amino-acid infusion for nephroprotection. The total injected activity was 7.4 GBq (200 mCi), with 3.7 GBq (100 mCi) per session.

Follow-up PET/CT with [^{68}Ga]Ga-DOTATATE in October 2019 and November 2020 demonstrated stable diffuse lesions in bones, largest in the spine (L5 and sacrum) with decreasing SUVmax up to 35, along with stable lesions in the right neck with lower somatostatin receptor expression (postoperative site at the right common carotid artery and group II lymph nodes, SUVmax values up to 17 in November 2020). The patient did not have anemia prior to the second treatment (hemoglobin level of 13.6 g/dL in 2018), and at the time of PRRT sessions in March and June 2019, hemoglobin level was 13.1 and 12.3 g/dL. As of April 2021, the patient remained in a good overall clinical condition. Follow-up [^{68}Ga]Ga-DOTATATE PET/CT scans are shown in Figure 2.

In our patient, shortly after the disease recurred for the second time and temporal bone metastases were found, we have recognized a hereditary, malignant form of PGL4 syndrome with the c.689 G>A (p.Arg230His) mutation in exon 7 of the SDHB gene. The disease involved the carotid body (at the first disease presentation in 1997) and the temporal bone (with adherent dura mater), with dissemination to the long bones, skull, ribs and spine. Hormonal studies revealed only slight elevation of urinary metanephrines but not epinephrine, norepinephrine or dopamine. When it turned out that the disease is generalized, with multiple bone metastases, there was no option for resection. Metastatic paragangliomas and pheochromocytomas are also relatively radioresistant, as compared to bone metastases in breast cancer and lymphoma lesions (*8*). The patient underwent surgical treatment, however, when two metastatic tumors located within the spinal canal exerted a serious mass effect with myelopathy and an attempt of tumor embolization was ineffective in a critical moment of the disease. Resection of these two metastatic tumors resulted in a prompt and effective relief of neurological symptoms. This approach is in accordance with the recommendations and may also possibly improve survival, although there are no definitive data to support this (*9*).
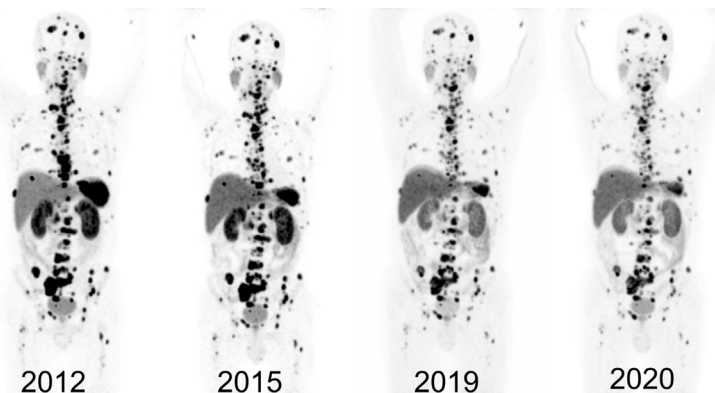
Figure 2. Somatostatin receptor imaging with [⁶⁸Ga]Ga-DOTATATE – response to treatment.

Both PRRT with radiolabelled somatostatin analogues and [¹³¹I]mIBG therapy have become established methods for treatment of disseminated paraganglioma (*10*). The efficacy and safety of most commonly used agents, [⁹⁰Y]Y-DOTATATE and [¹⁷⁷Lu]Lu-DOTATATE, in malignant paraganglioma has been described in a number of case reports and patient series. One of the largest recent series reported in the literature included 30 patients with inoperable or metastatic pheochromocytomas and paragangliomas (including 27 paragangliomas). Best tumor response was partial response in 7 (23%) patients and stable disease in 20 (67%) patients, while progressive disease was observed in 3 (10%) patients. The median progression-free survival was 91 months in patients with parasympathetic paragangliomas, 13 months in patients with sympathetic paragangliomas and 10 months in patients with metastatic pheochromocytomas. Grade 3/4 subacute haematotoxicity occurred in 6 (20%) of patients (*11*). In a recent systematic review, overall 12 studies were included, for a total of 201 patients with advanced (inoperable and metastatic) pheochromocytoma and paraganglioma who were treated with PRRT. A disease control rate of 84% was reported, and treatment-related adverse effects were minimal, with grade 3/4 neutropenia, thrombocytopenia, lymphopenia and nephrotoxicity observed in up to 11% of patients. Similar tumor response rates were noted for ⁹⁰Y- and ¹⁷⁷Lu-based agents (*12*). However, severe adverse reactions following [¹⁷⁷Lu]Lu-DOTATATE treatment were also reported in patients with paraganglioma, including catecholamine crisis and tumor lysis syndrome (*13*), as was marked progression of metastatic paraganglioma following initial partial response to PRRT (*14*).

PET/CT-based visualization of metastatic foci with very high uptake of [⁶⁸Ga]Ga-DOTATATE, with their confirmation by [¹⁸F]FDOPA PET/CT, was the reason for choosing this treatment method in the reported case. [¹²³I][¹³¹I]mIBG scintigraphy may be also considered, but mIBG scan revealed no uptake at the site of metastases. It is known that [¹²³I][¹³¹I]mIBG scintigraphy may be suboptimal in patients with special genotypic features such as those with VHL and SDHB gene mutation-related paraganglioma (*7*).

Systemic chemotherapy is recommended for unresectable and rapidly progressive pheochromocytoma/paraganglioma and in patients with high tumor burden or multiple bone metastases. A critical appraisal of the reports evaluating chemotherapy reveals, however, that these studies predominantly involved patients with retroperitoneal sympathetic catecholamine-secreting tumors and pheochromocytoma (*15,16*). Both the location and the parasympathetic origin of neck and head paraganglioma suggest cautious interpretation of these results in relation to hereditary malignant paraganglioma.

Recent years brought hope for a new effective chemotherapeutic temozolomide, used alone or in combination with other agents including thalidomide, capecitabine, gemcitabine, paclitaxel, and docetaxel (*17-19*). Temozolomide may be particularly useful in hereditary paraganglioma with SDHB gene mutation, which is associated with hypermethylation of the promoter for O-6-methylguanine-DNA methyltransferase (*17*). Experience with the drug is still limited, however, as in a recent case report and literature review, only 26 cases of metastatic pheochromocytoma/paraganglioma treated with temozolomide were identified globally (*20*).

In our patient, genetic testing revealed PGL4 syndrome associated with the Arg230His mutation in the SDHB gene. The mutation was reported previously (*21*), including in familial cases, although to date, there are only a few families bearing the Arg230His mutation described in the literature (*22-25*).

In one of these reports, the Arg230His mutation was identified in the context of high-altitude hypoxia-related paraganglioma in two members of the same family living in Guadalajara, Mexico, at over 1500 m above sea level (*23*). More than 40 years ago, it was noted that high altitude is associated with an increased incidence of paraganglioma (*26*). Many years later, the link between aberrant cellular oxygen sensing (pseudo-hypoxia) and development of tumors of sympathetic and parasympathetic origin has become a newly

investigated hypothesis (*27*). Molecular data showed that mutations in the genes coding for SDH subunits result in accumulation of succinate and inhibition of HIF-1 hydroxylases leading to stabilization of HIF-1 (*28,29*). HIF-1 and 2 are transcription factors that activate several genes that promote adaptation and survival under hypoxic conditions. They control energy, iron metabolism, erythropoiesis and development. Paragangliomas harboring mutations in SDH genes as well as the VHL gene are characterized by HIF stabilization, dysregulation and overexpression (*30*).

Our patient, unlike the two Mexican patients cited above, is a resident of Warsaw, located approximately 100 m above sea level, and has not had a history of living at a high altitude (besides two one-week holiday visits for skiing in the Italian Alps at about 1,800 m above sea level). He also has not had any conditions associated with frequent hypoxia episodes, such as sleep apnea syndrome, asthma or chronic obstructive pulmonary disease, or cyanotic heart disease. The only condition in his medical history, which could be associated with tissue hypoxia was iron deficiency anemia, identified at the time of diagnosis of disseminated disease.

In conclusion, we reported a family with the c.689G>A (p.Arg230His) mutation in the SDHB gene, with recurrent and later disseminated [131I]mIBG uptake-negative head and neck paraganglioma with multiple bone metastases in one family member, currently 49-year-old man who underwent PRRT with [90Y]Y/[177Lu]Lu-DOTATATE, with treatment repeated 6 years later due to disease progression, and who remains alive and in good overall clinical condition at 8 years of follow-up after the original presentation at our unit. Our case indicates that multiple imaging methods may be necessary to evaluate the extent of paraganglioma and determine the appropriate type of radionuclide therapy in disseminated inoperable cases, potentially contributing to improved outcomes. The genetic diagnosis allows screening among other family members and further follow-up of those affected.

Acknowledgements

References

1. Chen H, Sippel RS, O'Dorisio MS, Vinik AI, Lloyd RV, Pacak K, North American Neuroendocrine Tumor Society. The North American Neuroendocrine Tumor Society consensus guideline for the diagnosis and management of neuroendocrine tumors: pheochromocytoma, paraganglioma and medullary thyroid cancer. Pancreas. 2010; 39:775-783.

2. Lenders JW, Duh QY, Eisenhofer G, Gimenez-Roqueplo AP, Grebe SK, Murad MH, Naruse M, Pacak K, Young WF Jr; Endocrine Society. Pheochromocytoma and paraganglioma: An Endocrine Society clinical practice guideline. J Clin Endocrinol Metab. 2014; 99:1915-1942.

3. Mannelli M, Castellano M, Schiavi F, *et al*. Clinically guided genetic screening in a large cohort of Italian patients with pheochromocytomas and/or functional or nonfunctional paragangliomas. J Clin Endocrinol Metab. 2009; 94:1541-1547.

4. Fishbein L, Merrill S, Fraker DL, Cohen DL, Nathanson KL. Inherited mutations in pheochromocytoma and paraganglioma: why all patients should be offered genetic testing. Ann Surg Oncol. 2013; 20:1444-1450.

5. Vicha A, Musil Z, Pacak K. Genetics of pheochromocytoma and paraganglioma syndromes: new advances and future treatment options. Curr Opin Endocrinol Diabetes Obes. 2013; 20:186-191.

6. Venkatesan AM, Trivedi H, Adams KT, Kebebew E, Pacak K, Hughes MS. Comparison of clinical and imaging features in succinate dehydrogenase-positive versus sporadic paragangliomas. Surgery. 2011; 150:1186-1193.

7. Taïeb D, Timmers HJ, Hindié E, Guillet BA, Neumann HP, Walz MK, Opocher G, de Herder WW, Boedeker CC, de Krijger RR, Chiti A, Al-Nahhas A, Pacak K, Rubello D, European Association of Nuclear Medicine. EANM 2012 guidelines for radionuclide imaging of phaeochromocytoma and paraganglioma. Eur J Nucl Med Mol Imaging. 2012; 39:1977-1995.

8. Manneli M. Management and treatment of pheochromocytomas and paragangliomas. Ann N Y Acad Sci. 2006; 1073:405-416.

9. Huang KH, Chung SD, Chen SC, Chueh SC, Pu YS, Lai MK, Lin WC. Clinical and pathological data of 10 malignant pheochromocytomas: long-term follow up in a single institute. Int J Urol. 2007; 14:181-185.

10. Mamede M, Carrasquillo JA, Chen CC, Del Corral P, Whatley M, Ilias I, Ayala A, Pacak K. Discordant localization of 2-[18F]-fluoro-2-deoxy-D-glucose in 6-[18F]-fluorodopamine and [123I]-metaiodobenzylguanidine-negative metastatic pheochromocytoma sites. Nucl Med Commun. 2006; 27:31-36.

11. Zandee WT, Feelders RA, Duijzentkunst DAS, *et al*. Treatment of inoperable or metastatic paragangliomas and pheochromocytomas with peptide receptor radionuclide therapy using 177Lu-DOTATATE. Eur J Endocrinol. 2019; 181:45-53.

12. Satapathy S, Mittal BR, Bhansali A. Peptide receptor radionuclide therapy in the management of advanced pheochromocytoma and paraganglioma: A systematic review and meta-analysis. Clin Endocrinol (Oxf). 2019; 91:718-727.

13. Makis W, McCann K, McEwan AJ. The challenges of treating paraganglioma patients with 177Lu-DOTATATE PRRT: catecholamine crises, tumor lysis syndrome and the need for modification of treatment protocols. Nucl Med Mol Imaging. 2015; 49:223-230.

14. Wolf KI, Jha A, van Berkel A, Wild D, Janssen I, Millo

CM, Janssen MJR, Gonzales MK, Timmers HJKM, Pacak K. Eruption of metastatic paraganglioma after successful therapy with ^{177}Lu/^{90}Y-DOTATOC and ^{177}Lu-DOTATATE. Nucl Med Mol Imaging. 2019; 53:223-230.

15. Ayala-Ramirez M, Feng L, Habra MA, Rich T, Dickson PV, Perrier N, Phan A, Waguespack S, Patel S, Jimenez C. Clinical benefits of systemic chemotherapy for patients with metastatic pheochromocytoma or symphatetic extra-adrenal paragangliomas: insights from the largest single-institutional experience. Cancer. 2012; 118:2804-2812.

16. Huang H, Abraham J, Hung E, Averbuch S, Merino M, Steinberg SM, Pacak K, Fojo T. Treatment of malignant pheochromocytoma/paraganglioma with cyclophosphamide, vincristine, and dacarbazine: recommendation from a 22-year follow-up of 18 patients. Cancer. 2008; 113:2020-2028.

17. Hadoux J, Favier J, Scoazec JY, *et al*. SDHB mutations are associated with response to temozolomide in patients with metastatic pheochromocytoma or paraganglioma. Int J Cancer. 2014; 135:2711-2720.

18. Kulke MH, Stuart K, Enzinger PC, Ryan DP, Clark JW, Muzikansky A, Vincitore M, Michelini A, Fuchs CS. Phase II study of temozolomide and thalidomide in patients with metastatic neuroendocrine tumors. J Clin Oncol. 2006; 24:401-406.

19. Nozieres C, Walter T, Joly MO, Giraud S, Scoazec JY, Borson-Chazot F, Simon C, Riou JP, Lombard-Bohas C. A SDHB malignant paraganglioma with dramatic response to temozolomide-capecitabine. Eur J Endocrinol. 2012; 166:1107-1111.

20. Tong A, Li M, Cui Y, Ma X, Wang H, Li Y. Temozolomide is a potential therapeutic tool for patients with metastatic pheochromocytoma/paraganglioma-case report and review of the literature. Front Endocrinol (Lausanne). 2020; 11:61.

21. Andrews KA, Ascher DB, Pires DEV, *et al*. Tumour risks and genotype–phenotype correlations associated with germline variants in succinate dehydrogenase subunit genes SDHB, SDHC and SDHD. J Med Genet. 2018; 55:384-394.

22. Burnichon N, Rohmer V, Amar L, *et al*. The succinate dehydrogenase genetic testing in a large prospective series of patients with paragangliomas. J Clin Endocrinol Metab. 2009; 94:2817-2827.

23. Cerecer-Gil NY, Figuera LE, Llamas FJ, Lara M, Escamilla JG, Ramos R, Estrada G, Hussain AK, Gaal J, Korpershoek E, de Krijger RR, Dinjens WNM, Devilee P, Bayley JP. Mutation of SDHB is a cause of hypoxia-related high-altitude paraganglioma. Clin Cancer Res. 2010; 16:4148-4154.

24. Xekouki P, Szarek E, Bullova P, *et al*. Pituitary adenoma with paraganglioma/pheochromocytoma (3PAs) and succinate dehydrogenase defects in humans and mice. J Clin Endocrinol Metab. 2015; 100:E710-E719.

25. Gómez AM, Soares DC, Costa AAB, Pereira DP, Achatz MI, Formiga MN. Pheochromocytoma and paraganglioma: implications of germline mutation investigation for treatment, screening, and surveillance. Arch Endocrinol Metab. 2019; 63:369-375.

26. Saldana MJ, Saiem LE, Travezan R. High altitude hypoxia and chemodectomas. Hum Pathol. 1973; 4:251-263.

27. Opotowsky AL, Moco L, Ginns J, *et al*. Pheochromocytoma and paraganglioma in cyanotic congenital heart disease. J Clin Endocrinol Metab. 2015; 100:1325-1334.

28. Pollard PJ, Briere JJ, Alam NA, *et al*. Accumulation of Krebs cycle intermediates and over-expression of HIF1 alpha in tumors, which result from germline FH and SDH mutations. Hum Mol Genet. 2005; 14:2231-2239.

29. Selak MA, Armour SM, MacKenzie ED, Boulahbel H, Watson DG, Mansfield KD, Pan Y, Simon MC, Thompson CB, Gottlieb E. Succinate links TCA cycle dysfunction to oncogenesis by inhibiting HIF-alpha prolyl hydroxylase. Cancer Cell. 2005; 7:77-85.

30. Jochmanova I, Yang C, Zhuang Z, Pacak K. Hypoxia-inducible factor signaling in pheochromocytoma: turning the rudder in the right direction. J Natl Cancer Inst. 2013; 105:1270-1283.

Address correspondence to:
Piotr Jędrusik, Department of Internal Medicine, Hypertension and Vascular Diseases, Medical University of Warsaw, Banacha 1a, 02-097 Warsaw, Poland.
E-mail: pjedrusik@wum.edu.pl

Case Report

Mediastinal lymph node metastasis as a single expression of disease relapse in Ewing's sarcoma: multidisciplinary approach of two consecutive cases

Filippo Tommaso Gallina[1],*, Virginia Ferraresi[2], Alessio Annovazzi[3], Sabrina Vari[2], Paolo Visca[4], Daniele Forcella[1], Daniela Assisi[5], Enrico Melis[1], Francesco Facciolo[1]

[1] Department of Thoracic Surgery, IRCCS Regina Elena National Cancer Institute, Rome, Italy;
[2] Department of Medical Oncology 1, IRCCS Regina Elena National Cancer Institute, Rome, Italy;
[3] Nuclear Medicine Unit, IRCCS Regina Elena National Cancer Institute, Rome, Italy;
[4] Pathology Unit, IRCCS Regina Elena National Cancer Institute, Rome, Italy;
[5] Digestive Endoscopy Unit, IRCCS Regina Elena National Cancer Institute, Rome, Italy.

SUMMARY   Ewing's sarcoma of the bone is a rare, highly aggressive tumor that typically affects children and young adults. Progress in the treatment of Ewing's sarcoma has improved survival from about 10%, before the introduction of chemotherapy, to about 75% today for patients with localized tumors. On the contrary, metastatic disease still has a poor prognosis, and a multidisciplinary approach is essential to improve the outcome. Molecular techniques and new imaging modalities are affecting the diagnosis and classification of patients with Ewing's sarcoma. The most frequent sites of metastases in Ewing's sarcoma include lungs, bones and bone marrow. Lymph nodes are a rare site of metastatic spread, particularly in the mediastinum. In this report, we present two consecutive cases of patients with Ewing's Sarcoma, diagnosed, and treated at our institute. We focused particularly on the rarity of the atypical presentation of the disease and on the synergistic strategy to adopt as a model of networking in treating patients with rare diseases.

Keywords   Ewing's sarcoma, mediastinum, mediastinal lymphnodes, EBUS, EUS

1. Introduction

Ewing's sarcoma is a high-grade rare tumour that arises mainly from the bone (60% of cases) where it is the third most common malignancy (*1*). The age of peak incidence for Ewing's sarcoma is 15 years; men are slightly more affected than women with a ratio of 3:2. Ewing's sarcoma is predominantly observed in populations of Europe (~ 1.5 cases per million children, adolescents and young adults). On the other hand, people of Asia and Africa are less affected (~ 0.8 and ~ 0.2 cases per million per year, respectively) (*2*).

In the era of precision medicine, many investigations and molecular testing have attempted to search new prognostic factors in order to find a specific treatment for these types of tumors (*3*). Treatment of Ewing's sarcoma foresees a multidisciplinary approach including systemic aggressive polichemotherapy regimens and local therapy (surgery and/or radiotherapy for unresectable primitive sites or metastases) (*4,5*). Approximately 25% of patients with Ewing's sarcoma are diagnosed with advanced disease where typically the lung is the most

frequent metastatic site at diagnosis or at the moment of relapse (*6*). Other typical sites of metastases are the bone and bone marrow and in cases of suspicious lesions biopsies should be performed. In cases of multiple metastases, prognosis is generally poor. A small percentage of metastatic patients can however, still achieve lasting control of disease with combined therapeutic approaches including chemotherapy and radiotherapy on bulky disease or surgery on selected metastatic sites (*7*). Despite the lack of prospective studies aimed at evaluating the role of clinical and radiological surveillance in high-grade sarcomas, the prognostic value of early detection of local recurrence or distance metastases is recognized and a regular follow up policy is strongly recommended. Lymph node metastases of Ewing's sarcoma are extremely rare and there are still no cases of mediastinal lymph nodes as a single disease relapsing reported in the literature. In this report, we present two cases of patients with Ewing's sarcoma who showed a single recurrence on mediastinal lymph nodes on CT and FDG PET/CT, that were histologically confirmed *via* thoracic endoscopy. Before writing this

case report, we have obtained an informed consent from the patients.

2. Case Report

2.1. Case 1

A 32-year old male patient was admitted to our thoracic endoscopy unit. In January 2016, he was initially diagnosed with Ewing's Sarcoma of the right hip. The patient was enrolled in ISG-AIEOP EW1 (EudraCT: 2008-008361-35), arm B, a clinical trial and received neoadjuvant chemotherapy consisting of a VAI (vincristine, adriamycin, and ifosfamide) regimen for 4 courses. In May 2016, he underwent a resection of the right hip where the histological examination showed a pathological complete response. After surgery, he was treated as per *good responder* maintenance phase of the arm with VAI for 1 cycle and IE (ifosfamide and etoposide) for 4 cycles until October 2016. Subsequently, the patient underwent a physical examination, pelvis MRI and thorax CT scan every 4 months until September 2019, when a ^{18}F-FDG PET/CT scan showed a moderate FDG uptake (SUVmax = 3.7) in a small mediastinal left peri-bronchial lymph node, suspicious for metastasis (Figure 1A). A contrast enhanced CT scan (Figure 1B) performed one month later showed a significant increase in the size of the lymph node (28 *vs.* 15 mm). After some discussion at the sarcoma disease management team meeting, an endoscopic ultrasound fine needle aspiration biopsy was decided to be performed (EUS-FNAb). After deep sedation with propofol was induced by using an echo-endoscope, an examination of all

mediastinal lymph node stations was performed. In correspondence to station 8, a hypoechoic mass was found and an FNA was performed with a 22G Cook needle (Figure 2A). We obtained samples for cytological and histological examinations, both confirming a relapse of Ewing's sarcoma (Figure 2B). Immunohistochemical analysis showed a CD99+, CD45- and CKMNF116-, molecular analysis presented a EWSR11-FLI1 fusion transcript. The patient was then enrolled in a rEECur randomized clinical trial for metastatic disease (EudraCT number: 2014-000259-99), randomized in Topotecan plus a Cyclophosphamide (TC) arm, where he is still in treatment. The best response obtained after 2 cycles was partial, and the last CT scan showed an unvarying response. The patient has received 6 cycles of chemotherapy and is currently waiting for a CT re-evaluation of disease. Local treatment (radiotherapy or surgery) will be considered upon confirmation of response and chemotherapy might be continued until disease progression or severe toxicities.

2.2. Case 2

We evaluated a 74-year old male patient with hypertension and a history of stroke anamnesis. In May 2013, he noticed a persistent swelling of the left arm. For this reason, he underwent a biopsy, with a Ewing's Sarcomas diagnosis. The patient had 3 cycles of neoadjuvant chemotherapy with Epirubicin, Cyclophosphamide and Vincristine, and in December 2013 the patient's lesion underwent radical surgery, with 30% necrosis. He subsequently received 4 cycles of adjuvant chemotherapy with IE until May 2014. In
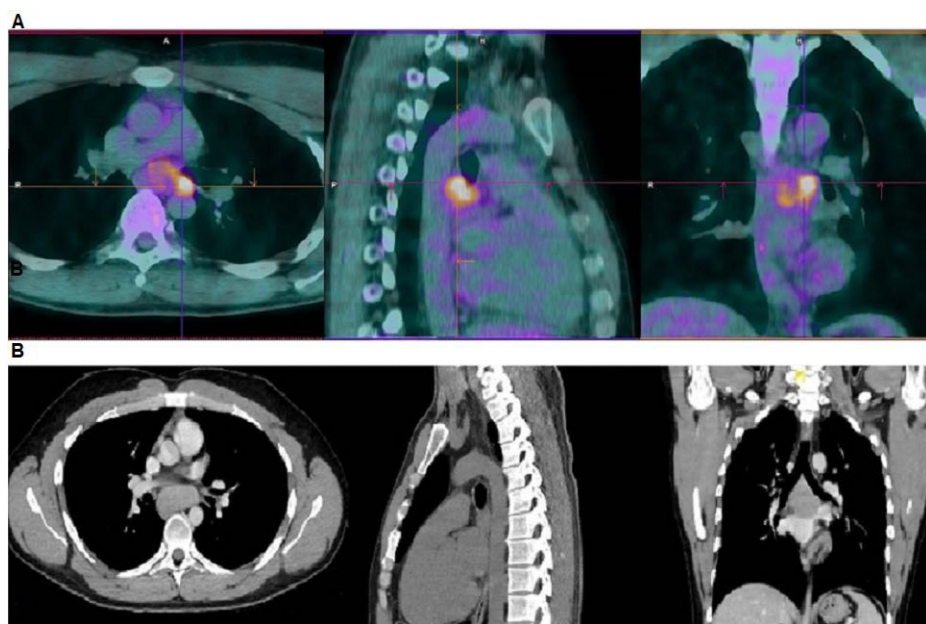

Figure 1. (A) Axial (left), sagittal (middle) and coronal (right) ^{18}F-FDG PET/CT fused views in a patient with Ewing sarcoma. A PET/CT performed during follow up showed a focal area of moderate FDG uptake (SUVmax = 3.7) in a small left para-esophageal lymph node, suspected for metastasis. **(B)** A contrast enhanced CT scan (Figure 1b) performed one month later showed a significant increase in the size of the lymph node (28 *vs.* 15 mm). The metastatic origin of the lymph node was then confirmed by transbronchial needle aspiration.
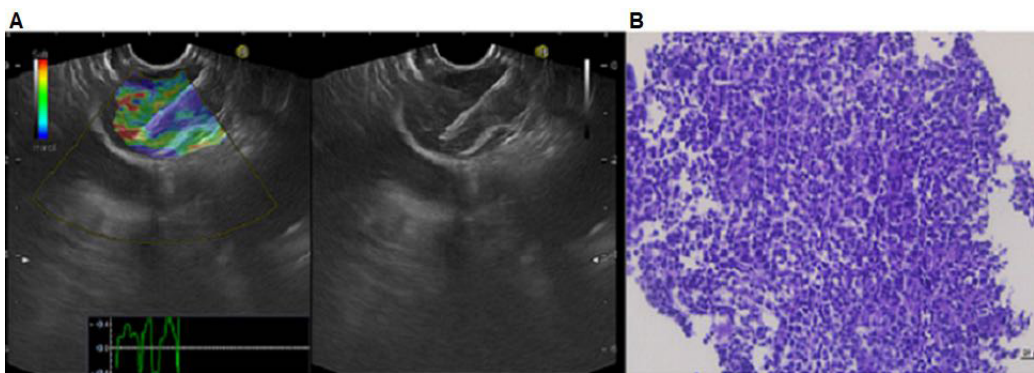
Figure 2. (A) Endoscopic ultrasound with elastography of the hypoechoic lymph node aspiration with 22G needle in correspondence of the para-oesophageal station. The elastography showed a predominantly blue pattern suspected for malignant lymph node. **(B)** Undifferentiated small round cell neoplasm consisting of relative monomorphic elements cohesive with hyperchromic nuclei and poor eosinophilic cytoplasm (All images are 20× magnification).
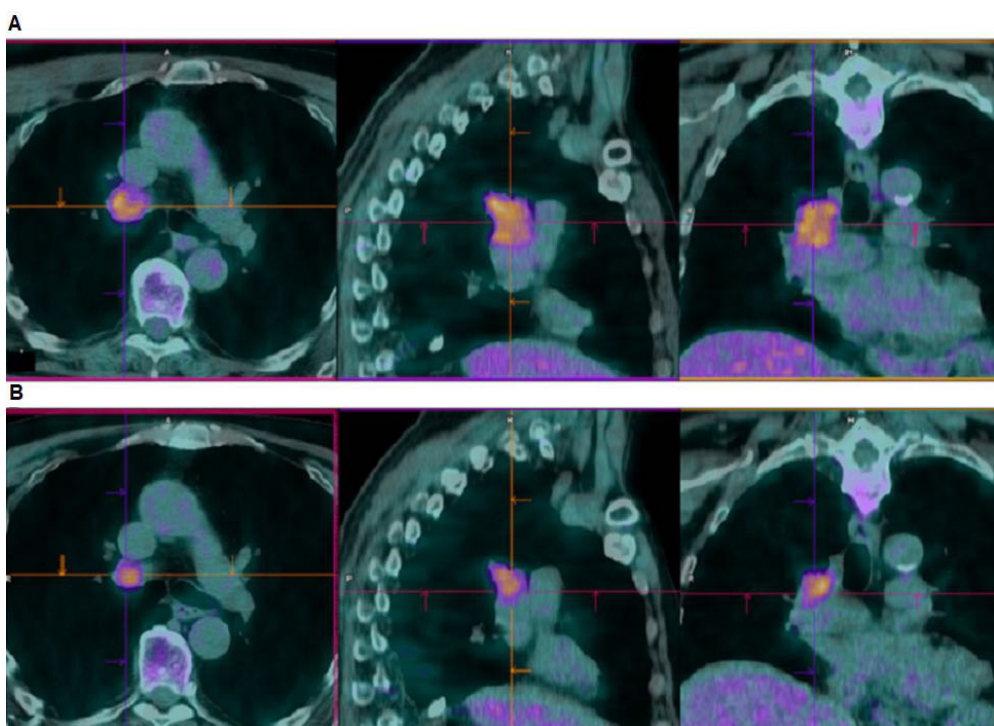

Figure 3. (A) Axial (left), sagittal (middle) and coronal (right) ^{18}F-FDG PET/CT fused views in a patient with Ewing sarcoma. A PET/CT performed during follow up showed an intense FDG uptake (SUVmax = 7.1) in a single right tracheobronchial metastatic lymph node (histologically confirmed). **(B)** A second PET/CT scan performed four months later undergoing chemotherapy revealed a significant reduction of the lymph node size (Metabolic Tumor Volume 10.8 *vs.* 32.4 cc), despite a persistently high FDG uptake (SUVmax = 7.2).

March 2019, the patient was admitted to right upper lobe wedge resection for a single pulmonary metastasis. An ^{18}F-FDG PET/CT scan performed for restaging in December 2019 showed high focal FDG uptake in a 26 × 33 mm mediastinal lymphadenopathy, station 4R (lower paratracheal lymph nodes) (Figure 3A). After having held an oncological multidisciplinary meeting, an endobronchial ultrasound with a transbronchial needle aspiration biopsy (EBUS-TBNAb) was decided to be carried out. The exam was performed under deep sedation with propofol and local oral anaesthesia. After inserting the echo-bronchoscope, we evaluated all

mediastinal stations and in correspondence to the right lower paratracheal station, we found a hypoechoic lesion that crossed the limit of station 10R with no evidence of clear cleavage plane. We performed a TBNA with a 22G Cook needle and obtained enough tissue sampling for cytological and histological examinations (Figure 4A). The histopathological response was consistent with a Ewing's sarcoma metastatic lymph node and the immunohistochemical analysis showed a CD99+, CD45- and CKMNF116- (Figure 4B). The molecular analysis confirmed the diagnosis showing a EWSR11-FLI1 fusion transcript. Since January 2020, the patient has been
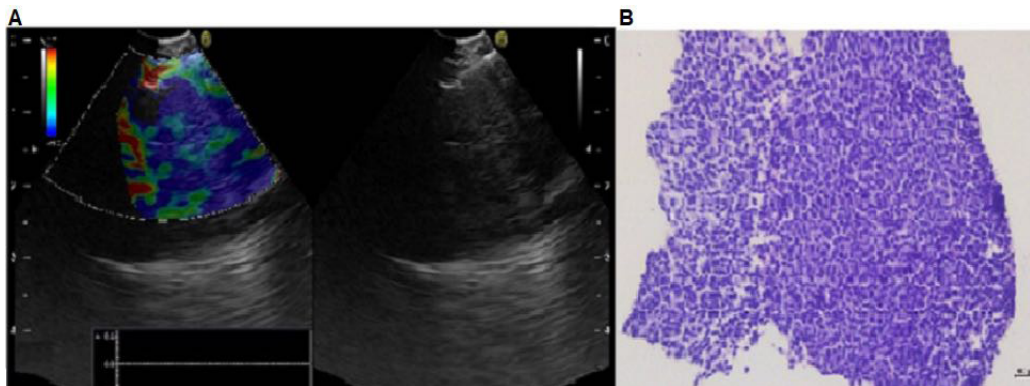
Figure 4. (A) Endobronchial ultrasound with elastography of the hypoechoic lymph node aspiration with a 22G needle in correspondence of the right lower paratracheal station and right hilar station. The elastography showed a predominantly blue pattern suspected for malignant lymph node. **(B)** Undifferentiated small round cell neoplasm consisting of relative monomorphic elements cohesive with hyperchromic nuclei and poor eosinophilic cytoplasm (All images are 20× magnification).

treated with first-line chemotherapy using Temozolomide and Irinotecan (TEMIRI regimen), attenuated for age and comorbidities. Despite a dose reduction, the patient reported irinotecan related gastrointestinal toxicity (persistent grade 2 diarrhoea) requiring intravenous fluid supplementation, leading to drug discontinuation. The patient-maintained treatment with temozolomide as a single agent obtaining a metabolic stabilization of the disease at first re-evaluation of disease in April 2020 (Figure 3B).

3. Discussion

The prognosis for patients with metastatic Ewing's sarcoma is generally poor (*1*). Despite aggressive systemic and local therapies, a small percentage of patients can still achieve long-term disease control, depending on time to relapse and extension and sites of metastatic disease. Lung and pleural metastases show in fact better prognosis compared to patients with bone metastases and bone marrow involvement.

Even though a standardized surveillance policy has not yet been approved in high-grade sarcomas, accepted and well established guidelines indicate that locoregional imaging using MRI and chest X-ray/CT should be carried out after completing chemotherapy for localized disease approximately every 3 months for the first 2 years; every 6 months for years 3-5, every 6-12 months for years 5-10, and thereafter every 0.5-2 years. Specifically, in Ewing's sarcoma and other bone sarcomas, bone scan imaging was also extensively used in patient follow ups due to its high accuracy for the detection of bone metastases. More recently, techniques such as ^{18}F-FDG PET/CT or whole-body MRI are increasingly being adopted into routine practice but require further evaluation in clinical trials (*8*).

Metastases on lymph nodes are extremely rare, especially in the mediastinum. After all, searching on PubMed using the keywords "Ewing's sarcoma relapse", "Ewing's sarcoma lymph node", "mediastinal Ewing's sarcoma relapse" and "metastatic Ewing's sarcoma",

there are only a few cases of metastatic lymph nodes reported in the literature. Weshi *et al.* in an analysis of 57 patients with extra skeletal Ewing's sarcoma, reported five cases of primary lymph node disease and only one patient with first relapse on lymph nodes (*9*). Somarouthu *et al.* reported the clinical outcomes of 26 patients with extra skeletal Ewing's sarcoma where 4 patients presented lymph node metastatic disease (*10*). In a retrospective study of a single institution, Huh *et al.* presented 5 patients with metastatic disease in mediastinal lymph nodes. The authors reported that lymph node metastases were commonly found in patients with primary extra-skeletal Ewing's sarcoma of the torso, including the abdomen, lung, peritoneum, pleura, and paravertebral region, compared to patients affected with the disease on the extremities, head, and neck (*11*).

The peculiarity of the cases described herein is that both patients with skeletal Ewing's sarcoma presented a mediastinal lymphadenopathy PET positive as a single localization of disease relapse. Our patients presented the primary tumor on the left arm and on the right hip. Both patients presented a single disease relapse in a single mediastinal lymph node station. We considered this condition to be metastatic disease and they were treated with an appropriate chemotherapy regimen. The first follow up after the treatment of the relapsing disease showed a partial response for patient 1 and metabolic stability for patient 2. In regard to the poor prognosis of metastatic Ewing's sarcoma, we can therefore consider the response to treatment satisfying. To our knowledge, there are no similar cases described in the literature.

The use of ^{18}F-FDG PET/CT has been shown to be helpful in the initial evaluation, restaging and monitoring treatment response in patients with Ewing Sarcoma (*12*). In particular, PET-CT plays an important role in detection of bone metastases, showing a more accurate detection than bone scintigraphy. The presence of FDG-positive lymph nodes on PET/CT scan should be evaluated carefully for possible false positive findings due to inflammation. A different approach was carried

out for the two patients: in case 1, due to a moderate FDG uptake, we required a short-term CT evaluation to confirm a suspicious lymph node. In case 2, an intense FDG uptake suggested a possible metastasis so we proceeded to directly carry out a histological confirmation.

Thoracic endoscopy is the safest and most feasible technique to evaluate the mediastinum and should be used when staging lung cancer patients and investigating suspected extra-thoracic cancer relapse (*13*). In our patients, we used EUS-FNA for subcarinal station, whereas, for right lower paratracheal stations and right hilum station EBUS-TBNA it is mandatory. By using these mini-invasive techniques, we can sample enough material to perform a quick histological and cytological diagnosis and start appropriate multimodality therapy (*14*). Compared to mediastinoscopy, EBUS-TBNA and EUS-FNA are less invasive and can be performed in an outpatient regimen with moderate sedation (*15*). The association between EBUS and EUS allows improvement of the quality standard of diagnosis in terms of sensitivity, specificity, and accuracy. Only a few patients needed surgery to achieve the mediastinal lymph node biopsy. One of the main limitations of these types of procedures is that their accuracy strongly depends on the operator's skills.

There are no standardized chemotherapy regimens to treat recurrent Ewing's sarcoma (*16,17*). In the immunotherapy era, there are currently in progress few clinical trials assessing checkpoint inhibitors that interrupt the repressive crosstalk between cancer and immune cells, either as a single agent or combined with conventional chemotherapy (*18*). Unfortunately, clinical responses in trials remain anecdotal but highlight the necessity to improve characterization of the tumor micro-environment to unlock the immunotherapeutic response (*19*). Despite novel therapeutic strategies for Ewing's sarcoma that include IGF-1 receptor (IGF-1R)-targeted antibodies combined with mTOR inhibitors (mTORi), as well as chemotherapy-PARP combinations, which could represent new prospects for the future, the prognosis remains poor (*20,21*).

Treating elderly patients with Ewing's sarcoma is really challenging due to greater aggressiveness and toxicity of the chemotherapy regimens that prove to be effective in the younger population, as well as a lack of prospective clinical trials evaluating this extremely rare subpopulation of patients. Despite very good clinical conditions and a 25% dose reduction from the first cycle of the TEMIRI regimen, our 74-year old patient was not able to tolerate the combination of drugs and therefore continued with oral temozolomide alone.

When a very rare disease presents itself, as demonstrated by our two patients, a synergistic strategy should be put into place by giving the patient the best therapeutic options. This strategy is mainly made up of three steps. First, a strict follow-up is conducted by the oncologist in accordance with international guidelines. Second, an imaging evaluation by a dedicated nuclear medicine doctor is performed. Third, an accurate and fast diagnosis using less invasive thoracic endoscopic techniques and a histological examination are carried out. All these steps lead to the beginning of a personalized therapeutic course based on patient characteristics using the most innovative therapy protocols. The therapeutic algorithm for single site relapse of Ewing's sarcoma is not well defined. A multidisciplinary discussion in centers with high expertise on Ewing's sarcoma is absolutely required for a correct diagnosis and therapy of the patient with single site lymph node metastasis to offer treatment with potentially still curative intentions.

In conclusion, although very rare, mediastinal lymph node relapsing should always be considered in cases of radiological suspicion. If lymph nodes are the only suspicious site of metastatic disease on a CT or PET/CT scan, a histological examination should quickly be carried out in order to exclude inflammatory diseases like sarcoidosis or other neoplastic conditions.

References

1. Grünewald TGP, Cidre-Aranaz F, Surdez D, Tomazou EM, de Álava E, Kovar H, Sorensen PH, Delattre O, Dirksen U. Ewing sarcoma. Nat Rev Dis Primers. 2018; 4:5.
2. Balamuth NJ, Womer RB. Ewing's sarcoma. Lancet Oncol. 2010; 11:184-192.
3. Casey DL, Lin TY, Cheung NV. Exploiting signaling pathways and immune targets beyond the standard of care for Ewing sarcoma. Front Oncol. 2019;9:537.
4. Gaspar N, Hawkins DS, Dirksen U, *et al.* Ewing sarcoma: Current management and future approaches through collaboration. J Clin Oncol . 2015; 33:3036-3046.
5. Haeusler J, Ranft A, Boelling T, Gosheger G, Braun-Munzinger G, Vieth V, Burdach S, van den Berg H, Juergens H, Dirksen U. The value of local treatment in patients with primary, disseminated, multifocal Ewing sarcoma (PDMES). Cancer. 2010; 116:443-450.
6. Scurr M, Judson I. How to treat the Ewing's family of sarcomas in adult patients. Oncologist. 2006; 11:65-72.
7. Stahl M, Ranft A, Paulussen M, Bölling T, Vieth V, Bielack S, Görtitz I, Braun-Munzinger G, Hardes J, Jürgens H, Dirksen U. Risk of recurrence and survival after relapse in patients with Ewing sarcoma. Pediatr Blood Cancer. 2011; 57:549-553.
8. Casali PG, Bielack S, Abecassis N, *et al.* Bone sarcomas:

ESMO-PaedCan-EURACAN Clinical Practice Guidelines for diagnosis, treatment and follow-up. Ann Oncol. 2018; 29(Suppl 4):iv79-iv95.

9. El Weshi A, Allam A, Ajarim D, Al Dayel F, Pant R, Bazarbashi S, Memon M. Extraskeletal Ewing's sarcoma family of tumours in adults : Analysis of 57 patients from a single institution. Clin Oncol (R Coll Radiol). 2010; 22:374-381.

10. Somarouthu BS, Shinagare AB, Rosenthal MH, Tirumani H, Hornick JL, Ramaiya NH, Tirumani SH. Multimodality imaging features, metastatic pattern and clinical outcome in adult extraskeletal Ewing sarcoma: experience in 26 patients. Br J Radiol. 2014; 87:20140123.

11. Huh J, Kim KW, Park SJ, Kim HJ, Lee JS, Ha HK, Tirumani SH, Ramaiya NH. Imaging features of primary tumors and metastatic patterns of the extraskeletal Ewing sarcoma family of tumors in adults: A 17-year experience at a single institution. Korean J Radiol. 2015; 16:783-790.

12. Costelloe CM, Chuang HH, Daw NC. PET/CT of osteosarcoma and Ewing sarcoma. Semin Roentgenol. 2017; 52:255-268.

13. Annema JT, Versteegh MI, Veseliç M, Voigt P, Rabe KF. Endoscopic ultrasound-guided fine-needle aspiration in the diagnosis and staging of lung cancer and its impact on surgical staging. J Clin Oncol. 2005; 23:8357-8361.

14. Sakairi Y, Nakajima T, Yoshino I. Role of endobronchial ultrasound-guided transbronchial needle aspiration in lung cancer management. Expert Rev Respir Med. 2019; 13:863-870.

15. Call S, Obiols C, Rami-Porta R. Present indications of surgical exploration of the mediastinum. J Thorac Dis. 2018; 10(Suppl 22):S2601-S2610.

16. Hunold A, Weddeling N, Paulussen M, Ranft A, Liebscher C, Jürgens H. Topotecan and cyclophosphamide in patients with refractory or relapsed Ewing tumors. Pediatr Blood Cancer. 2006; 47:795-800.

17. Ferrari S, del Prever AB, Palmerini E, Staals E, Berta M, Balladelli A, Picci P, Fagioli F, Bacci G, Vanel D. Response to high-dose ifosfamide in patients with advanced/recurrent Ewing sarcoma. Pediatr Blood Cancer. 2009; 52:581-584.

18. Heymann MF, Schiavone K, Heymann D. Bone sarcomas in the immunotherapy era. Br J Pharmacol. 2021; 178:1955-1972.

19. Guven DC, Kilickap S, Yildirim HC, Ceylan F, Bas O, Dizdar O. Chemoimmunotherapy for the salvage treatment of Ewing sarcoma: A case report. J Oncol Pharm Pract. 2021; 27:1281-1283.

20. Amin HM, Morani AC, Daw NC, *et al.* IGF-1R/mTOR Targeted Therapy for Ewing Sarcoma: A Meta-Analysis of Five IGF-1R-Related Trials Matched to Proteomic and Radiologic Predictive Biomarkers. Cancers (Basel). 2020; 12:1768.

21. van Maldegem AM, Bovée JV, Peterse EF, Hogendoorn PC, Gelderblom H. Ewing sarcoma: The clinical relevance of the insulin-like growth factor 1 and the poly-ADP-ribose-polymerase pathway. Eur J Cancer. 2016; 53:171-180.

Address correspondence to:
Filippo Tommaso Gallina, Thoracic Surgery, National Cancer Institute "Regina Elena" Rome Via Elio Chianesi 53, 00144 Rome, Italy.
Email: filippo.gallina@ifo.gov.it

Letter

Mild congenital myopathy due to a novel variation in *SPEG* gene

Mirac Yildirim[1],*, Ozgur Balasar[2], Engin Kose[3], Melih Timucin Dogan[4]

[1] Department of Pediatric Neurology, Ankara University Faculty of Medicine, Ankara, Turkey;
[2] Department of Medical Genetics, Konya Research and Training Hospital, Konya, Turkey;
[3] Department of Pediatric Metabolism and Nutrition, Ankara University Faculty of Medicine, Ankara, Turkey;
[4] Department of Pediatric Cardiology, Konya Research and Training Hospital, Konya, Turkey.

SUMMARY   Centronuclear myopathies (CNMs) are a subgroup of congenital myopathies (CMs) characterized by muscle weakness, genetic heterogeneity, and predominant type 1 fibers and increased central nuclei in muscle biopsy. Mutations in CNM-causing genes such as *MTM1*, *DNM2*, *BIN1*, *RYR1*, *CACNA1S*, *TTN*, and extraordinary rarely *SPEG* (striated muscle preferentially expressed protein kinase) have been identified for about 60-80% of patients. Herein, we report a case of CM due to a novel variation in the *SPEG* gene, manifested by mild neonatal hypotonia, muscle weakness, delayed motor milestones, and ophthalmoplegia, without dilated cardiomyopathy. We identified a novel variation [c.153C>T (p.Asn51=) in exon 1] in the *SPEG* gene with whole-exome sequencing and confirmed by Sanger sequencing. Mild intellectual disability has not been associated with SPEG-related CM in the previous reports. We suggest that this report expands the phenotypic spectrum of SPEG-related CM, and further case reports are required to expand the genotype-phenotype correlations.

Keywords   congenital myopathy, striated muscle preferentially expressed protein kinase, SPEG, centronuclear myopathy, intellectual disability

Congenital myopathies (CMs) are a heterogeneous group of muscle diseases usually characterized by muscle weakness and hypotonia at birth or in infancy. The severity of clinical presentation ranges from mild hypotonia due to delayed motor skills to severe muscle weakness that causes death due to cardiac or respiratory involvement in the neonatal period (*1*).

Centronuclear myopathies (CNMs) are a subgroup of CMs. The histological manifestations include an increase in the number of fibers with central nuclei and the predominance of type I fibers (*2*). Mutations in genes such as *MTM1*, *DNM2*, *BIN1*, *RYR1*, *CACNA1S*, and *TTN* have been identified for about 60-80% of patients with CNM. In recent studies, the mutations in the *SPEG* gene (striated muscle preferentially expressed protein kinase) have been associated with CNM in a small case series (*3-7*). Herein, we report a case of CM due to a novel variation in the *SPEG* gene, which is manifested by intellectual disability, a new clinical finding.

We present a case of 7-year-old boy who presented with motor developmental delay. He was born after uneventful pregnancy and delivery, with third-degree consanguineous marriage of his parents. There was a family history with three siblings (two girls and a boy) death with similar severe phenotypic characteristics

(Figure 1A). At birth, he had mild hypotonia without respiratory distress or swallowing difficulty. The motor milestones were delayed, head control developed at 1-year-old, and unsupported sitting at 2-year-old. He has never been able to walk with or without support. Social and language skills were mildly delayed.

According to the findings of physical examination at 7-year-old, his weight, height, and head circumference were between the 3rd and 10th percentile. He had a high arched palate, facial weakness, nasal speech, episodic weak cough, pectus excavatum, mild scoliosis, pes planovalgus, vertical supranuclear ophthalmoplegia, globally absent deep tendon reflexes, axial hypotonia, and contracture of bilateral ankles (Figure 1B). His maximum muscle strength was sitting without support. He had mild intellectual disability [intelligence quotient (IQ) test score was 55].

In laboratory tests, serum creatine kinase (CK) levels were mildly elevated (240 and 252 UI/L; reference range: 0-170 UI/L). Plasma and urine amino acids, tandem mass spectrometry, and urine organic acids were unremarkable. Liver and renal function tests and blood gases analysis were normal. At 5-year, 6-month-old, brain MRI and abdominal ultrasound findings were unremarkable. At 7-year-old, electrocardiogram and echocardiogram were normal (ejection fraction:
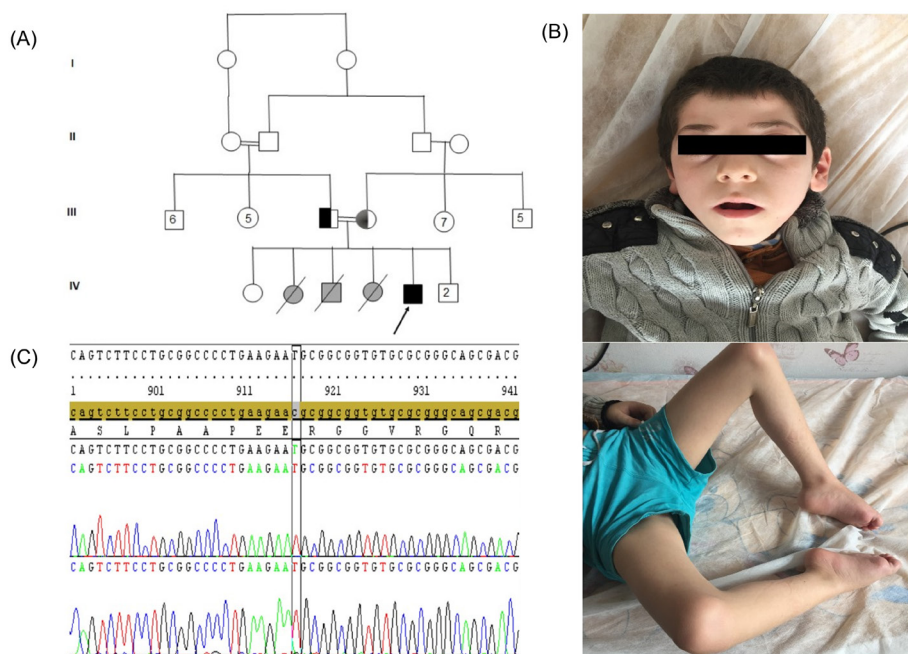
Figure 1. (A) Pedigree of the family; **(B)** Physical examination of patient; **(C)** Sequencing of SPEG variant c.153C>T with Sanger sequencing. Informed consent for genetic analysis and publication of clinical reports and photographs were obtained from patient's parents.

65%, shortening fraction: 32%). The ophthalmological evaluation revealed external ophthalmoplegia. Whole-exome sequencing was performed as the parents did not consent to the muscle biopsy. We identified a novel homozygous variation of c.153C>T (p.Asn51=) in exon 1 of the *SPEG* gene, and the variant was confirmed by Sanger sequencing (Figure 1C).

To date, in the majority of patients with *SPEG* mutations were reported with neonatal hypotonia, muscle weakness, delayed motor milestones, facial weakness, ophthalmoplegia, respiratory support or nasogastric tube feeding requirement, and dilated cardiomyopathy (*4-7*). Consistent with the previously reported cases, our case presented with neonatal hypotonia, delayed motor milestones, intellectual disability, muscle weakness, scoliosis, pes planovalgus, pectus excavatum, and ophthalmoplegia. However, dilated cardiomyopathy, which was reported in most of the cases with *SPEG* mutation, was not present in our case. Similarly, cases with *SPEG* gene mutations present with milder clinical features and delayed motor milestones without dilated cardiomyopathy were recently reported (*3,8*). The present patient is the third case in the literature who did not develop dilated cardiomyopathy despite reaching the age of 7. We believe that more reports of cases with *SPEG* gene mutation will lead us to better understand the clinical variation of the disease and its genotype-phenotype correlation.

One of the major pathogenic pathways of *SPEG* function is the interaction with *MTM1*. The region in the C-terminal of the *SPEG* gene (amino acid 2530-2674) is required for *MTM1* interaction (*5*). In the literature, it was found that *SPEG* mutations leading to loss of interaction between *MTM1* and C-terminal were associated with more severe phenotypes such as death in the neonatal period and dilated cardiomyopathy (*4,5*). Although presenting with mild neonatal hypotonia and delayed motor milestones, the present case was able to sit unsupported at two years of age, did not require ventilatory support or nasogastric tube feeding, and did not develop dilated cardiomyopathy. We suggest that our case had a milder clinical phenotype because of having a novel homozygous variation outside of C-terminal in the *SPEG* gene. However, we did not perform a muscle biopsy to investigate whether central nuclei were present.

To conclude, in previous reports, mild intellectual disability and elevation of CK levels have been associated with other CM subgroups, but not with SPEG-related CM (*1-3,8*). Our case expands the phenotypic spectrum, and we suggest that SPEG-related CM can be associated with mild phenotypes with intellectual disability. Further case reports on SPEG-related CM are required to expand the genotype-phenotype correlations.

Conflict of Interest: The authors have no conflicts of interest to disclose.

References

1. Nance JR, Dowling JJ, Gibbs EM, Bönnemann CG. Congenital myopathies: an update. Curr Neurol Neurosci Rep. 2012; 12:165-174.

2.   Romero NB, Bitoun M. Centronuclear myopathies. Semin Pediatr Neurol. 2011; 18:250-256.
3.   Qualls AE, Donkervoort S, Herkert JC, D'gama AM, Bharucha-Goebel D, Collins J, Chao KR, Foley AR, Schoots MH, Jongbloed JDH, Bönnemann CG, Agrawal PB. Novel *SPEG* mutations in congenital myopathies: Genotype-phenotype correlations. Muscle Nerve. 2019; 59:357-362.
4.   Wang H, Castiglioni C, Kaçar Bayram A, Fattori F, Pekuz S, Araneda D, Per H, Erazo R, Gümüş H, Zorludemir S, Becker K, Ortega X, Bevilacqua JA, Bertini E, Cirak S. Insights from genotype-phenotype correlations by novel *SPEG* mutations causing centronuclear myopathy. Neuromuscul Disord. 2017; 27:836-842.
5.   Agrawal PB, Pierson CR, Joshi M, *et al*. SPEG interacts with myotubularin, and its deficiency causes centronuclear myopathy with dilated cardiomyopathy. Am J Hum Genet. 2014; 95:218-226.
6.   Wang H, Schänzer A, Kampschulte B, Daimagüler HS, Logeswaran T, Schlierbach H, Petzinger J, Ehrhardt H, Hahn A, Cirak S. A novel *SPEG* mutation causes non-compaction cardiomyopathy and neuropathy in a floppy infant with centronuclear myopathy. Acta Neuropathol Commun. 2018; 6:83.
7.   Tang J, Ma W, Chen Y, Jiang R, Zeng Q, Tan J, Jiang H, Li Q, Zhang VW, Wang J, Tang H, Luo L. Novel SPEG variant cause centronuclear myopathy in China. J Clin Lab Anal. 2020; 34:e23054.
8.   Lornage X, Sabouraud P, Lannes B, Gaillard D, Schneider R, Deleuze JF, Boland A, Thompson J, Böhm J, Biancalana V, Laporte J. Novel *SPEG* mutations in congenital myopathy without centralized nuclei. J Neuromuscul Dis. 2018; 5:257-260.

*Address correspondence to:
Mirac Yildirim, Department of Pediatric Neurology, Ankara University Faculty of Medicine, Ankara, RI 06590, Turkey.
E-mail: miracyildirim81@hotmail.com

IRDR
Intractable & Rare Diseases Research

Guide for Authors

1. Scope of Articles

Intractable & Rare Diseases Research (Print ISSN 2186-3644, Online ISSN 2186-361X) is an international peer-reviewed journal. Intractable & Rare Diseases Research devotes to publishing the latest and most significant research in intractable and rare diseases. Articles cover all aspects of intractable and rare diseases research such as molecular biology, genetics, clinical diagnosis, prevention and treatment, epidemiology, health economics, health management, medical care system, and social science in order to encourage cooperation and exchange among scientists and clinical researchers.

2. Submission Types

Original Articles should be well-documented, novel, and significant to the field as a whole. An Original Article should be arranged into the following sections: Title page, Abstract, Introduction, Materials and Methods, Results, Discussion, Acknowledgments, and References. Original articles should not exceed 5,000 words in length (excluding references) and should be limited to a maximum of 50 references. Articles may contain a maximum of 10 figures and/or tables. Supplementary Data are permitted but should be limited to information that is not essential to the general understanding of the research presented in the main text, such as unaltered blots and source data as well as other file types.

Brief Reports definitively documenting either experimental results or informative clinical observations will be considered for publication in this category. Brief Reports are not intended for publication of incomplete or preliminary findings. Brief Reports should not exceed 3,000 words in length (excluding references) and should be limited to a maximum of 4 figures and/or tables and 30 references. A Brief Report contains the same sections as an Original Article, but the Results and Discussion sections should be combined.

Reviews should present a full and up-to-date account of recent developments within an area of research. Normally, reviews should not exceed 8,000 words in length (excluding references) and should be limited to a maximum of a maximum of 10 figures and/or tables and 100 references. Mini reviews are also accepted, which should not exceed 4,000 words in length (excluding references) and should be limited to a maximum of 5 figures and/or tables and 50 references.

Policy Forum articles discuss research and policy issues in areas related to life science such as public health, the medical care system, and social science and may address governmental issues at district, national, and international levels of discourse. Policy Forum articles should not exceed 3,000 words in length (excluding references) and should be limited to a maximum of 5 figures and/or tables and 30 references.

Case Reports should be detailed reports of the symptoms, signs, diagnosis, treatment, and follow-up of an individual patient. Case reports may contain a demographic profile of the patient but usually describe an unusual or novel occurrence. Unreported or unusual side effects or adverse interactions involving medications will also be considered. Case Reports should not exceed 3,000 words in length (excluding references) and should be limited to a maximum of 5 figures and/or tables and 30 references.

Communications are short, timely pieces that spotlight new research findings or policy issues of interest to the field of global health and medical practice that are of immediate importance. Depending on their content, Communications will be published as "Comments" or "Correspondence". Communications should not exceed 1,500 words in length (excluding references) and should be limited to a maximum of 2 figures and/or tables and 20 references.

Editorials are short, invited opinion pieces that discuss an issue of immediate importance to the fields of global health, medical practice, and basic science oriented for clinical application. Editorials should not exceed 1,000 words in length (excluding references) and should be limited to a maximum of 10 references. Editorials may contain one figure or table.

News articles should report the latest events in health sciences and medical research from around the world. News should not exceed 500 words in length.

Letters should present considered opinions in response to articles published in *Intractable & Rare Diseases Research* in the last 6 months or issues of general interest. Letters should not exceed 800 words in length and may contain a maximum of 10 references. Letters may contain one figure or table.

3. Editorial Policies

For publishing and ethical standards, *Intractable & Rare Diseases Research* follows the Recommendations for the Conduct, Reporting, Editing, and Publication of Scholarly Work in Medical Journals (*http://www.icmje.org/recommendations*) issued by the International Committee of Medical Journal Editors (ICMJE), and the Principles of Transparency and Best Practice in Scholarly Publishing (*https://doaj.org/bestpractice*) jointly issued by the Committee on Publication Ethics (COPE), the Directory of Open Access Journals (DOAJ), the Open Access Scholarly Publishers Association (OASPA), and the World Association of Medical Editors (WAME).

Intractable & Rare Diseases Research will perform an especially prompt review to encourage innovative work. All original research will be subjected to a rigorous standard of peer review and will be edited by experienced copy editors to the highest standards.

Ethics: *Intractable & Rare Diseases Research* requires that authors of reports of investigations in humans or animals indicate that those studies were formally approved by a relevant ethics committee or review board. For research involving human experiments, a statement that the participants gave informed consent before taking part (or a statement that it was not required and why) should be indicated. Authors should also state that the study conformed to the provisions of the Declaration of Helsinki (as revised in 2013). When reporting experiments on animals, authors should indicate whether

the institutional and national guide for the care and use of laboratory animals was followed.

Conflict of Interest: All authors are required to disclose any actual or potential conflict of interest including financial interests or relationships with other people or organizations that might raise questions of bias in the work reported. If no conflict of interest exists for each author, please state "There is no conflict of interest to disclose".

Submission Declaration: When a manuscript is considered for submission to *Intractable & Rare Diseases Research*, the authors should confirm that 1) no part of this manuscript is currently under consideration for publication elsewhere; 2) this manuscript does not contain the same information in whole or in part as manuscripts that have been published, accepted, or are under review elsewhere, except in the form of an abstract, a letter to the editor, or part of a published lecture or academic thesis; 3) authorization for publication has been obtained from the authors' employer or institution; and 4) all contributing authors have agreed to submit this manuscript.

Cover Letter: The manuscript must be accompanied by a cover letter prepared by the corresponding author on behalf of all authors. The letter should indicate the basic findings of the work and their significance. The letter should also include a statement affirming that all authors concur with the submission and that the material submitted for publication has not been published previously or is not under consideration for publication elsewhere. The cover letter should be submitted in PDF format. For example of Cover Letter, please visit: Download Centre (*https://www.irdrjournal.com/downcentre*).

Copyright: When a manuscript is accepted for publication in *Intractable & Rare Diseases Research*, the transfer of copyright is necessary. A JOURNAL PUBLISHING AGREEMENT (JPA) form will be e-mailed to the authors by the Editorial Office and must be returned by the authors as a scan. Only forms with a hand-written signature are accepted. This copyright will ensure the widest possible dissemination of information. Please note that your manuscript will not proceed to the next step in publication until the JPA Form is received. In addition, if excerpts from other copyrighted works are included, the author(s) must obtain written permission from the copyright owners and credit the source(s) in the article.

Peer Review: *Intractable & Rare Diseases Research* uses single-blind peer review, which means that reviewers know the names of the authors, but the authors do not know who reviewed their manuscript. The external peer review is performed for research articles by at least two reviewers, and sometimes the opinions of more reviewers are sought. Peer reviewers are selected based on their expertise and ability to provide high quality, constructive, and fair reviews. For research manuscripts, the editors may, in addition, seek the opinion of a statistical reviewer. Consideration for publication is based on the article's originality, novelty, and scientific soundness, and the appropriateness of its analysis.

Suggested Reviewers: A list of up to 3 reviewers who are qualified to assess the scientific merit of the study is welcomed. Reviewer information including names, affiliations, addresses, and e-mail should be provided at the same time the manuscript is submitted online. Please do not suggest reviewers with known conflicts of interest, including participants or anyone

with a stake in the proposed research; anyone from the same institution; former students, advisors, or research collaborators (within the last three years); or close personal contacts. Please note that the Editor-in-Chief may accept one or more of the proposed reviewers or may request a review by other qualified persons.

Language Editing: Manuscripts prepared by authors whose native language is not English should have their work proofread by a native English speaker before submission. If not, this might delay the publication of your manuscript in *Intractable & Rare Diseases Research*.

The Editing Support Organization can provide English proofreading, Japanese-English translation, and Chinese-English translation services to authors who want to publish in *Intractable & Rare Diseases Research* and need assistance before submitting a manuscript. Authors can visit this organization directly at *http://www.iacmhr.com/iac-eso/support.php?lang=en*. IAC-ESO was established to facilitate manuscript preparation by researchers whose native language is not English and to help edit works intended for international academic journals.

4. Manuscript Preparation

Manuscripts are suggested to be prepared in accordance with the "Recommendations for the Conduct, Reporting, Editing, and Publication of Scholarly Work in Medical Journals", as presented at *http://www.ICMJE.org.*

Manuscripts should be written in clear, grammatically correct English and submitted as a Microsoft Word file in a single-column format. Manuscripts must be paginated and typed in 12-point Times New Roman font with 24-point line spacing. Please do not embed figures in the text. Abbreviations should be used as little as possible and should be explained at first mention unless the term is a well-known abbreviation (*e.g.* DNA). Single words should not be abbreviated.

Title page: The title page must include 1) the title of the paper (Please note the title should be short, informative, and contain the major key words); 2) full name(s) and affiliation(s) of the author(s), 3) abbreviated names of the author(s), 4) full name, mailing address, telephone/fax numbers, and e-mail address of the corresponding author; and 5) conflicts of interest (if you have an actual or potential conflict of interest to disclose, it must be included as a footnote on the title page of the manuscript; if no conflict of interest exists for each author, please state "There is no conflict of interest to disclose"). Please visit Download Centre and refer to the title page of the manuscript sample.

Abstract: The abstract should briefly state the purpose of the study, methods, main findings, and conclusions. For articles that are Original Articles, Brief Reports, Reviews, Policy Forum articles, or Case Report, a one-paragraph abstract consisting of no more than 250 words must be included in the manuscript. For Communications, Editorials, News, or Letters, a brief summary of main content in 150 words or fewer should be included in the manuscript. Abbreviations must be kept to a minimum and non-standard abbreviations explained in brackets at first mention. References should be avoided in the abstract. Three to six key words or phrases that do not occur in the title should be included in the Abstract page.

Introduction: The introduction should be a concise statement of the basis for the study and its scientific context.

Materials and Methods: The description should be brief but with sufficient detail to enable others to reproduce the experiments. Procedures that have been published previously should not be described in detail but appropriate references should simply be cited. Only new and significant modifications of previously published procedures require complete description. Names of products and manufacturers with their locations (city and state/country) should be given and sources of animals and cell lines should always be indicated. All clinical investigations must have been conducted in accordance with Declaration of Helsinki principles. All human and animal studies must have been approved by the appropriate institutional review board(s) and a specific declaration of approval must be made within this section.

Results: The description of the experimental results should be succinct but in sufficient detail to allow the experiments to be analyzed and interpreted by an independent reader. If necessary, subheadings may be used for an orderly presentation. All figures and tables must be referred to in the text.

Discussion: The data should be interpreted concisely without repeating material already presented in the Results section. Speculation is permissible, but it must be well-founded, and discussion of the wider implications of the findings is encouraged. Conclusions derived from the study should be included in this section.

Acknowledgments: All funding sources should be credited in the Acknowledgments section. In addition, people who contributed to the work but who do not meet the criteria for authors should be listed along with their contributions.

References: References should be numbered in the order in which they appear in the text. Citing of unpublished results, personal communications, conference abstracts, and theses in the reference list is not recommended but these sources may be mentioned in the text. In the reference list, cite the names of all authors when there are fifteen or fewer authors; if there are sixteen or more authors, list the first three followed by *et al*. Names of journals should be abbreviated in the style used in PubMed. Authors are responsible for the accuracy of the references. The EndNote Style of *Intractable & Rare Diseases Research* could be downloaded at **EndNote** (*https://www.irdrjournal.com/examples/Intractable_Rare_Diseases_Research.ens*).

Examples are given below:

Example 1 (Sample journal reference):

Inagaki Y, Tang W, Zhang L, Du GH, Xu WF, Kokudo N. Novel aminopeptidase N (APN/CD13) inhibitor 24F can suppress invasion of hepatocellular carcinoma cells as well as angiogenesis. Biosci Trends. 2010; 4:56-60.

Example 2 (Sample journal reference with more than 15 authors):

Darby S, Hill D, Auvinen A, *et al*. Radon in homes and risk of lung cancer: Collaborative analysis of individual data from 13 European case-control studies. BMJ. 2005; 330:223.

Example 3 (Sample book reference):
Shalev AY. Post-traumatic stress disorder: Diagnosis, history and life course. In: Post-traumatic Stress Disorder, Diagnosis, Management and Treatment (Nutt DJ, Davidson JR, Zohar J, eds.). Martin Dunitz, London, UK, 2000; pp. 1-15.

Example 4 (Sample web page reference):

World Health Organization. The World Health Report 2008 – primary health care: Now more than ever. *http://www.who.int/whr/2008/whr08_en.pdf* (accessed September 23, 2010).

Tables: All tables should be prepared in Microsoft Word or Excel and should be arranged at the end of the manuscript after the References section. Please note that tables should not in image format. All tables should have a concise title and should be numbered consecutively with Arabic numerals. If necessary, additional information should be given below the table.

Figure Legend: The figure legend should be typed on a separate page of the main manuscript and should include a short title and explanation. The legend should be concise but comprehensive and should be understood without referring to the text. Symbols used in figures must be explained. Any individually labeled figure parts or panels (A, B, *etc*.) should be specifically described by part name within the legend.

Figure Preparation: All figures should be clear and cited in numerical order in the text. Figures must fit a one- or two-column format on the journal page: 8.3 cm (3.3 in.) wide for a single column, 17.3 cm (6.8 in.) wide for a double column; maximum height: 24.0 cm (9.5 in.). Please make sure that the symbols and numbers appeared in the figures should be clear. Please make sure that artwork files are in an acceptable format (TIFF or JPEG) at minimum resolution (600 dpi for illustrations, graphs, and annotated artwork, and 300 dpi for micrographs and photographs). Please provide all figures as separate files. Please note that low-resolution images are one of the leading causes of article resubmission and schedule delays.

Units and Symbols: Units and symbols conforming to the International System of Units (SI) should be used for physicochemical quantities. Solidus notation (*e.g*. mg/kg, mg/mL, mol/mm^2/min) should be used. Please refer to the SI Guide *www.bipm.org/en/si/* for standard units.

Supplemental data: Supplemental data might be useful for supporting and enhancing your scientific research and *Intractable & Rare Diseases Research* accepts the submission of these materials which will be only published online alongside the electronic version of your article. Supplemental files (figures, tables, and other text materials) should be prepared according to the above guidelines, numbered in Arabic numerals (*e.g*., Figure S1, Figure S2, and Table S1, Table S2) and referred to in the text. All figures and tables should have titles and legends. All figure legends, tables and supplemental text materials should be placed at the end of the paper. Please note all of these supplemental data should be provided at the time of initial submission and note that the editors reserve the right to limit the size and length of Supplemental Data.

5. Submission Checklist

The Submission Checklist will be useful during the final checking of a manuscript prior to sending it to *Intractable & Rare Diseases Research* for review. Please visit Download Centre and download the Submission Checklist file.

6. Online Submission

Manuscripts should be submitted to *Intractable & Rare Diseases Research* online at *https://www.irdrjournal.com*. The manuscript file should be smaller than 5 MB in size. If for any reason you are unable to submit a file online, please contact the Editorial Office by e-mail at *office@irdrjournal.com*

7. Accepted Manuscripts

Proofs: Galley proofs in PDF format will be sent to the corresponding author *via* e-mail. Corrections must be returned to the editor (*office@irdrjournal.com*) within 3 working days.

Offprints: Authors will be provided with electronic offprints of their article. Paper offprints can be ordered at prices quoted on the order form that accompanies the proofs.

Page Charge: No page charges will be levied to authors for the publication of their article except for reprints.

Misconduct: *Intractable & Rare Diseases Research* takes seriously all allegations of potential misconduct and adhere to the ICMJE Guideline (*http://www.icmje.org/recommendations*) and COPE Guideline (*http://publicationethics.org/files/Code_of_conduct_for_journal_editors.pdf*). In cases of suspected research or publication misconduct, it may be necessary for the Editor or Publisher to contact and share submission details with third parties including authors' institutions and ethics committees. The corrections, retractions, or editorial expressions of concern will be performed in line with above guidelines.

(As of June 2020)

Intractable & Rare Diseases Research
Editorial and Head Office
Pearl City Koishikawa 603,
2-4-5 Kasuga, Bunkyo-ku,
Tokyo 112-0003, Japan.
E-mail: office@irdrjournal.com